Title
Regulation and Recruitment of Human Telomerase

Author
Sexton, Alec Nathan

Publication Date
2014

Peer reviewed|Thesis/dissertation

Regulation and Recruitment of Human Telomerase

by

Alec Nathan Sexton

A dissertation submitted in partial satisfaction of the

requirements for the degree of

Doctor of Philosophy

in

Molecular and Cell Biology

in the

Graduate Division

of the

University of California, Berkeley

Committee in charge:

Professor Kathleen Collins, Chair
Professor Donald Rio
Professor Michael Rape
Assistant Professor Danica Chen

Spring 2014

Abstract

Regulation and Recruitment of Human Telomerase

by

Alec Nathan Sexton

Doctor of Philosophy in Molecular and Cell Biology
University of California, Berkeley
Kathleen Collins, Chair

Linear chromosomes lose terminal sequence with every cell division due to incomplete replication by the eukaryotic replisome. Sequence must be added back to DNA ends, called telomeres, in order to deter instability that would occur as loss of end sequence encroached on genic DNA. Human telomeres are elongated by a ribonucleoprotein enzyme called telomerase, composed of the protein, TERT, and the RNA, hTR, which adds telomeric sequence onto DNA ends through reverse transcription off of its internal RNA template. Telomerase ensures indefinite replicative potential through maintenance of these ends, and is thus important for both normal cellular growth, and uncontrolled cell growth observed in most cancers.

Regulation of hTR accumulation is a multi step process involving many protein partners. Defects in the biogenesis pathway lead to reduced levels of hTR and impaired telomere maintenance. I show that the G-quadruplex resolvase DHX36 binds to hTR dependent on hTR's 5' guanosines. The binding occurs through the unique N-terminal domain of DHX36 which has demonstrated specificity for G-quadruplexes. Furthermore, stable accumulation of hTR depends on the presence of the 5' guanosines, implicating DHX36-mediated resolution of the 5' end of hTR in stable accumulation of the RNA.

Recruitment of mature telomerase to its substrate is dependent on the telomere binding protein TPP1. Specifically, it has been shown that the oligonucleotide/oligosaccharide-binding fold (OB) of TPP1 is important for recruitment of telomerase to the telomere. Using directed mutagenesis, I identified a discrete OB fold surface of TERT-TPP1 interaction, later termed the TEL patch. Importantly, the TEL patch is physically distinct from other regions that are essential for binding other shelterin proteins that maintain telomeric integrity and guard against recognition of the telomere end by DNA damage response proteins. Using genetic manipulation of human embryonic stem cells, I determined that the TEL patch is essential for recruitment to the telomere in a cellular system. Furthermore, through a separate residue, L104, TPP1 dictates the responsiveness of telomerase to telomere length. Together, these findings open up new targets for pharmaceutical inhibition of telomerase activity in cancer.

ACKNOWLEDGEMENTS

Today science is a collaborative effort, and I have had innumerable people help me through both practicing science at the bench and the life that revolves around that practice. First and foremost, my advisor Kathy Collins has been an incredible asset and advocate for me. She has shown me how to think critically about experiments, to always mind the details, and how to maintain a driving fascination for new scientific questions. Late in my graduate work I was also extremely fortunate to collaborate with new faculty member Dirk Hockemeyer. He clearly has a great career ahead of him and I count myself lucky to have been there for the start.

I also thank my committee, Don Rio, Michael Rape, and Danica Chen. Their feedback has helped to improve both the details of my projects as well as the overall direction of my graduate work.

The Collins lab has had many people travel through it in the time that I have been at Berkeley, all of whom I owe thanks in one way or another for scientific advice and moral support. Emily Egan was my patient rotation mentor, and continued to dole out advice and support whenever I needed it. Barbara Eckert was a master of protein biochemistry and, along with Emily, a reluctant audience to many of my jokes. Aaron Robart was my first baymate in the lab, and a good one. He was replaced by Alex Wu in what will later be referred to as "the Great Baymate Swap of 2011." Alex is certainly the best biochemist, one of the funniest people I know, a person of refined taste, and a frequenter of all fine dining establishments. To Heather Upton, who now takes up the heavy mantle of Rad Czar, I say Godspeed. Dan Youmans began working with me as Intrepid Junior Lab Assistant, First Class, and excelled quickly. I have no doubt he will be successful in graduate and medical school, and in intramural soccer leagues to come. Sam Regalado in the Hockemeyer lab is an excellent technician and also has a great scientific career ahead of him, and was an enormous help to me in my last year. For memorable discussions about all things science and other, I thank Mary Couvillion, Bosun Min, Jacob Vogan, Tristan Bell, Brian Farley, Kyungah Hong, Kasper Andersen, George Katibah, Chiba Kunitoshi, Ryan Forster, and all of my classmates.

My family has always encouraged me and given me the freedom and independence to pursue my goals. And finally I would like to thank Dorothy, my partner, for being patient and supportive in everything I do, even through many late nights in lab.

TABLE OF CONTENTS

ABSTRACT 1

ACKNOWLEDGEMENTS i

TABLE OF CONTENTS ii

CHAPTER ONE: Human telomerase assembly and functional interactions 1

CHAPTER TWO:The 5’ guanosine tracts of human telomerase RNA are recognized by the G-quadruplex binding domain of the RNA helicase DHX36 and function to increase RNA accumulation 5

Abstract 5

Introduction 6

Materials and methods 8

Results 10

Discussion 15

Figures 17

CHAPTER THREE: Specificity requirements for human telomere protein interaction with telomerase holoenzyme 25

Abstract 25

Introduction 26

Materials and Methods 29

Results 31

Discussion 35

Figures 37

CHAPTER FOUR: Genetic dissection of multiple roles for human TPP1 in stem cell telomere length homeostasis 45

Abstract 45

Introduction 46

Materials and Methods 48

Results 50

Discussion 54

Figures 56

REFERENCES 78

CHAPTER ONE

Human telomerase assembly and functional interactions

Telomerase is the enzyme responsible for maintaining the ends of chromosomes. Incomplete replication due to the use of RNA primers during DNA synthesis results in a progressive shortening of chromosome ends, or telomeres (Blackburn and Collins, 2011). The human telomerase ribonucleoprotein (RNP), composed minimally of a protein, TERT, and an integral RNA, hTR, synthesizes six nucleotide TTAGGG repeat using a complementary sequence contained in hTR to compensate for the loss of DNA during replication and maintain genomic integrity. Human telomeres are made up of approximately 5-15 kb of TTAGGG•CCCTAA double stranded (ds) DNA repeats with approximately 50-150 nucleotides (nt) of single stranded (ss) DNA G-rich overhang. Belying its importance in cell growth, this activity is largely restricted to highly proliferative cells such as certain hematopoietic cell populations, stem cells, germ line cells, and approximately 90% of cancers (Cifuentes-Rojas and Shippen, 2012; Kim et al., 1994; Lansdorp, 2005). Conversely, telomeres that become eroded due to uncompensated DNA replication and telomere loss can become recognized as dsDNA breaks, leading to cellular senescence and genomic instability (Artandi and Attardi, 2005).

Composition of the telomere

The ultimate destination for telomerase, the end of the telomere, is a highly ordered DNA-protein complex. Six proteins, TRF1, TRF2, RAP1, TIN2, TPP1, and POT1, collectively called the shelterin complex, bind to telomeres and contribute to telomere length regulation, protection from recognition of DNA ends as dsDNA breaks, and telomerase recruitment (Palm and de Lange, 2008). TRF1 and TRF2 both specifically bind telomeric dsDNA, while POT1 specifically binds telomeric ssDNA. TIN2 serves as a structural bridge from TRF1 and TRF2 to TPP1, which then connects to POT1. TPP1 has been implicated in the recruitment of telomerase to the telomere, while the TPP1:POT1 heterodimer has been shown in some studies to increase telomerase processivity (Abreu et al., 2010; Wang et al., 2007; Xin et al., 2007; Zhong et al., 2012).

While shelterin is the most well established protein complex found at the human telomere, others exist as well. In budding yeast, the ssDNA binding protein is Cdc13, which along with the proteins Stn1 and Ten1, forms the CST complex (Price et al., 2010). The components of the CST complex are RPA homologs which bind ssDNA and result in telomere uncapping and induction of the DNA damage response when any component is deleted. A CST complex has been identified in mammals, composed homologs of the yeast CST complex CTC1, STN1, and TEN1(Miyake et al., 2009). It colocalizes with many, but not all telomeres throughout the cell cycle. The function of mammalian CST is still under investigation, but it seems that it does not occupy the same telomere-capping role *per se* as in *S. cerevisiae*, because its binding to telomeres is independent of POT1, which is also involved in telomere end

protection. Deletion or depletion, however, of any of the CST components in mammals results in activation of the DNA damage response, telomere end fusions, C-strand degradation, and inefficient DNA replication in the telomere (Gu et al., 2012; Miyake et al., 2009; Stewart et al., 2012a). CST also has interactions with shelterin components through TPP1 (with STN1 and CTC1) and POT1 (with CTC1), possibly suggesting more involvement with telomere structure or telomerase activity (Chen et al., 2012; Wan et al., 2009). The involvement of CST in recruitment or activity of telomerase is interesting considering that in *S. cerevisiae* Cdc13 is responsible for recruiting yeast telomerase through a telomerase accessory protein, Est1, and this interaction is dependent on Cdc13 binding to Stn1 and Ten1 (Li et al., 2009).

Biogenesis of telomerase components

Telomerase in human cells is first regulated at the level of biogenesis of its components. A complicated array of sequence polymorphisms, transcription factor interactions and epigenetic modifications collaborate to influence telomerase component levels (Cairney and Keith, 2008; Daniel et al., 2012). In humans, the TERT mRNA transcript is undetectable in most somatic tissues and is found to be upregulated in many cancerous tissues, whereas hTR accumulates at low levels (approximately 1000 molecules per cell) in all tissues (Avilion et al., 1996; Meyerson et al., 1997). After initial transcription in the case of hTR, and initial transcription and translation for TERT, multiple proteins must interact with the two telomerase components for proper accumulation and localization (Egan and Collins, 2012). hTR is bound on its 3' stem H/ACA motif by a core set of H/ACA proteins that are required for its stability and accumulation, as well as on its 3' stem-loop 4 nt CAB box by TCAB/WDR79, which localizes hTR to Cajal Bodies (Egan and Collins, 2010; Tomlinson et al., 2006; Venteicher et al., 2009).

The importance of these interactions is underscored by mutations that have been found in these proteins that prevent binding to hTR, and consequently mislocalized or poorly accumulated mature hTR (Walne and Dokal, 2009). TERT itself is shown to be important for hTR localization also, as knockdown of TERT results in mislocalization of hTR from Cajal Bodies (Tomlinson et al., 2008). It remains unclear whether TERT generally contributes to hTR stability outside of S-phase, given the facts that during this time TERT localizes to the nucleolar periphery, that hTR localization to Cajal Bodies is only observed in cancer cells, and that localization to Cajal Bodies, even when present, is not strictly required for telomere maintenance when telomerase components are overexpressed (Stern et al., 2012). In addition to these relatively well explored interactions hTR binding proteins, a number of other proteins have been found to have interactions with hTR, the significance of which have yet to be fully realized.

Recruitment of telomerase to telomeres

The sheer scarcity of both the telomeric substrate (184 after replication in S-phase, or more in aneuploid cell lines) and the fully assembled telomerase enzyme (a roughly estimated 25-50 in HeLa cells), coupled with the fact that in human cells with maintained telomeres each telomere appears to be extended by telomerase exactly one time during S-phase, implies a

specific and ordered recruitment of telomerase to the DNA ends (Cohen et al., 2007; Zhao et al., 2011). While most of the events that lead to telomere loading of telomerase are unknown, many studies have implicated telomeric proteins and domains of TERT that are important in this process.

The telomeric protein TPP1 was initially shown to be an integral part of the shelterin complex, serving as a link between TIN2 and the ssDNA binder POT1 (Houghtaling et al., 2004a; Liu et al., 2004; Ye et al., 2004). Further studies showed it to be able to associate with active telomerase and potentially contribute to an increase in telomerase activity (Wang et al., 2007; Xin et al., 2007). Moreover, the OB fold of TPP1 recruits telomerase to the telomere and is essential for long term proliferative potential. Tethering of the OB domain alone to the telomere results in the binding of TERT to the telomere and subsequent telomere maintenance (Abreu et al., 2010; Tejera et al., 2010). In fact, overexpression of TPP1 is known to cause telomere shortening, likely due to occupying the TERT telomere recruitment site, in effect a dominant negative (Houghtaling et al., 2004a; Ye et al., 2004; Zhong et al., 2012). Whether TPP1 binding of TERT near to its substrate is enough to initiate telomere elongation, or whether other steps are required for loading of telomerase onto the extreme ssDNA 3' end is not yet known. The progression of the DNA replication fork through the telomere, coupled with modifications made to telomeric proteins during cell cycle progression that induce remodeling of telomeric chromatin would suggest that the state and composition of the telomere during elongation is dynamic (Deng et al., 2009; McKerlie and Zhu, 2011).

Regions of TERT itself responsible for proper recruitment to telomeres have been identified through mutational screens that separate in vitro catalytic activity from in vivo telomere maintenance. These TERT regions, called DAT (for dissociates activities of telomerase), show activity in cell extract, but are unable to immortalize cells, potentially due to telomerase recruitment defects. Two regions in particular, in the TERT N-terminal region and the C-terminal extremis, can be mutated without loss of catalytic activity but loss of function for telomere maintenance (Armbruster et al., 2001; Counter et al., 1998). Recruitment to the telomere is specifically implicated as being impaired because tethering of these mutants to the telomeric proteins POT1 or TRF2 increases telomere maintenance (Armbruster et al., 2003, 2004). Two other residues within the N-terminal domain, R132 and V144, have also been implicated in recruitment of TERT to the telomere based on lack of telomeric localization of R132D or V144M TERT by immunofluorescence in cells (Stern et al., 2012; Zhong et al., 2012).

Telomerase biology in pluripotent cells

Almost all of the previous research carried out on telomere and telomerase biology in human has utilized immortalized cell lines where telomerase expression is aberrantly upregulated. Additionally, many studies utilize stable integration of retroviral constructs, or transient overexpression of telomere and telomerase components. While these approaches have been fruitful for identifying dynamic interactions among telomerase components, they necessarily come with several caveats including non-physiological expression or stoichiometry

of components, competition from endogenous proteins, aneuploid chromosomes, and generally abnormal cellular contexts when compared with typical human physiology. Human embryonic stem cells (hESCs), however, represent a discrete developmental state where telomerase components are expressed and telomeres are maintained (Thomson, 1998).

While mechanistic studies in hESCs to date are few, induced pluripotent stem cells have already shown promise as a valuable system for investigating telomerase biology. This is expecially true in cases where reversion to a pluripotent state reactivates maintenance of telomeres, and allows investigation of disease causing telomerase mutants. This has shown that even in a cell line where telomeres are normally maintained, mutations that cause Dyskeratosis Congenita impair maintenance of telomere length, leading to telomere shortening and cell death over time (Batista et al., 2011).

Although many of the complex steps leading to telomerase recruitment to telomeres have been discovered, still more of the process remains a black box. This work details several new contributions to our understanding of telomerase regulation. First, I showed that an RNA helicase, DHX36, is implicated in binding to a tract of guanosines in the 5' tail of hTR (Sexton and Collins, 2011). The stability of hTR in vivo is shown to depend on the presence of these guanosines, which have been shown to form a G-quadruplex structure, in vitro. Proper biogenesis of hTR thus may rely on the interaction between this structural motif and DHX36. Second, I find that the interaction between TPP1 and active telomerase depends on an acidic loop on TPP1's OB fold (Sexton et al., 2012). Significantly, this is the same surface of interaction found on other TPP1 homologs in various yeasts, demonstrating a deep evolutionary conservation of telomerase protein interactions. Additionally, several TERT residues in the TEN domain also are required for binding of active telomerase to TPP1. Finally I have shown TPP1 roles to be essential in hESC context.

CHAPTER TWO

The 5’ Guanosine Tracts in Human Telomerase RNA Recruit the G-quadruplex Binding Domain of the RNA Helicase DHX36 and Function to Increase RNA Accumulation

Based on Sexton and Collins, Molecular and Cellular Biology, 2011

Abstract

Telomerase promotes telomere maintenance by copying a template within its integral RNA subunit to elongate chromosome ends with new telomeric repeats. Motifs have been defined within the telomerase RNA that contribute to mature RNA accumulation, holoenzyme catalytic activity or enzyme recruitment to telomeres. Here we describe a motif of human telomerase RNA (hTR) not previously characterized in cellular context comprised of several guanosine tracts near the RNA 5’ end. These guanosine tracts together are recognized by the DExH-box RNA helicase DHX36. The helicase domain of DHX36 does not mediate hTR binding; instead, hTR interacts with the N-terminal accessory domain of DHX36 known to bind specifically to the parallel-strand G-quadruplex substrates resolved by the helicase domain. The steady-state level of DHX36-hTR interaction is low, but hTR guanosine-tract substitutions substantially reduce mature hTR accumulation and thereby reduce telomere maintenance. These findings suggest that G-quadruplex formation in the hTR precursor improves the escape of immature RNP from degradation, but subsequently the G-quadruplex may be resolved in favor of a longer terminal stem. We conclude that G-quadruplex formation within hTR can stimulate telomerase-mediated telomere maintenance.

Introduction

Telomerase is a RNP reverse transcriptase that extends the ends of eukaryotic chromosomes by new telomeric repeat synthesis (Blackburn and Collins, 2011; Blackburn et al., 2006). Enzyme activity requires the two universally conserved subunits of a functional telomerase RNP: the telomerase RNA and telomerase reverse transcriptase protein (TERT). Other proteins associate with telomerase RNA and/or TERT to promote their cellular accumulation and association or to engage the biologically active telomerase holoenzyme with telomere substrates (Collins, 2006; Stern and Bryan, 2008). In multicellular eukaryotes, somatic cells down-regulate telomerase-mediated telomere maintenance as a tumor suppression mechanism (Shay and Keith, 2008). The progressive telomere attrition evident in most human somatic cell lineages with cell division cumulatively increases the likelihood of telomere unmasking as a signal for the DNA damage response (O'Sullivan and Karlseder, 2010). Telomerase activation is critical for long-term cellular proliferation, as reflected in the near-universal increase of telomerase subunit expression and activity in immortalized cell lines and cancers (Harley, 2008).

Phylogenetic sequence comparisons, directed mutagenesis and studies of disease-linked mutations have uncovered a complexity of sequence requirements for human telomerase RNA (hTR) folding, processing and protein interactions (Chen et al., 2000; Collins, 2008; Robart and Collins, 2010). As a nascent transcript of RNA polymerase II, the hTR precursor recruits two sets of the H/ACA-motif RNA binding proteins dyskerin, NHP2 and NOP10 in a chaperoned multistep process culminating in the exchange of RNP biogenesis factors for the fourth stably associated H/ACA-motif RNP protein GAR1 (Egan and Collins, 2010; Fu and Collins, 2007). Proper assembly of the hTR H/ACA-motif with dyskerin, NHP2 and NOP10 is essential for precursor maturation and produces the biologically stable telomerase RNP (Collins, 2008).

The RNA binding protein WDR79/TCAB1 can bind to the loop of the hTR 3' stem and through this interaction increase the retention of hTR in Cajal bodies (Cristofari et al., 2007a; Egan and Collins, 2010; Jády et al., 2006; Tycowski et al., 2009; Venteicher et al., 2009). Two regions within hTR separated by the 5' stem of the H/ACA motif (Fig. 1A) are necessary and sufficient for TERT binding and RNP activity (Mitchell and Collins, 2000). In addition to the motifs described above that promote hTR function in telomere maintenance, other hTR motifs provide opportunities for negative regulation (Collins, 2008; Fu and Collins, 2007).

DHX36 (also known as RHAU and G4R1) is a DExH-box RNA helicase independently discovered as mediator of AU-rich element mRNA degradation and as a resolvase for G-quadruplex DNA in vitro (Tran et al., 2004; Vaughn et al., 2005). Subsequent studies expanded the function of DHX36 to include more global roles in regulating mRNA expression and to include resolvase activity on a model RNA as well as DNA quadruplex of parallel strand orientation (Creacy et al., 2008; Iwamoto et al., 2008; Lattmann et al., 2010). A previous mass-spectrometry analysis of human telomerase holoenzyme affinity purified by tagged TERT (Fu and Collins, 2007) unreliably identified DHX36 and several other helicase-domain proteins

(unpublished results), with the inconclusive identifications based on only a single peptide sequence (in the case of DHX36) or peptide detection in parallel mock purifications from cells lacking tagged TERT (in the case of RuvBL1/RuvBL2, the Unigene designations for proteins also known as TIP49 or pontin and TIP48 or reptin, respectively). Helicase-domain proteins participate broadly in RNA processing, RNP biogenesis and RNP regulation with strand-separating, strand-annealing and RNP remodeling activities potentially relevant to telomerase RNP maturation and function (Jankowsky and Fairman, 2007). DHX36 in particular has several potentially relevant substrates, because model oligonucleotides with the sequence of human telomeric DNA, telomeric RNA or the 5' region of hTR can form Hoogsteen base-paired G-quadruplex structures in vitro (Bryan and Baumann, 2010; Collie et al., 2010; Gros et al., 2008; Li et al., 2007; Randall and Griffith, 2009; Xu et al., 2010). We therefore investigated whether DHX36 associates with human telomerase and if so whether the interaction has defined sequence requirements or a more chaperone-like general specificity.

Here we demonstrate that guanosine tracts clustered near the hTR 5' end can be recognized by DHX36 and in particular by the DHX36 N-terminal domain specific for binding to G-quadruplex structures in vitro (Lattmann et al., 2010). Curiously, substitutions within the hTR guanosine tracts substantially reduce mature RNA accumulation. Variants of hTR disrupted for G-quadruplex formation still support robust telomerase holoenzyme catalytic activity and high repeat addition processivity. However, a reduced level of steady-state accumulation compromises their function in telomere maintenance. Together these findings uncover a stimulatory role for G-quadruplex formation in promoting the biological function of human telomerase.

Materials and methods

Cell lines and constructs

All cell lines were grown in DMEM with 10% fetal bovine serum, penicillin and streptomycin. Transient transfection of 293T cells with DNA expression constructs was performed with calcium phosphate as previously described (Fu and Collins, 2003). Whole cell extract was prepared 48 h after transfection by freeze-thaw cell lysis as previously described (Mitchell et al., 1999). The 1774TERT cell line, created by ectopic TERT expression in primary fibroblasts from an X-linked dyskeratosis congenita patient (Wong., J.M.Y., and Collins, 2006), and HT-1080 cells were stably transduced by retroviral infection as previously described (Wong., J.M.Y., and Collins, 2006). Constructs for hTR and hTR-U64 expression from the U3 promoter were in a pBS vector backbone (Fu and Collins, 2003); all other transiently transfected constructs were in the pcDNA 3.1 (+) vector backbone and retrovirally transduced constructs were in the pBABEpuro vector backbone. Proteins were N-terminally tagged with three FLAG peptides, two tandem protein A domains (zz) or a TAP tag composed of tandem protein A domains, a protease cleavage site and a calmodulin-binding peptide.

Purification and detection of RNA and protein

For tagged protein purifications, clarified whole cell extract corresponding to 0.5-1.0 mg total protein was added to tubes with 10 µl rabbit IgG agarose (Sigma) or FLAG M2 antibody resin (Sigma) pre-washed 3x 5 min in IP buffer (10 mM HEPES at pH 8, 10% glycerol, 150 mM NaCl, 0.1% NP40). Samples were incubated at room temperature for 2 h with rotation, then beads were washed 3x 5 min in wash buffer (IP buffer with added 0.4% NP40 and 0.1% Triton-X100). RNA was extracted by TRIzol according to the manufacturer's protocol (Invitrogen), and a 5' end-labeled probe complementary to hTR nucleotides 51-72 was used for blot hybridization as previously described (Mitchell et al., 1999). An in vitro transcript of mature hTR nucleotides 1-160 was added before RNA extraction from bound samples for use as a recovery control (RC). The input RNA loading control (LC) is an endogenous RNA that cross-hybridizes to the hTR probe (Fu and Collins, 2007). For all RNA inputs of samples used for immunopurifications, the amount loaded corresponds to 10% of the total.

For hTR detection in total cellular RNA of retrovirally transduced cell lines, 2 µg or 10 µg RNA was used for 1774TERT or HT1080 cell lines, respectively. Tagged proteins were detected with rabbit IgG (for TAP- or zz-tagged proteins) or mouse anti-FLAG M2 monoclonal antibody (for FLAG-tagged proteins) and secondary antibodies imaged by the LI-COR Odyssey system. Immunoblot input samples were normalized to contain 10 µg total protein each, which corresponds to between 2% and 4% of total protein input.

Telomerase activity and telomere length assays

The direct primer extension activity assay was performed using resin-immobilized purified holoenzyme as previously described (Robart and Collins, 2010). The PCR-amplified TRAP activity assay was performed using total cell lysate or resin-bound samples as previously

described (Fu and Collins, 2006). The TRAP internal control (IC) is an oligonucleotide competitor for amplification that generates a product longer than the telomerase product ladder. All activity assay samples were diluted in IP buffer. Telomere length was determined by in-gel hybridization using a 5'-end-labeled telomeric-repeat oligonucleotide as previously described (Fu and Collins, 2007), except for the inclusion of additional genomic DNA purification steps before and after RsaI and HinfI digestion. DNA fragment size was determined by staining an excised DNA ladder lane of the gel with ethidium bromide.

Results

DHX36 association with human telomerase RNP

We probed the association of TERT and hTR with DHX36 and a panel of other helicase-domain proteins including RuvBL1 and RuvBL2, two interacting multimeric proteins previously demonstrated to play a critical role in chaperoning general H/ACA RNP biogenesis and hTR accumulation (Huen et al., 2010; Venteicher et al., 2009). Comparing across the helicase-domain proteins, hTR was most robustly associated with DHX36 over a range of wash stringency conditions (data not shown). Whole-cell extracts from 293T cells transiently transfected to express N-terminally zz-tagged TERT and/or N-terminally 3xFLAG-tagged (F) DHX36 were used to recover TERT on IgG agarose and immunoblot for associated DHX36. There was not a readily detectable association between overexpressed tagged TERT and DHX36 with or without concurrent expression of additional hTR (Fig. 1B). There was also no readily detectable association if TERT was F-tagged and DHX36 was TAP-tagged (data not shown). On the other hand, TAP-tagged DHX36 did copurify hTR with or without concurrent overexpression of TERT (Fig. 1C, lanes 6-7; note that mature hTR frequently migrates as a doublet due to partial folding during denaturing gel electrophoresis). As a background control, no hTR was recovered with IgG agarose in the absence of TAP-DHX36 (Fig. 1C, lane 8). Because 293T cells have endogenous TERT, we further assessed the TERT-dependence of DHX36 interaction with hTR using an RNA lacking a high-affinity TERT binding site. The hTR-U64 chimera replaces the 3' half of hTR, including the H/ACA motif and the major TERT binding site atop the H/ACA-motif 5' stem (Fig. 1A), with the H/ACA small nucleolar RNA U64. Despite severely crippled TERT interaction (Mitchell et al., 1999), hTR-U64 retained robust association with DHX36 (Fig. 1C, lane 10). Together these results support the conclusion that DHX36 associates with hTR in a manner that does not require hTR interaction with TERT.

We next investigated whether DHX36 associates with hTR in a manner that is mutually exclusive with TERT interaction and RNP catalytic activity. We compared the copurification of hTR and telomerase catalytic activity by tagged DHX36 versus tagged dyskerin. Two subunits of dyskerin are incorporated in each biologically assembled telomerase RNP (Egan and Collins, 2010), so the majority hTR population of catalytically inactive RNP and the TERT-containing catalytically active holoenzyme are both enriched by the control F-tagged dyskerin. Compared to F-tagged dyskerin, F-tagged DHX36 recovered less of the overexpressed hTR (Fig. 2A, lanes 3-4) and proportionally less telomerase activity detected by the PCR-amplified TRAP assay (Fig. 2B, lanes 7-8). Nonetheless, F-tagged DHX36 did enrich both hTR and telomerase activity relative to background detected in the absence of an F-tagged protein (Fig. 2A, compare lane 1 to lane 3; Fig. 2B, compare lane 5 to lane 7). As a specificity control, the small nuclear RNA U2 was not enriched by DHX36 or dyskerin. Overexpressing hTR increased both hTR and telomerase activity copurification with F-DHX36, but even endogenous levels of hTR and telomerase holoenzyme activity were specifically copurified (Fig. 2A, compare lanes 1-3; Fig. 2B, compare lanes 5-7). The RNP enriched by DHX36 appeared much lower in specific activity

than the RNP enriched by TERT, suggesting that like dyskerin DHX36 is not preferentially associated with the catalytically active telomerase holoenzyme. These conclusions were reproducible across different extracts and tagged subunit purifications (data not shown).

Comparing the telomerase RNP purification yield from tagged dyskerin versus tagged DHX36 is not strictly quantitative due to potential differences in tagged protein competition with endogenous untagged protein, but it seems likely that the stoichiometry of hTR association with DHX36 is less than that of its association with dyskerin. We were unable to detect specific enrichment of telomerase activity in association with endogenous DHX36 using a commercially available DHX36 antibody, potentially for technical reasons (commercial antibodies have not been reported to purify DHX36 RNP complexes). Also, because the hTR structure that recruits DHX36 would be subsequently resolved by DHX36 activity (see below), in a steady-state distribution, very little of the endogenous telomerase RNP could have associated DHX36.

RNA-motif and protein-domain specificity of hTR-DHX36 interaction

To address the sequence specificity of hTR-DHX36 interaction, we first considered the 5' half of hTR that supports DHX36 interaction in the hTR-U64 chimera (Fig. 1C). Aside from the template/pseudoknot motifs required for catalytic activity in association with TERT, this region includes a putative single-stranded 5' leader and domain-closing P1 helix that could be sites of DHX36 interaction (Fig. 3A). Notably, rodent evolution has truncated the telomerase RNA 5' end to a starting position almost immediately 5' of the template (Chen et al., 2000). Despite this appearance of functional dispensability, the hTR P1 helix serves an important role in template boundary definition: hTR sequence substitutions that disrupt P1 base-pairing reduce the fidelity of repeat synthesis and are associated with human disease (Chen and Greider, 2003; Robart and Collins, 2010). Synthetic RNAs harboring hTR sequence 5' of the template can fold as a G-quadruplex (Gros et al., 2008; Li et al., 2007). Importantly, unlike DNA, RNA uniformly adopts the parallel strand orientation of quadruplex in vitro and in vivo (Bryan and Baumann, 2010; Collie et al., 2010; Randall and Griffith, 2009; Xu et al., 2010). DHX36 has the ability to bind and resolve a model intermolecular G-quadruplex RNA (Creacy et al., 2008). We therefore tested whether DHX36 binding requires the hTR 5’ G-tracts with quadruplex-forming potential.

Tracts of 2-3 consecutive guanosines were substituted to replace two guanosines with two cytidines (pairs of substituted guanosines are shaded in Fig. 3A). We coexpressed wild-type or variant hTR with hTR-U64 as an internal transfection control, recovered DHX36-associated RNAs by immunopurification and quantified the input and bound hTR and hTR-U64. Most of the hTR G-tract substitutions reduced mature hTR accumulation relative to coexpressed hTR-U64 (Fig. 3B; hTR Accumulation indicates hTR level normalized to hTR-U64). We then determined the relative percentage of input hTR associated with DHX36 (Fig 3B; hTR Bound/Input). Substitutions GG2-3CC, GG12-13CC and GG16-17CC in the 3-G tracts of the 5' leader drastically reduced hTR-DHX36 interaction, as did the G12C and G13C single-nucleotide substitutions of the central 3-G tract (Fig. 3B, lanes 3-4 and 6-9). For these hTR variants, the amount of bound hTR approached the low level of background from copurification of

endogenous wild-type hTR (Fig. 3B, lane 2). The substitution GG8-9CC in the only 2-G tract of the 5' leader reduced DHX36 interaction to a lesser extent (Fig. 3B, lane 5). Within the first few base-pairs of P1, the GG21-22CC substitution strongly inhibited DHX36 interaction (Fig. 3B, lane 10). A more central P1 substitution GG26-27CC reduced DHX36 interaction more than did the CC199-200GG substitution of the complementary strand, but the compensatory combination of substitutions rescued DHX36 interaction with hTR (Fig. 3B, lanes 11-13). These results implicate several guanosine tracts near the hTR 5’ end as contributors to DHX36 interaction.

Potentially any combination of four G-tracts at a nascent hTR 5’ end could fold as an intramolecular quadruplex to form a DHX36 binding site. Results above suggest that folding favors inclusion of the 5' leader 3-G tracts GGG1-3, GGG11-13, GGG15-17. In alternative folds the fourth strand could be contributed by GG8-9, GGG21-23 or GGGG25-28. Formation of P1 would disfavor incorporation of the central P1 GGGG25-28 tract more than the GGG21-23 tract toward the base of the stem. Indeed, results from hTR chemical modification and enzymatic digestion after folding in vitro or in vivo support complete base-pairing of central P1 GGGG25-28 but a more dynamic or mixed population of structures involving GGG21-23 and/or the partner cytidines at the base of P1 (Antal et al., 2002). Curiously, all of the multiple-guanosine tracts in the hTR 5’ leader are partially protected from modification compared to guanosines around the template, and the GGG11-13 and GGG15-17 tracts are sites of pauses to reverse transcription. The only hTR 5’-end guanosine not protected from modification after folding in vitro or in vivo is the singlet G6 (Antal et al., 2002), which substituted in G6C hTR had no impact on DHX36 interaction (data not shown). Together the previous findings and our results above suggest that at least some hTR RNPs have folded guanosine-tract structure(s) recognized by DHX36.

To investigate the DHX36 domain requirements for hTR interaction, we compared hTR copurification with full-length and truncated DHX36 proteins (Fig. 4A), with or without the E335A active-site substitution that abrogates helicase catalytic activity (Iwamoto et al., 2008). The unique N-terminal domain of DHX36 alone (amino acids 1-200) copurified hTR as well as or better than the full-length protein, whereas the helicase domain (amino acids 201-1008) did not support any detectable hTR interaction (Fig. 4B, lanes 1-5). The catalytic-dead full-length protein retained hTR interaction comparable to wild-type DHX36, and catalytic-dead helicase domain did not gain hTR interaction (Fig. 4B, lanes 6-7). The DHX36 N-terminal domain alone showed the same specificity of hTR interaction as full-length DHX36, with binding abrogated by the G12C hTR substitution (Mut; Fig. 4C). In cells expressing G12C hTR, tagged DHX36 enriched only the low level of endogenous hTR that also copurified with DHX36 in the absence of any recombinant hTR (Fig. 4C, lanes 3 and 5). Likewise, from input extracts containing abundant G12C hTR, the DHX36 N-terminal domain and the catalytic-dead full-length protein copurified only a low level hTR likely to be entirely of endogenous wild-type sequence (Fig. 4C, lanes 6 and 8). In comparison, the DHX36 helicase domain copurified neither recombinant G12C hTR nor endogenous wild-type hTR (Fig. 4C, lanes 7 and 9).

These results extend previous studies of DHX36 RNA binding specificity in vitro, which revealed that the DHX36 N-terminal domain is sufficient for binding to the intermolecular G-

quadruplex model substrate that can be resolved by the helicase domain in full-length DHX36 (Creacy et al., 2008; Lattmann et al., 2010). Different from previous findings, we did not detect increased RNA association with full-length DHX36 compared to the DHX36 N-terminal domain alone. The previously inferred contribution of the helicase domain to G-quadruplex binding may have been a consequence of a difference in folding of the recombinant full-length protein expressed in insect cells versus the recombinant N-terminal domain expressed in *E. coli*, or it could reflect helicase domain binding to the long single-stranded regions of the model quadruplex generated by intermolecular annealing of an $A_{15}G_5A_{15}$ oligonucleotide.

Biological function of the hTR guanosine-tract motif

To address the functional role of the hTR G-tracts recognized by DHX36, we first assessed whether disruption of these sequences affected hTR-TERT interaction or the catalytic activity of holoenzyme assembled in vivo. We coexpressed each of a panel of hTR sequence variants with tagged TERT in 293T cells, recovered the F-tagged TERT and assayed for coenrichment of hTR. As predicted from the known hTR determinants of TERT binding (Mitchell and Collins, 2000), none of the hTR 5'-end sequence substitutions prevented hTR-TERT interaction (Fig. 5, top panels). Furthermore, in agreement with established requirements for activity reconstitution using TERT and minimized hTR domains in vitro (Chen and Greider, 2005; Mitchell and Collins, 2000), none of the hTR 5'-end sequence substitutions notably inhibited holoenzyme activity or repeat addition processivity (Fig. 5, bottom panel). As expected based on the role of P1 in template 5' boundary definition (Chen and Greider, 2003; Robart and Collins, 2010), unpairing central P1 increased the synthesis of products one nucleotide longer than the normal ladder (Fig. 5, lanes 6-7; longer products are marked with a filled arrowhead). Compensatory stem substitutions that repaired central P1 suppressed this defect (Fig. 5, lane 8). Template boundary bypass was less severe in the hTR GG21-22CC holoenzyme disrupted for pairing of the P1 base (Fig. 5, lane 5), consistent with the relatively modest template 5' boundary bypass imposed by the disease-linked hTR C204G variant compared to a P1 disruption closer to the template (Robart and Collins, 2010).

We next investigated the impact of G-tract disruptions on hTR function in telomere maintenance. Some but not all cell lines will show an increase in the steady-state accumulation of mature hTR when hTR precursor is overexpressed from an integrated retroviral expression construct. Fibroblasts from X-linked dyskeratosis congenita patients that ectopically express TERT maintain exceptionally short telomeres due to the limiting level of endogenous hTR, and so additional hTR expression induces rapid telomere elongation to a stably maintained longer telomere length set-point (Wong., J.M.Y., and Collins, 2006). This provides a sensitized system for detecting even partial inhibition of hTR function in telomere elongation (Errington et al., 2008). We stably transduced the 1774TERT X-linked dyskeratosis congenita fibroblast cell line with the negative-control empty vector, positive-control wild-type hTR expression vector and expression vectors encoding hTR variants that compromise the DHX36 interaction indicative of G-quadruplex formation (GG12-13CC, G12C, GG16-17CC and GG21-22CC). Following

selection for retroviral integration, polyclonal cell populations were harvested at increasing population doublings to assay hTR accumulation, telomerase activity in cell extract and telomere length. As observed previously (Errington et al., 2008; Wong., J.M.Y., and Collins, 2006), each cell line rapidly reached a new telomere length set-point (data not shown).

Each of the hTR G-tract variants accumulated at a reduced steady-state level compared to wild-type hTR, although still substantially above the endogenous hTR level in cells transduced with the empty vector (Fig. 6A). Consistent with the levels of hTR accumulation, cell lines expressing hTR G-tract variants had levels of telomerase activity in cell extract that were greater than the empty vector control, as detected by TRAP assay (Fig. 6B). The cell lines expressing hTR G-tract variants stably maintained telomeric restriction fragment lengths (Fig. 6C, lanes 3-6) that were intermediate between the cells expressing empty vector (lane 2) and the cells expressing wild-type hTR (lane 1). We repeated this test of hTR function for the G12C hTR variant in HT-1080 human fibrosarcoma cells. Integration of the wild-type hTR expression construct produced a much more modest increase in steady-state hTR accumulation and telomerase activation than was obtained in 1774TERT cells, likely due to the higher endogenous level of hTR (Figs. 7A and 7B). As in the primary fibroblast system, HT-1080 cells stably expressing G12C hTR elongated telomeres relative to the empty vector control, but the extent of telomere elongation was reduced in comparison to cells expressing additional wild-type hTR (Fig. 7C; duplicate lanes are independent loading). In summary, in both cell types, hTR G-tract variants supported a reduced level of telomere elongation due in part or whole to compromised hTR accumulation.

Discussion

Proteins required for hTR biogenesis and accumulation can limit telomerase-mediated telomere maintenance, as evident in inherited diseases of human telomerase deficiency (Savage and Alter, 2009). Here we uncover a previously unsuspected recognition of hTR by the DExH-box RNA helicase DHX36. Consistent with previous studies of DHX36 activity as a G-quadruplex binding factor (Creacy et al., 2008; Vaughn et al., 2005), we found that DHX36-hTR interaction requires multiple G-tracts at the hTR 5' end. Also consistent with a concurrent study (Lattmann et al., 2010), our results suggest that the N-terminal domain of DHX36 is necessary and sufficient for association with G-tract RNA. The hTR binding site for DHX36 contains closely spaced G-tracts that would be favored by dilute concentration in vivo to fold as an intramolecular quadruplex, in contrast to the $A_{15}G_5A_{15}$ model substrate forced to fold as an intermolecular quadruplex in vitro. Nonetheless, the highly preferred parallel strand orientation of G-quadruplex RNA would give the model RNA oligonucleotide and endogenously folded hTR a similar structure of stacked guanosines for recognition by DHX36 (Collie et al., 2010).

Using hTR variants that retain TERT interaction and holoenzyme catalytic activity, we examined the significance of the hTR G-tracts in cellular context. G-tract substitutions including the single-nucleotide change G12C reduced hTR function in telomere elongation in part or whole by reducing the steady-state level of mature hTR. The decrease in RNP accumulation could be due to loss of DHX36 interaction, but we suspect instead that DHX36 binds hTR in the process of resolving a G-quadruplex structure that itself is the determinant of RNP accumulation. Because the majority of hTR RNP is not bound by DHX36 at steady-state yet disruption of the DHX36 interaction site on hTR severely reduces mature hTR accumulation, we propose that a large fraction of hTR precursor folds to contain a quadruplex that acts transiently in an early stage of RNP biogenesis to protect the RNA from degradation. This quadruplex structure would subsequently be recognized and likely unfolded by DHX36, resulting in DHX36 release (Fig. 8). The unstructured hTR 5' region could potentially refold as quadruplex, but this may often be competed by formation of a complete P1. A quadruplex involving only the 5' leader from P1 would fold with less than optimal stability due to the necessary inclusion of a 2-G tract. Also, the mature hTR trimethylated 5' cap structure could diminish the stability of quadruplexes formed with the 5' guanosine. DHX36 recognition and resolution of a structure formed by the majority of nascent hTR transcripts would account for the highly stabilizing biological role of the hTR guanosine tracts and yet the low steady-state level of DHX36 association with active telomerase RNP. Vertebrate telomerase RNAs that lack a guanosine-rich 5' leader could compensate for this loss by increased precursor expression or other stabilizing influences such as more rapid 5' cap modification.

DHX36 has a primarily nucleoplasmic but partially cytoplasmic distribution and has multiple ascribed functions in the regulation of mRNA expression and turnover (Iwamoto et al., 2008; Tran et al., 2004). The pleiotropic impact of DHX36 depletion on mRNA levels complicates any analysis of a direct influence of DHX36 on telomere biology, particularly given

that only a minor fraction of the total cellular DHX36 would be required to saturate interaction with the scarce telomerase RNP. Because DHX36 recognition of hTR is mediated by the N-terminal protein domain, the helicase domain would be poised for association with nearby potential substrates. In addition to acting as a resolvase for structured regions of hTR, more speculatively, the helicase domain of hTR-bound DHX36 could act on telomeric DNA or telomeric RNA quadruplexes. DHX36 resolution of telomeric RNA or telomeric DNA quadruplexes would be expected to activate telomerase for telomere elongation (Bryan and Baumann, 2010; Feuerhahn et al., 2010), with the prediction that disruption of the hTR binding site for DHX36 would result in telomere shortening.

Figure 1

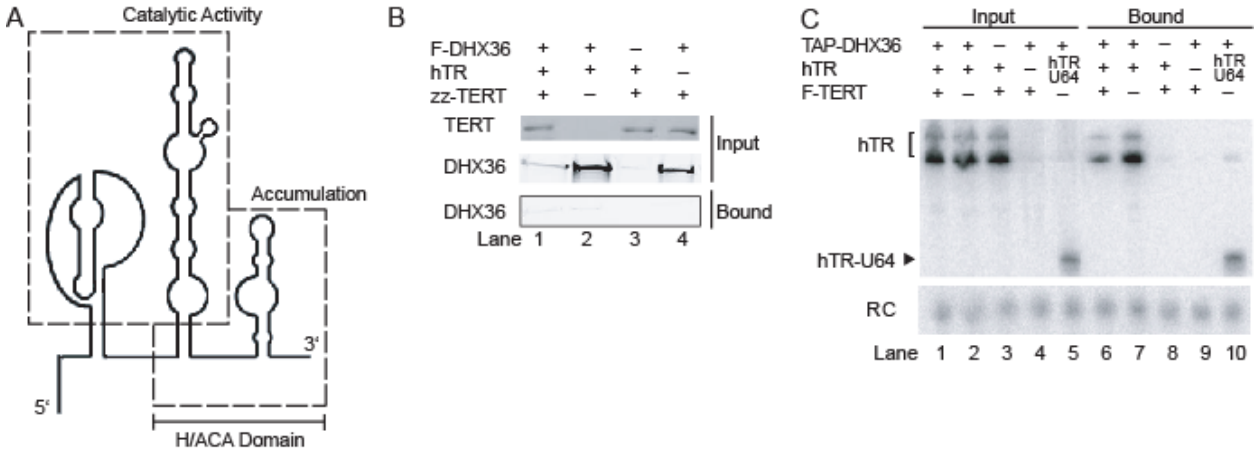

Figure 1: DHX36 associates with hTR independent of TERT. (A) Schematic of hTR structural domains and their roles. (B) Extracts from transfected 293T cells were enriched for zz-TERT using IgG agarose and assayed for DHX36 copurification by FLAG antibody immunoblot. (C) Extracts from transfected 293T cells were enriched for TAP-DHX36 using IgG agarose and assayed for hTR copurification by blot hybridization. RC is the recovery control. Note that lane 6 bound hTR is less than lane 7 bound hTR due to a reproducibly lower level of DHX36 accumulation when it was coexpressed with TERT, as evident in (B).

Figure 2

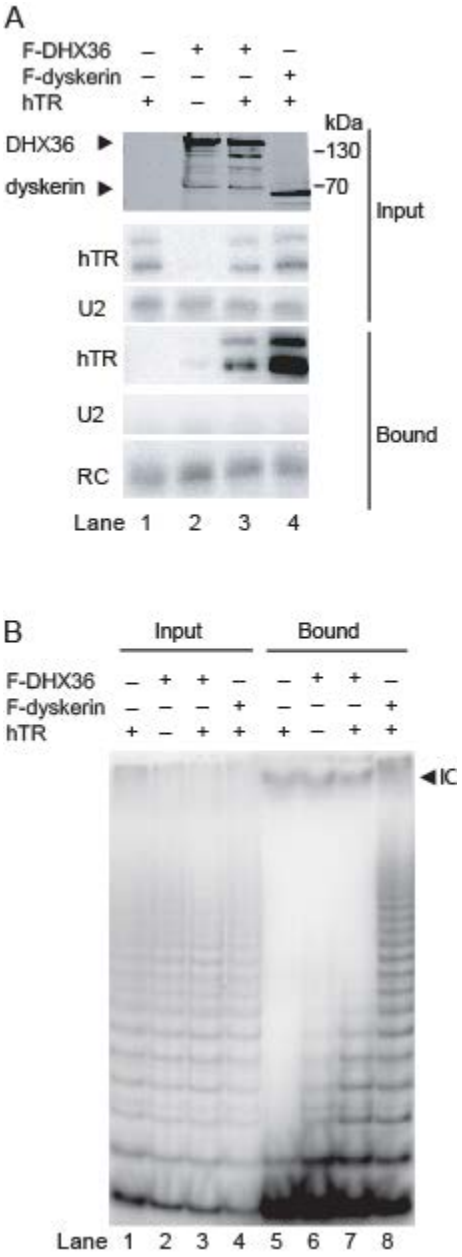

Figure 2: DHX36 copurifies predominantly an inactive telomerase RNP population. (A) Extracts from transfected 293T cells were used to detect F-tagged protein inputs. Input and bound samples were used to detect hTR and the control U2 small nuclear RNA by blot hybridization. (B) TRAP assays of cell extract representing 0.1% of each input sample or 50% of each FLAG-antibody purified sample. IC is a TRAP assay competitive internal control.

Figure 3

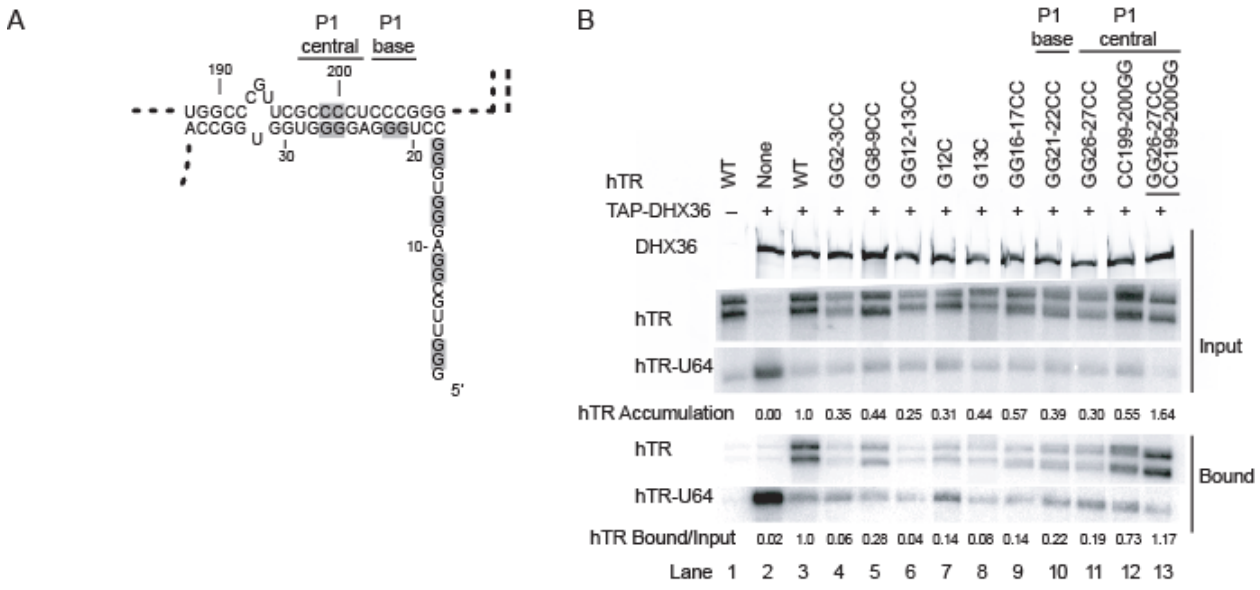

Figure 3: DHX36 binding to hTR requires several guanosine tracts at the RNA 5' end. (A) Schematic of hTR 5' leader and P1 sequence. Positions of sequence substitutions are shaded. (B) Extracts from 293T cells transfected to express TAP-DHX36, hTR-U64 and wild-type (WT) or variant hTR were enriched for DHX36 using IgG agarose and analyzed for hTR and hTR-U64 copurification by blot hybridization. Accumulation of hTR is normalized to the coexpressed hTR-U64, and Bound/Input is bound hTR normalized to input hTR; all intensity values were first corrected for local background before normalization.

Figure 4

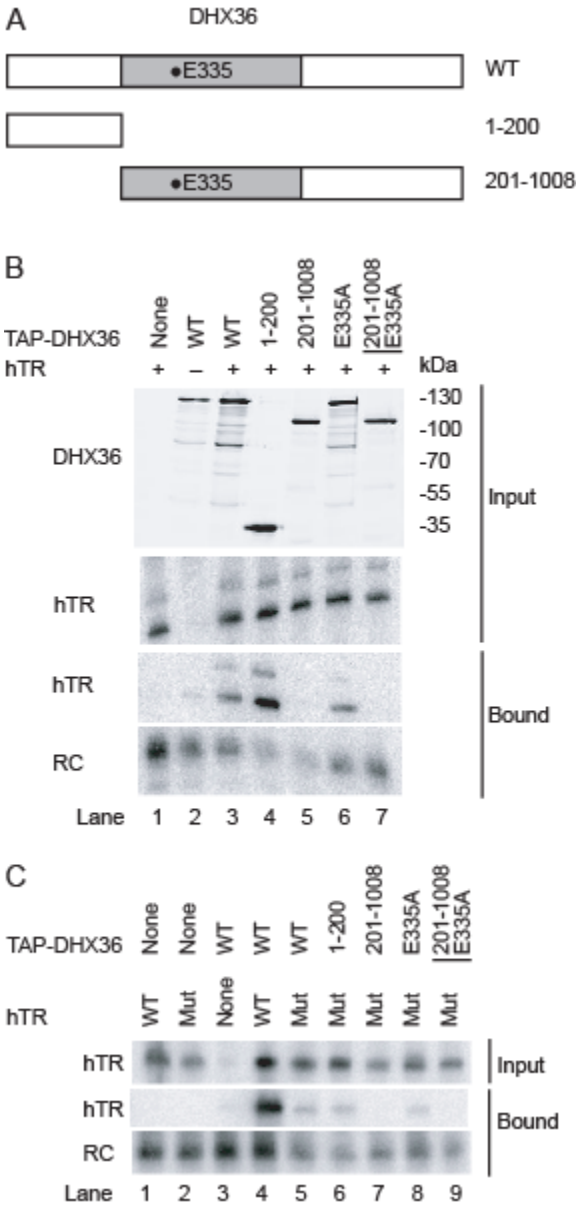

Figure 4: The N-terminal domain of DHX36 is necessary and sufficient for sequence-specific association with hTR. (A) Schematic of DHX36 protein domain expression. The helicase-motif region is shaded and the position of the E335 substitution that abrogates catalytic activity is indicated. (B, C) Extracts from transfected 293T cells expressing recombinant wild-type (WT) or G12C (Mut) hTR and full-length, truncated and/or substituted TAP-DHX36 were enriched using IgG agarose and analyzed for hTR copurification by blot hybridization.

Figure 5

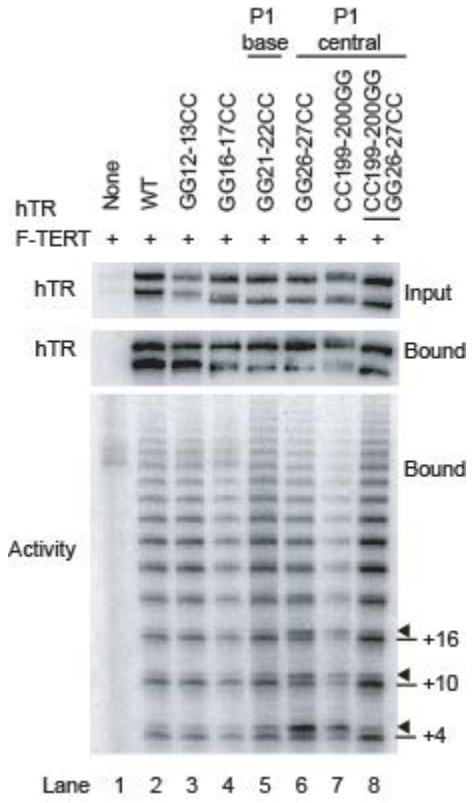

Figure 5: Variants of hTR with a disrupted G-tract motif and loss of DHX36 association retain TERT association and support telomerase holoenzyme catalytic activity. Extracts from transfected 293T cells were enriched for F-TERT and assayed for copurification of hTR by blot hybridization. Purified telomerase holoenzymes were then assayed for telomerase activity by direct extension of the telomeric-repeat primer $(T_2AG_3)_3$, with products resolved by denaturing gel electrophoresis. The predominant products from complete repeat synthesis are indicated by the number of nucleotides added to the primer (+4, +10, +16), while products one nucleotide longer due to template boundary bypass synthesis are indicated with a filled arrowhead.

Figure 6

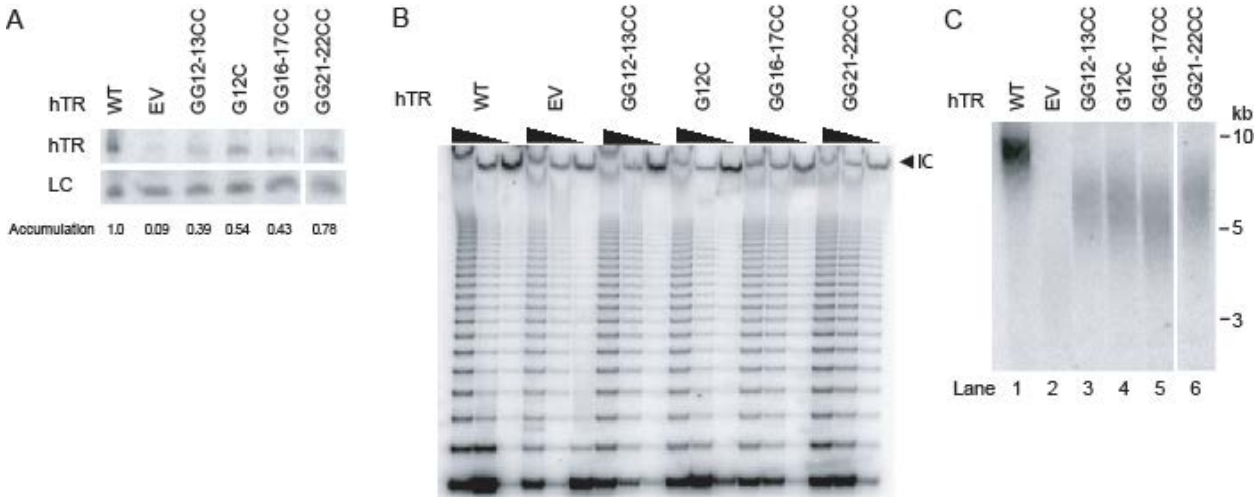

Figure 6: Substitutions in the 5' guanosine tracts reduce hTR steady-state accumulation and telomere maintenance in 1774TERT fibroblast cell lines. Note that adjacent panels were cropped from the same blot exposure. (A) Total RNA extracted from 1774TERT cell lines expressing the indicated form of recombinant hTR (WT indicates wild-type, EV indicates empty vector) was used to detect hTR by blot hybridization. A cross-reacting RNA provides the loading control (LC) used to normalize relative hTR accumulation. (B) TRAP assay detection of telomerase activity from cell extracts using 2 µg total protein and sequential 1:3 dilutions. (C) In-gel hybridization of telomeric restriction fragments was used to compare telomere lengths. Note that adjacent panels were cropped from the same blot exposure. Analysis of multiple time points of culture growth (not shown) confirmed that these telomere lengths are stably maintained in telomere length homeostasis.

Figure 7

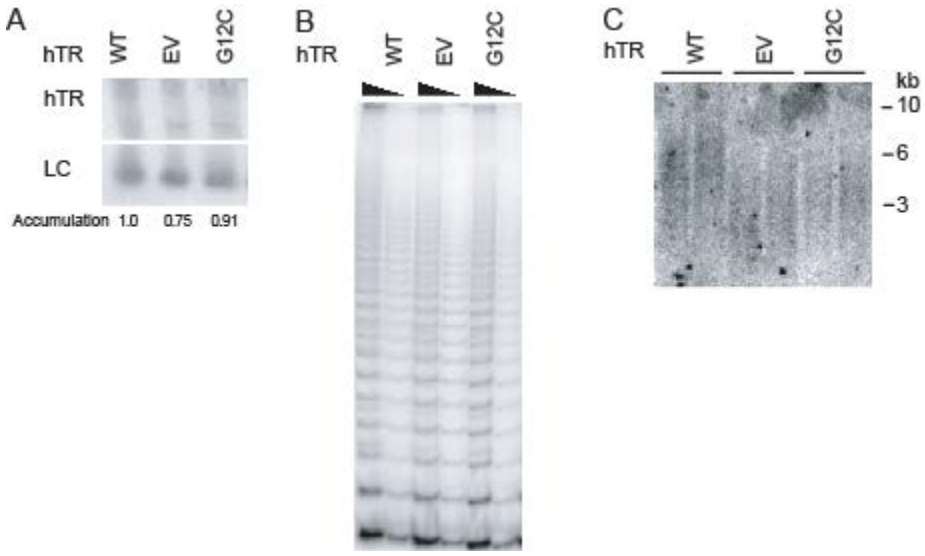

Figure 7: Substitution G12C reduces hTR steady-state accumulation and telomere maintenance in HT-1080 cells. (A) Total RNA extracted from HT-1080 cell lines expressing the indicated form of recombinant hTR was used to detect hTR and the loading control by blot hybridization. (B) TRAP assay detection of telomerase activity from whole cell extracts using 1 µg total protein and a 1:10 dilution. (C) In-gel hybridization of telomeric restriction fragments was used to compare telomere lengths. Duplicate lanes are independent loadings of the same genomic DNA digest. Analysis of multiple time points of culture growth (not shown) confirmed that these telomere lengths are stably maintained in telomere length homeostasis.

Figure 8

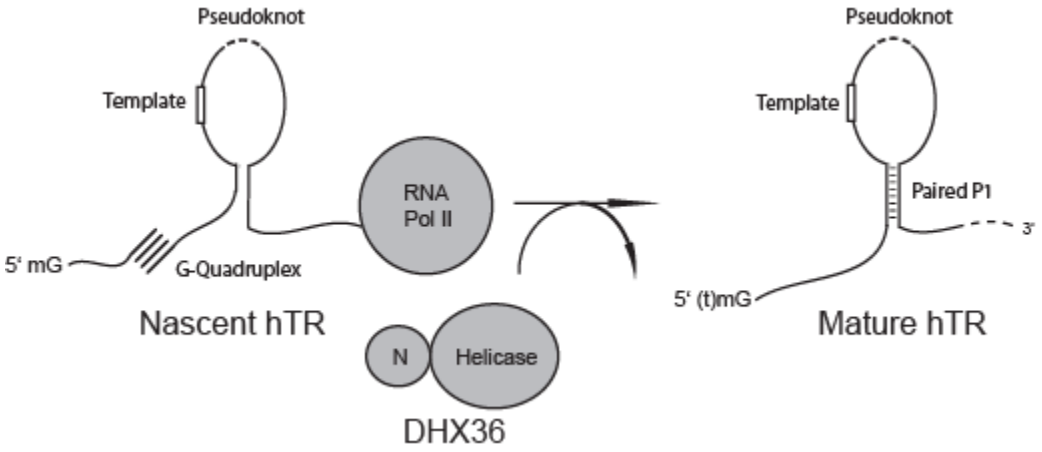

Figure 8: Model of proposed action of DHX36 on hTR biogenesis.

CHAPTER THREE

Specificity Requirements for Human Telomere Protein Interaction with Telomerase Holoenzyme

Based on Sexton et al., Journal of Biological Chemistry, 2012

Abstract

Human telomeres are maintained by the enzyme telomerase, which uses a template within its integral RNA subunit (hTR) and telomerase reverse transcriptase protein (TERT) to accomplish the synthesis of single-stranded DNA repeats. Many questions remain unresolved about the cellular regulation of telomerase subunits and the fully assembled telomerase holoenzyme, including the basis for the specificity of binding and acting on telomeres. Previous studies have revealed that the telomere protein TPP1 is necessary for stable TERT and hTR association with telomeres in vivo. Here, we expand the biochemical characterization and understanding of TPP1 interaction with TERT and the catalytically active telomerase holoenzyme. Using extracts from human cells, we show that TPP1 interacts sequence-specifically with TERT when TERT is assembled into holoenzyme context. In holoenzyme context, the TERT N-terminal (TEN) domain mediates a TPP1 interaction. Assays of stable subunit complexes purified after their cellular assembly suggest that other telomere proteins do not necessarily influence TPP1 association with telomerase holoenzyme or alter its impact on elongation processivity. We show that a domain of recombinant TPP1 comprised of an oligonucleotide/oligosaccharide binding (OB) fold recapitulates the full-length protein interaction specificity for the TERT TEN domain assembled into telomerase holoenzyme. By global analysis of TPP1 side-chain requirements for holoenzyme association, we demonstrate a selective requirement for the amino acids in one surface-exposed protein loop. Our results reveal the biochemical determinants of a sequence-specific TPP1-TERT interaction in human cells, with implications for the mechanisms of TPP1 function in recruiting telomerase subunits to telomeres and in promoting telomere elongation.

Introduction

The conventional DNA synthesis machinery incompletely copies linear chromosome ends. Therefore, genome integrity is dependent on a specialized mechanism of telomere maintenance. Most eukaryotes compensate for the replication-coupled loss of terminal telomeric repeats by *de novo* repeat synthesis (Blackburn et al., 2006). The ribonucleoprotein (RNP) telomerase accomplishes this addition by using single-stranded chromosome 3' ends as primers for reverse transcription of the RNA template (Collins, 2011). Importantly, as shown in many species including humans, telomere elongation by telomerase is restricted in the cell cycle. This regulation constrains the opportunity for DNA break repair by telomere addition; it also limits the extent of authentic telomere elongation, which may be critical for achieving a balanced telomere length homeostasis (Hug and Lingner, 2006; Stewart et al., 2012b).

Telomerase and its substrate telomeres have an unexpectedly elaborate subunit composition (Egan and Collins, 2012; Palm and de Lange, 2008). Current models suggest that the biologically active telomerase holoenzyme and the elongation-competent state of a telomere are both created only transiently, and thus they are scarce when considering a whole cell. In human cells, TERT and the 451 nucleotide (nt) mature hTR co-localize with each other and with telomeres intermittently and asynchronously (Jády et al., 2006; Tomlinson et al., 2006). Even stably assembled telomeric chromatin is in dynamic exchange at the level of individual subunits (Mattern et al., 2004). Telomere-specific proteins include two double-stranded DNA binding factors (TRF1 and TRF2) specific for the typically ~5-10 kbp of TTAGGG•CCCTAA repeats and one single-stranded DNA binding protein (POT1) associated with some or all of the ~50 nt guanosine-rich 3' single-stranded overhang (Palm and de Lange, 2008). Additional components of end-protective shelterin protein complexes include the TRF1/2-interacting protein TIN2 and the TIN2- and POT1-interacting protein TPP1 (Palm and de Lange, 2008).

Beyond regulating recombination and repair, shelterin proteins also regulate telomerase access to telomeres (Bianchi and Shore, 2008). TPP1 has been implicated as a mediator of telomerase recruitment, with a dependence on the TPP1 OB-fold (Abreu et al., 2010; Tejera et al., 2010). TPP1 is required for co-localization of hTR with telomeres, assayed by *in situ* hybridization, and for TERT association with telomeres, assayed by co-immunopurification (IP) of cross-linked chromatin. The telomerase subunit recruitment role of TPP1 in vivo depends on its interaction with TIN2 through the TPP1 TIN2 binding domain (TBD) and thus on a population of TPP1 tethered to double-stranded telomeric repeats (Abreu et al., 2010). Curiously, telomerase recruitment by TPP1 in vivo does not require POT1, which would tether TPP1 to single-stranded telomeric repeats (Abreu et al., 2010). The ability of TPP1 to bridge telomeres to telomerase is also supported by TPP1 co-IP of telomerase catalytic activity.

Human telomerase recruitment to telomeres is stimulated by hTR concentration in Cajal bodies (Cristofari et al., 2007a; Stern et al., 2012). However, Cajal body association is not required *per se* in cells with high telomerase expression levels (Fu and Collins, 2007; Stern et al., 2012; Zhao et al., 2011). Even with these important recent insights, the mechanisms remain

unknown that dictate the specificity of cellular stabilization of hTR RNP assembly with TERT and interaction of these subunits with a telomere. The co-dependence of hTR and TERT association with telomeres suggests that either telomeres nucleate holoenzyme assembly or that they greatly stabilize the preassembled holoenzyme.

In addition to physical recruitment of telomerase to telomeres, TPP1 could influence telomere-bound telomerase catalytic activity. For example, a conformation of telomerase holoenzyme favored by TPP1 binding could promote enzyme interaction with single-stranded DNA. Studies of the yeast TPP1 ortholog, Est3, are illuminating as precedent for this potential TPP1 function. Est3 interacts directly with yeast TERT (Est2), which can be recapitulated using recombinant Est3 and Est2 TEN domain (Talley et al., 2011; Yen et al., 2011). Est3 side-chain substitutions guided by modeling with the TPP1 OB-fold structure (20) have led to the definition of Est3 sequence requirements for Est2 interaction and telomerase catalytic activation in vitro and in vivo (Lee et al., 2008; Talley et al., 2011; Yu et al., 2008). The stimulation of Est2 RNP activity by Est3 addition in vitro (Lee et al., 2010; Talley et al., 2011) could result directly from stable binding, if Est3 binding to Est2 favors the active RNP conformation.

In activity assays of a minimal human telomerase RNP reconstituted from TERT and hTR in rabbit reticulocyte lysate (RRL), a complex of recombinant POT1 and a bacterially expressed N-terminal region of TPP1 containing the OB-fold domain (OBD) and the POT1 binding domain (PBD) increases repeat addition processivity (RAP) by slowing primer dissociation and increasing template translocation (Latrick and Cech, 2010; Wang et al., 2007; Zaug et al., 2010). The RAP-stimulatory influence of purified recombinant POT1-TPP1 complex is abrogated by a G100V substitution in the TERT TEN domain (Zaug et al., 2010). This glycine is within the human TERT N-terminal dissociation-of-activities (DAT) region implicated in the in vivo coupling of telomerase catalytic activity to telomere elongation (Armbruster et al., 2001). Recently, a single amino acid substitution in the human TERT TEN domain (R132D) was demonstrated to dramatically inhibit the stable telomere association of TERT and hTR (Stern et al., 2012).

Here we define the biochemical specificity of TPP1 interaction with TERT and the catalytically active telomerase holoenzyme using extracts from human cells. We find that TPP1-TERT association monitored by co-IP is largely not reflective of TPP1 association with functional RNP and is not dependent on the TEN domain. In contrast, TPP1 interaction with the catalytically active telomerase holoenzyme is strictly dependent on the TEN domain and is abrogated by the TERT G100V substitution. The interaction of TPP1 and telomerase holoenzyme is not dependent on TPP1 association with TIN2 or POT1, suggesting that it could occur in any shelterin context of TPP1 in vivo. We exploit a bacterially expressed TPP1 OBD, as well as the OBD or full-length TPP1 expressed in human cells, to define the surface side-chains of TPP1 required for binding to telomerase holoenzyme. TPP1 association with the catalytically active telomerase holoenzyme was exquisitely sensitive to disruption of one TPP1 surface loop. Remarkably, this region of the TPP1 OBD is analogous to the loop in yeast Est3 that mediates its interaction with Est2 and the stimulation of Est2 RNP catalytic activity (Lee et al., 2008; Talley

et al., 2011). Our findings suggest that TPP1 and Est3 provide a conserved surface for assembly of telomere-bound telomerase holoenzyme.

Materials and Methods

Protein expression.

Full-length TPP1 includes amino acids 88-544 of the GenBank sequence NM_001082486.1. The OBD included amino acids 88-249. Deletion of the TPP1 PBD removed amino acids 250-334, while deletion of the TBD removed amino acids 335-544. Expression constructs for full-length TERT, TEN domain (amino acids 1-325), and TERT core (amino acid 326 to the protein C-terminus) have been previously described (Robart and Collins, 2011). Expression constructs for other proteins used the same pcDNA3.1 vector backbone. All tags were N-terminal fusions. For all experiments other than the protein-protein interaction assays shown in Fig. 1, hTR was co-over-expressed in the transfected 293T cells using pBS-U3-hTR-500 (Fu and Collins, 2003). Bacterial expression of the TPP1 OBD used the pACYC vector backbone.

Protein purification.

Transfected 293T cell extracts were made by freeze-thaw lysis (Robart and Collins, 2011). IPs from human cell extract were done with lysate adjusted to 150 mM NaCl in binding buffer (BB) containing 10 mM HEPES pH 7.5, 150 mM NaCl, 10% glycerol, and 0.1% NP-40. When indicated, complexes bound to FLAG M2 antibody resin (Sigma) were eluted in BB containing 150 ng/µl triple FLAG peptide (Sigma).

Bacterially expressed six-histidine tagged (6xHis) TPP1 OBD was purified using Ni-NTA agarose (Qiagen). Cell lysis buffer (LB) contained 50 mM Tris-HCl pH 8.0, 50 mM NaH_2PO_4, 400 mM NaCl, 10% glycerol, and 10 mM imidazole supplemented with 0.1 mg/ml lysozyme, 0.1 mM phenylmethanesulfonylfluoride, and 2 mM beta-mercaptoethanol. After protein binding for 2 h at 4°C, Ni-NTA resin was washed in LB adjusted to 600 mM NaCl and then eluted in LB with 150 mM NaCl and 300 mM imidazole. Purified protein was rebound to Ni-NTA resin in LB with 150 mM NaCl and 1 mM DTT. SDS-PAGE analysis verified that the vast majority of purified TPP1 OBD re-bound to Ni-NTA resin. After washing, the resin-immobilized TPP1 OBD was incubated with transfected 293T cell extract containing over-expressed f-TERT and hTR for 1 h at 4°C and then washed with LB adjusted to 150 mM NaCl and 1 mM DTT.

Detection of protein, RNA, and telomerase catalytic activity.

Immunoblots were done to detect the protein tags using rabbit IgG (Sigma), FLAG M2 antibody (Sigma), and anti-myc peptide antibody (Santa Cruz Biotechnology). Equivalency of tagged protein and hTR expression levels was verified across extracts (data not shown). Northern blots detected hTR with an oligonucleotide probe complementary to hTR nts 51-72, which also detects the recombinant hTR fragment added to samples prior to RNA extraction and precipitation as a recovery control (RC). The Bound/Input hTR ratio was calculated by subtracting general blot background from each Input and Bound quantified intensity, adjusting these values for the RC to control for any variation in RNA gel loading, dividing Bound by Input, and normalizing to a Bound/Input ratio of 1 for the relevant wild-type sample.

Direct primer extension assays were performed as previously described (Robart and Collins, 2011), using the primer $(T_2AG_3)_3$ and radiolabeled dGTP. Reactions shown were stopped after 1 h. A 5'-end-labeled 12 nt single-stranded DNA was added to the precipitation mix as a loading control (LC). RAP quantification was carried out as previously described (Latrick and Cech, 2010), followed by normalization across samples. Relative specific activity was determined by normalizing the total product intensity from an entire gel lane to the intensity of the loading control (LC), followed by normalization across samples.

Results

TPP1 interactions with TERT.

We began by adapting a previously developed TERT *trans* complementation system (Robart and Collins, 2011) to investigate whether physical association of TPP1 and TERT is mediated through the TERT TEN domain. For human TERT domains expressed by transient transfection of human 293T cells, a TERT core region lacking the TEN domain can assemble with hTR RNP to produce an enzyme active for single-repeat synthesis. If the TEN domain is expressed as a polypeptide separate from the TERT core, it functions in *trans* with the TERT core RNP to trap single-stranded DNA substrate and also confer elongation RAP. This functional *trans* complementation requires a productive docking conformation of the TEN domain on the TERT core RNP (Robart and Collins, 2011).

To address the specificity of TPP1 interaction with TERT, we assayed TPP1 interaction with full-length TERT versus the separate TERT core and TEN domain. FLAG (f)-tagged TPP1 co-expressed with tandem Protein A domain (zz)-tagged TERT was enriched by binding to FLAG antibody resin, followed by peptide elution to eliminate any non-specific zz-TERT background (Fig. 1*A*, lane 1). Co-purification of zz-TERT with f-TPP1 was detected by immunoblot (Fig. 1*A*, lane 2). In addition to wild-type sequence, we tested full-length TERT and TEN domain polypeptides containing either the G100V substitution that abrogates recombinant TPP1-POT1 stimulation of RAP (Zaug et al., 2010) or a six amino acid substitution of residues 92-97 (NDAT) that prevents telomerase holoenzyme from maintaining telomere length (Armbruster et al., 2001). Apparently specific co-IP by TPP1 was detected for all three full-length TERTs: wild-type, G100V, and NDAT (Fig. 1*A*, lanes 1-6). Unexpectedly, f-TPP1 also enriched the autonomous TEN domain independent of its sequence substitutions (Fig. 1*A*, lanes 7-12).

The results above suggested that TPP1 co-IP of TERT could reflect associations at multiple sites of interaction. TPP1 is a multi-domain protein with structurally independent surfaces for telomerase holoenzyme association (the OBD), binding to POT1 (the PBD), and binding to TIN2 (the TBD) from the protein N-terminus to C-terminus (Palm and de Lange, 2008). Therefore, some of the TERT-TPP1 interaction detected by co-IP could be indirect, for example requiring TIN2 (Yang et al., 2011). To examine the dependence of TPP1 co-IP of TERT on shelterin subunit associations, we compared TERT co-IP by full-length TPP1, a TPP1 internal domain deletion that eliminates POT1 binding (ΔPBD), or a TPP1 C-terminal truncation that eliminates TIN2 binding (ΔTBD). Co-expressed zz-TERT was clearly enriched by all of the f-TPP1 polypeptides, with no background binding of zz-TERT from a cell extract lacking f-tagged TPP1 (Fig. 1*B*, lanes 1-4). Surprisingly, the TERT core and independent TEN domain were both enriched by each of the f-tagged TPP1 polypeptides (Fig. 1*B*, lanes 5-12). These results indicate that TPP1 interactions with TERT detected by co-IP are not dependent on a specific TERT domain or on TPP1 association with other shelterin subunits. We note that the f-tagged TPP1 OBD alone did not co-IP a level of co-expressed zz-tagged TERT, TERT core, or TEN domain

that was readily detectable by immunoblot (data not shown), despite its association with telomerase holoenzyme (see below).

TPP1 interaction with telomerase holoenzyme.

Given the domain-unspecific associations of TPP1 and TERT detected by protein-protein interaction, despite using what should be physiologically folded proteins in human cell extracts, we next asked whether there was more specificity of TPP1 interaction with the catalytically functional telomerase holoenzyme. By the direct telomeric primer extension assay, we found that telomerase holoenzyme was co-enriched by f-TPP1 from cell extracts with over-expressed zz-TERT and hTR but not from control extracts lacking either the f-tagged TPP1 or over-expressed telomerase holoenzyme (Fig 2*A*, lanes 1-3). In contrast to the TERT immunoblot results, telomerase holoenzyme co-IP with TPP1 was dramatically reduced by the TEN domain G100V substitution (Fig. 2*A*, lane 4). As a control, we tested a TEN domain Y176A substitution that reduced RRL-reconstituted RNP catalytic activity to a similar extent as the G100V substitution but preserved the stimulation of RAP by recombinant TPP1-POT1 complex (24). The Y176A TERT holoenzyme did co-IP with f-TPP1 as expected (Fig. 2*A*, lane 5), establishing the specificity of disruption by the G100V substitution.

We verified that the TERT G100V substitution did not disrupt in vivo telomerase holoenzyme assembly, as monitored by primer extension activity of f-tagged wild-type or G100V TERT co-expressed with hTR (Fig. 2*A*, lanes 6-7). The f-tagged G100V TERT purification recovered less holoenzyme activity than wild-type TERT, consistent with activity assays of the RRL-reconstituted enzyme (Zaug et al., 2010). Northern blot detection of hTR demonstrated that purification of f-tagged G100V TERT co-enriched hTR comparably to wild-type TERT, in the presence or absence of co-expressed TPP1 (Fig. 2*B*, lanes 2-5). Thus, the holoenzyme assembled by human cell expression of G100V TERT is compromised in the specific activity of primer elongation. A small difference in hTR co-IP with wild-type versus G100V TERT was detected in some experiments, perhaps due to a reduced stability of the G100V TERT holoenzyme in cell extract.

Because the G100V TERT substitution affects RNP catalytic activity, we used Northern blot detection of hTR as the readout for quantification of telomerase holoenzyme association with TPP1. Although f-TPP1 co-IP of zz-TERT was unaffected by the G100V substitution (Fig. 2*C*, immunoblot panels), the G100V substitution dramatically reduced f-TPP1 co-IP of hTR (Fig. 2*C*, Northern blot panels). This reduction was specific for the G100V substitution, because the Y176A substitution had only a slight impact on TPP1 co-IP of hTR (Fig. 2*C*, compare lanes 3-5), perhaps due to reduced stability of the Y176A TERT holoenzyme in cell extract.

To directly establish the TERT TEN domain contribution to telomerase holoenzyme association with TPP1, without altering TEN domain sequence, we used the TERT domain *trans* complementation system. Co-expression of f-TPP1 with full-length TERT and hTR allowed robust detection of hTR co-IP with f-TPP1 (Fig. 2*D*, lane 1). Co-expression of f-TPP1, TERT core, and hTR did not allow a similarly high level of hTR co-IP with TPP1 unless the TEN domain was also co-expressed (Fig. 2*D*, lanes 2 and 4). No background binding of hTR RNP to

FLAG antibody resin was detected (Fig. 2*D*, lane 3). We conclude that TPP1 physical association with telomerase holoenzyme is strongly influenced by the presence of the TERT TEN domain. We note that the side-chain of G100 is not proven to be part of the direct site of TPP1 binding; instead, for example, the G100V disruption could affect TEN domain docking on the TERT core RNP, which in turn could affect TEN domain interaction with TPP1.

Shelterin subunit requirements for TPP1 association with telomerase holoenzyme.

To investigate whether TPP1 association with telomerase holoenzyme is biochemically coupled to its assembly into shelterin complexes, we compared holoenzyme activity co-IP by f-TERT, f-TPP1, f-TIN2, and f-POT1. Additionally we tested holoenzyme activity co-IP by the f-tagged TPP1 OBD alone, which supports TPP1 interaction with telomerase holoenzyme but removes the TPP1 domains necessary for its associations with TIN2 and POT1. Extracts were prepared from cells that co-expressed hTR, TERT, and one or more shelterin subunits (Fig. 3*A*). Consistent with the expected TPP1-bridged interaction between shelterin and telomerase, the co-IP of telomerase activity with f-TIN2 or f-POT1 was greatly increased by co-expression of myc (m)-tagged TPP1 (data not shown).

The relative specific activity of purified f-tagged telomerase holoenzyme complexes was calculated from the ratio of telomerase product intensity to hTR. The f-TERT co-IP of telomerase activity enriched a slightly higher specific activity of telomerase holoenzyme than was obtained by co-IP of zz-tagged TERT with f-TPP1 (Fig. 3*B*, lanes 1-2). This difference could derive entirely or in part from the difference in TERT tagging. However, all zz-TERT complexes purified by f-TPP1, f-TIN2, f-POT1, or f-TPP1 OBD had similar specificity activity (Fig. 3*B*, lanes 2-5). Furthermore, the purified complexes showed similar RAP, as quantified from individual product DNAs within the first ~100 nt added (the quantified region is indicated by the bracket at right in Fig. 3*B*), which was reproducible in independent experiments (data not shown). Based on our assays of telomerase holoenzyme complexes purified before the activity assay, we conclude that TPP1 association does not necessarily stimulate the increase in RAP that is conferred by addition of recombinant POT1-TPP1 complexes to RRL-reconstituted human telomerase RNP or human cell extract (Latrick and Cech, 2010; Wang et al., 2007; Zaug et al., 2010). We note that in vitro RAP can vary significantly depending on the assay conditions, and thus present and previous results could differ due to any of numerous variables in the assays.

A TPP1 sequence requirement for interaction with telomerase holoenzyme.

To establish a biochemically specific assay for TPP1 OBD association with telomerase holoenzyme, we sought conditions under which the catalytically active telomerase holoenzyme would interact with the TPP1 OBD but not other OBDs. Purified recombinant TPP1 OBD was immobilized on Ni-NTA agarose and then assessed for its ability to recruit telomerase holoenzyme from an extract of cells with over-expressed f-TERT and hTR. A low background level of holoenzyme association was detected with control Ni-NTA agarose lacking any bound protein (Fig. 4*A*, lane 1), and therefore this background was monitored in every experiment. With

specificity, telomerase holoenzyme was enriched by the TPP1 OBD (Fig. 4*A*, lanes 2-3) and not by the N-terminal or C-terminal OBD of the *Tetrahymena* telomerase subunit Teb1 (Fig. 4*A*, lanes 4-7)(Min and Collins, 2009).

We also established the interaction specificity of recombinant TPP1 OBD by comparing its ability to co-purify the catalytically active wild-type telomerase holoenzyme versus telomerase holoenzyme with the TERT G100V substitution. Because the G100V TERT holoenzyme has less activity than the wild-type holoenzyme, it was necessary to compare their binding to the TPP1 OBD by comparing catalytic activity enrichment. Therefore, we first purified holoenzyme from extracts of cells over-expressing hTR and f-tagged wild-type or G100V TERT. Holoenzyme containing G100V TERT had relatively less catalytic activity, as expected (Fig. 4*B*, lanes 1-2). The TPP1 OBD enriched wild-type TERT holoenzyme, with bound activity comparable to 10% of the total binding input (Fig. 4*B*, lanes 3-4). In contrast, the TPP1 OBD did not associate with any of the G100V TERT holoenzyme (Fig. 4*B*, lanes 5-6).

We undertook a broad scope of TPP1 OBD mutagenesis to define the sequence specificity of TPP1 OBD association with telomerase holoenzyme. Side chains from numerous surfaces of the TPP1 OBD structure (Wang et al., 2007) were individually substituted to alanine, except for the K233 side chain of ubiquitin conjugation (Rai et al., 2011) that was tested as a substitution to arginine. Each sequence variant of the TPP1 OBD was bacterially expressed and purified. Holoenzyme recruitment from cell extract was then assayed for the wild-type and 41 variant TPP1 OBDs (Fig. 4*C*). This approach revealed that TPP1 OBD interaction with the catalytically active telomerase holoenzyme is selectively dependent on a cluster of side chains spanning amino acids 167 to 172 (bracketed in Fig. 4*C*), which occur in a protein loop (see below for a TPP1 OBD surface representation).

We confirmed this specificity of TPP1 OBD interaction with telomerase holoenzyme by assaying co-IP of enzyme catalytic activity with f-TPP1 OBD variants expressed in human cells (Fig. 5). Individual substitutions of the side chains of W167 through F172 strongly disrupted holoenzyme co-IP, and two additional side-chain substitutions nearby in the domain fold (L183A and E215A) had an intermediate effect (Fig. 5*A*, indicated by the bracket and asterisks). None of the other side-chain substitutions imposed a substantial or reproducible inhibition (Fig. 5*B*).

Finally, we used full-length TPP1 to examine the significance of the TPP1 OBD side chains implicated in holoenzyme interaction. Full-length f-tagged TPP1 with the wild-type sequence or an OBD side-chain substitution was co-expressed in cells with zz-TERT and hTR. Substitutions of the TPP1 OBD from W167 to F172 did not uniformly reduce TERT co-IP (Fig. 6*A*), but all of these substitutions did drastically reduce the co-IP of holoenzyme catalytic activity (Fig. 6*B*). As a control for the specificity of the loss of active telomerase holoenzyme interaction, we verified that none of the TPP1 OBD sequence substitutions compromised the f-TPP1 co-IP of TIN2 or POT1 (data not shown). These results pinpoint a surface of the TPP1 OBD that mediates the association of TPP1-containing shelterin complexes with the catalytically active telomerase holoenzyme (Fig. 6*C*).

Discussion

We set out to understand a potentially synergistic set of interactions that bridge telomerase subunits to shelterin subunits. In the physiological context of telomerase recruitment to telomeres in vivo, it seemed likely that multiple, perhaps sequentially reinforcing subunit interactions would have evolved to overcome the biochemical challenge inherent in the scarcity of both telomerase and chromosome ends. This challenge is particularly evident when considering the telomerase substrate requirement for 3'-terminal hydroxyl groups, which have an even lower abundance than telomeric repeats in general. Our results suggest the possibility of multiple TPP1-TERT interaction interfaces distributed between the TERT core and TEN domain. These interactions do not require TERT assembly into the catalytically active telomerase holoenzyme, so they could mediate TERT recruitment to telomeres prior to the biologically regulated association of TERT with hTR. However, we note that it is not established whether all of the TPP1-TERT interactions assayed by TERT co-IP with TPP1 are important for telomere elongation.

Unlike TPP1 co-IP of TERT protein alone, we could define a structural specificity of TPP1 co-IP of a catalytically active telomerase holoenzyme. Because the TEN domain of TERT alone did not have the high specificity of TPP1 interaction evident for the TEN domain in holoenzyme context, the TEN domain dependent TPP1 OBD interface for association with catalytically active telomerase may be highly sensitive to TEN domain conformation. The G100 region of the TEN domain is an excellent candidate surface for binding to the TPP1 OBD, but a direct physical method such as cross-linking will be required to conclusively establish the site of protein-protein contact. Beyond G100 itself, the surrounding N-terminal DAT region of the TEN domain is important for telomerase function in telomere elongation (Armbruster et al., 2001; Stern et al., 2012). It seems plausible that human TERT DAT sequence substitutions affect holoenzyme specific activity and telomere association through the same perturbations of TEN domain surfaces and/or overall conformation (Armbruster et al., 2003; Lee et al., 2003).

We had anticipated that mutually exclusive TPP1-TERT and TPP1-POT1 interactions would present an opportunity to confer the strict regulation of human telomeric DNA synthesis per telomere (Zhao et al., 2009, 2011). However, at a biochemical level, we find that the ability of TPP1 to associate with telomerase holoenzyme is not excluded by and is not dependent on TPP1-POT1 or TPP1-TIN2 interaction. This is evident from co-IP of telomerase holoenzyme activity with TPP1, POT1, or TIN2 and from holoenzyme activity co-IP with the TPP1 OBD alone. These observations raise the question of how telomerase holoenzyme interaction with TPP1 in vivo is sensitized to involve the telomere-bound, shelterin-assembled TPP1. Low endogenous levels of TPP1 may be critical for this specificity (Takai et al., 2010).

Extensive mutagenesis suggests that one loop of TPP1, including amino acids 167 to 172, is essential for TPP1 association with the catalytically active telomerase holoenzyme. Est3 amino acid substitutions in this loop of the OB-fold preclude Est2 binding and also Est3 stimulation of Est2 RNP catalytic activity (Lee et al., 2008; Talley et al., 2011). Stimulation of catalytic activity

could result from an Est3 binding specificity for the catalytically active Est2 conformation. The conservation of an interaction interface between Est3/TPP1 and holoenzyme-assembled TERT is striking given the divergence of human and yeast telomerases overall (Egan and Collins, 2012). It is possible that the TPP1 OBD interacts with DNA in addition to TERT, as suggested for Est3 proteins from certain yeasts (Yen et al., 2011), perhaps dependent on an elongation-specific holoenzyme conformation.

Figure 1

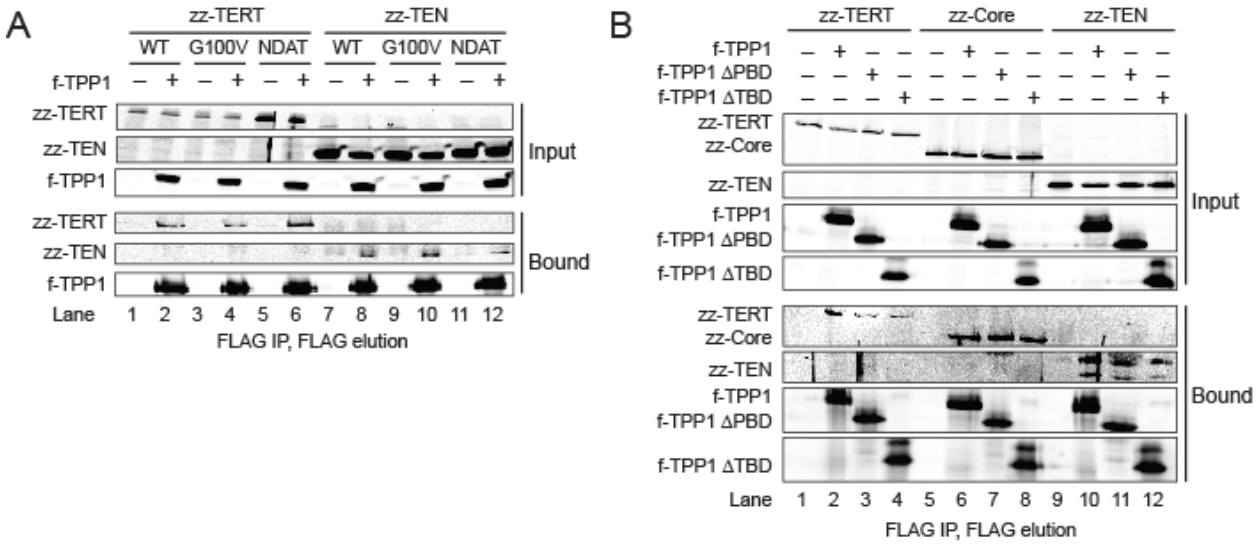

Figure 1: Domain interactions of TERT and TPP1. *A*, Immunoblot detection of f-TPP1 co-IP of zz-tagged full-length TERT or zz-TEN domain (TERT amino acids 1-325), each with wild-type (WT), G100V, or NDAT (92-97 NAAIRS) sequence. *B*, Immunoblot detection of zz-TERT, zz-Core (TERT lacking amino acids 1-325), or zz-TEN domain following IP of full-length f-TPP1 or f-TPP1 variants lacking the domain for TIN2 bidning (ΔTBD) or POT1 binding (ΔPBD).

Figure 2

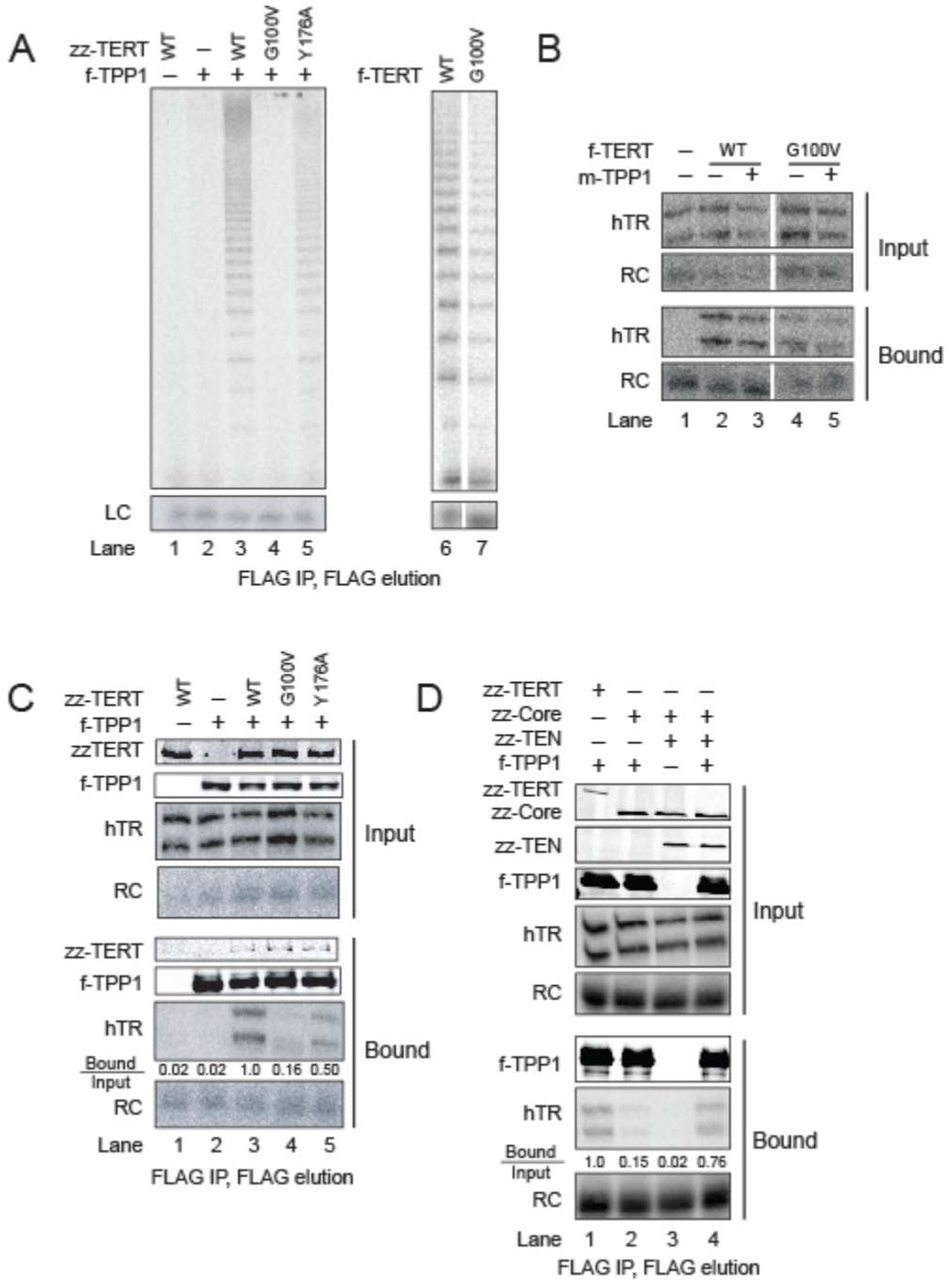

Figure 2: TEN-domain dependence of TPP1 association with telomerase holoenzyme. *A,* Telomerase catalytic activity associated with f-TPP1 from cells co-expressing hTR and the indicated zz-tagged TERT (lanes 1-5) or activity associated with the indicated f-tagged TERT co-expressed with hTR alone (lanes 6-7). Lanes 6 and 7 were cropped from the same exposure of the same gel. *B*, Northern blot detection of co-expressed hTR co-IPed with the indicated f-TERT in the presence or absence of co-expressed myc-tagged (m) TPP1. A

recombinant RNA recovery control (RC) was added to antibody resin before hTR extraction and is detected with the same end-labeled probe. All lanes were cropped from the same exposure of the same blot. *C*, Immunoblot and Northern blot detection of f-TPP1 co-IP of co-expressed zz-TERT and hTR. The Bound/Input ratio of hTR hybridization signal was calculated after normalization for the RNA RC (see Experimental Procedures). *D*, Immunoblot and Northern blot detection of f-TPP1 co-IP of co-expressed zz-tagged full-length or domain-truncated TERTs and hTR.

Figure 3

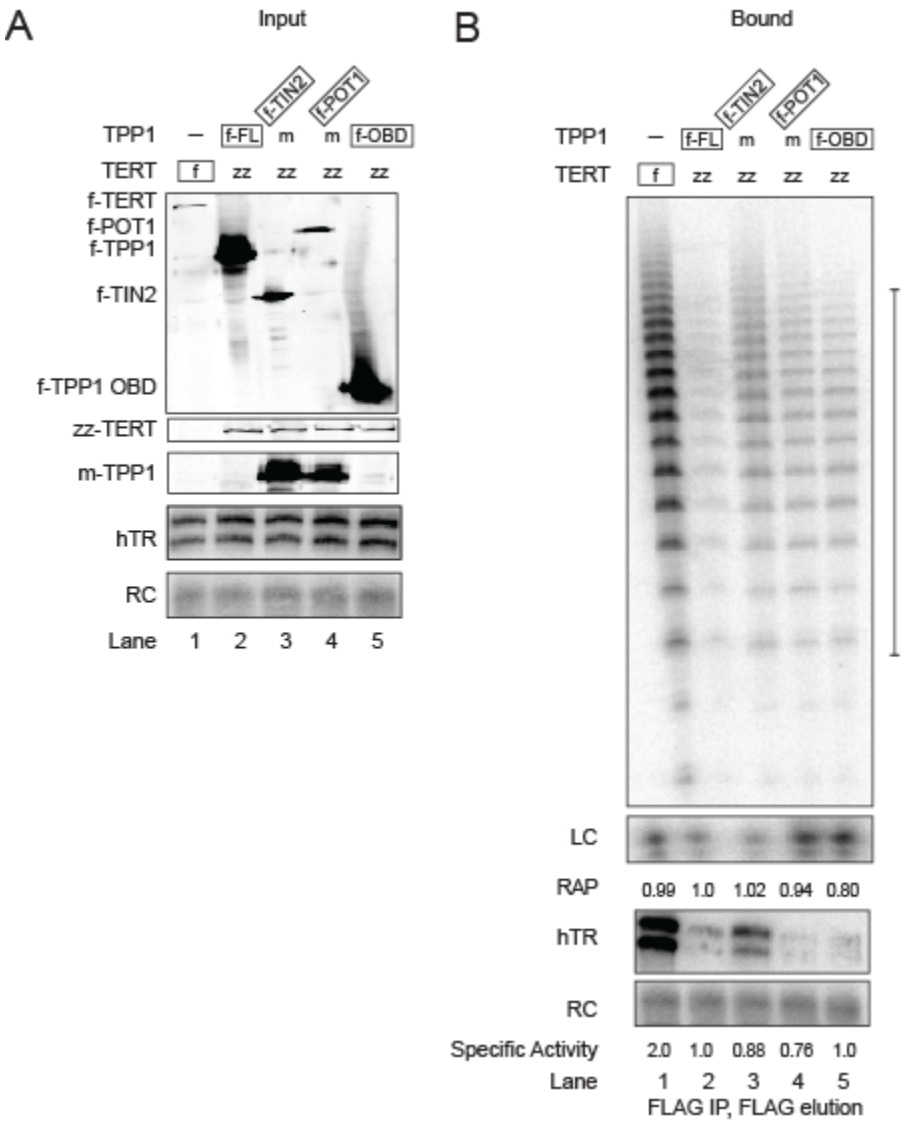

Figure 3: Influence of telomere-protein subcomplexes and domains on holoenyzyme RAP. ***A,*** Telomerase catalytic activity associated with complexes of the indicated f-tagged protein (TERT, TPP1, TIN2, or POT1) or f-tagged TPP1 domain variant (ΔPBD, ΔTBD, or OBD alone). Cells co-expressed hTR and untagged (ut) or zz-tagged TERT and/or myc-tagged TPP1 as indicated; the f-tagged subunit bound directly to antibody resin is boxed. Cell extract with no f-tagged protein was used in parallel to verify the reproducible absence of non-specific activity association with the antibody resin (data not shown). The bracket at right of the gel indicates the product DNAs used to calculate RAP; RAP values for the activity in each gel lane are shown in the bar graph below. *B*, Recombinant proteins at the indicated final concentrations were added directly to activity assays of f-TERT holoenyzme purified from cells co-over-expressing hTR. Activity assayed in lanes 1, 4, 7, and 10 was the buffer-only control for 6xHis-tagged TPP1 OBD, 6xHis-tagged Teb1 N-terminal OBD, BSA, or heat-killed BSA.

Figure 4

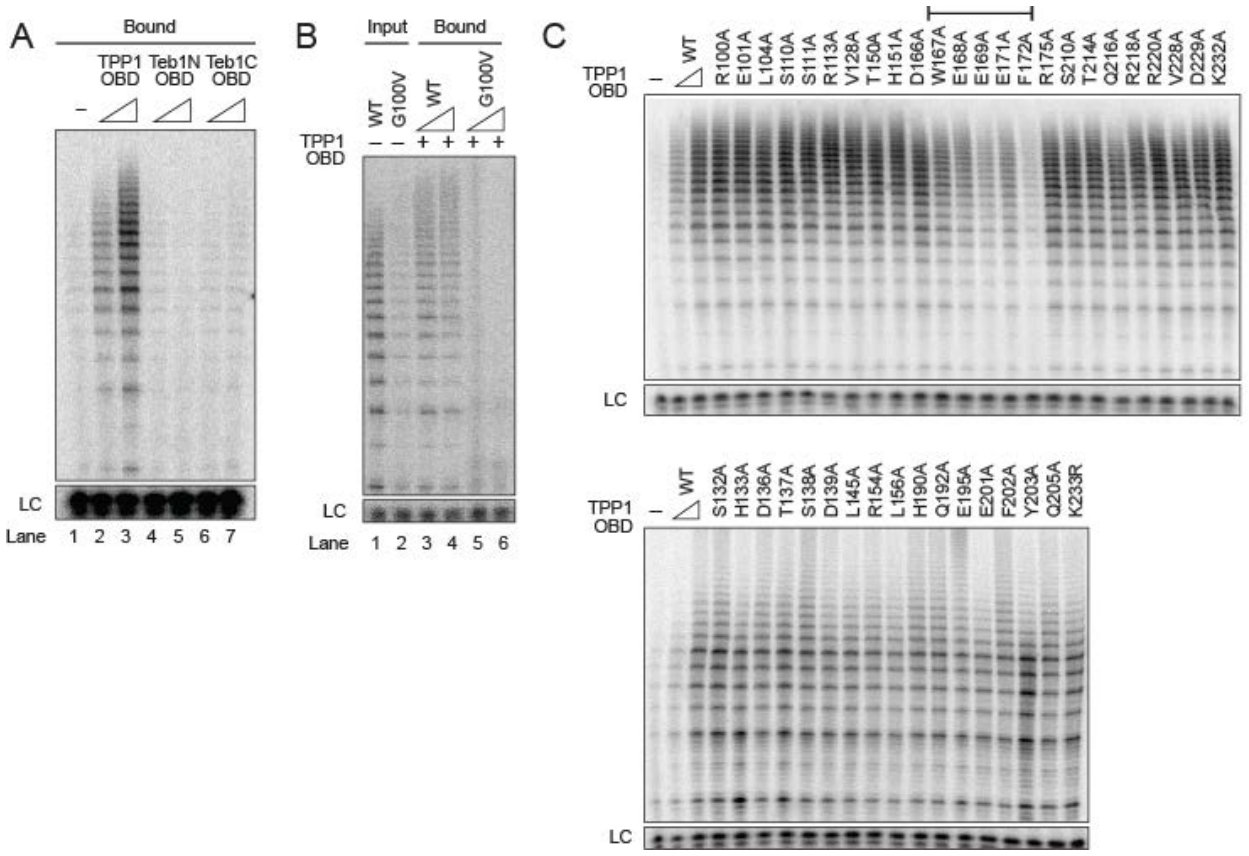

Figure 4: Identification of a TPP1 OBD surface required for holoenzyme interaction. *A,* Extract from cells co-expressing hTR and either WT or G100V f-tagged TERT were used for binding to Ni-NTA agarose with bacterially expressed TPP1 OBD (rTPP1 OBD). Either 100 pmole or 1 nmole of rTPP1 OBD was pre-bound to the resin and activity was assayed directly on resin without elution (lanes 3-6). Activity assays of the extract inputs (lanes 1-2) used 10% of the amount allowed to bind to rTTP1 OBD resin. *B*, Extract from cells co-expressing hTR and f-tagged TERT was used for holoenzyme binding to Ni-NTA agarose with 6xHis-tagged TPP1 OBD or the 6xHis-tagged N-terminal or C-terminal OBD of *Tetrahymena* Teb1. Either 100 pmole or 1 nmole of each purified recombinant OBD was pre-bound to the resin. A negative control monitored holoenzyme binding to resin lacking pre-bound OBD (lane 1). *C*, Telomerase holoenzyme activity binding to resin-immobilized WT TPP1 OBD or the TPP1 OBD variant indicated. Each panel begins with a negative control monitoring holoenzyme binding to resin lacking a TPP1 OBD. Either 20 or 100 pmole of WT or 100 pmole of sequence-variant rTTP1 OBD was pre-bound to the resin and activity was assayed directly on resin without elution. The bracket indicates variants with reproducibly and severely reduced co-IP of holoenzyme activity.

Figure 5

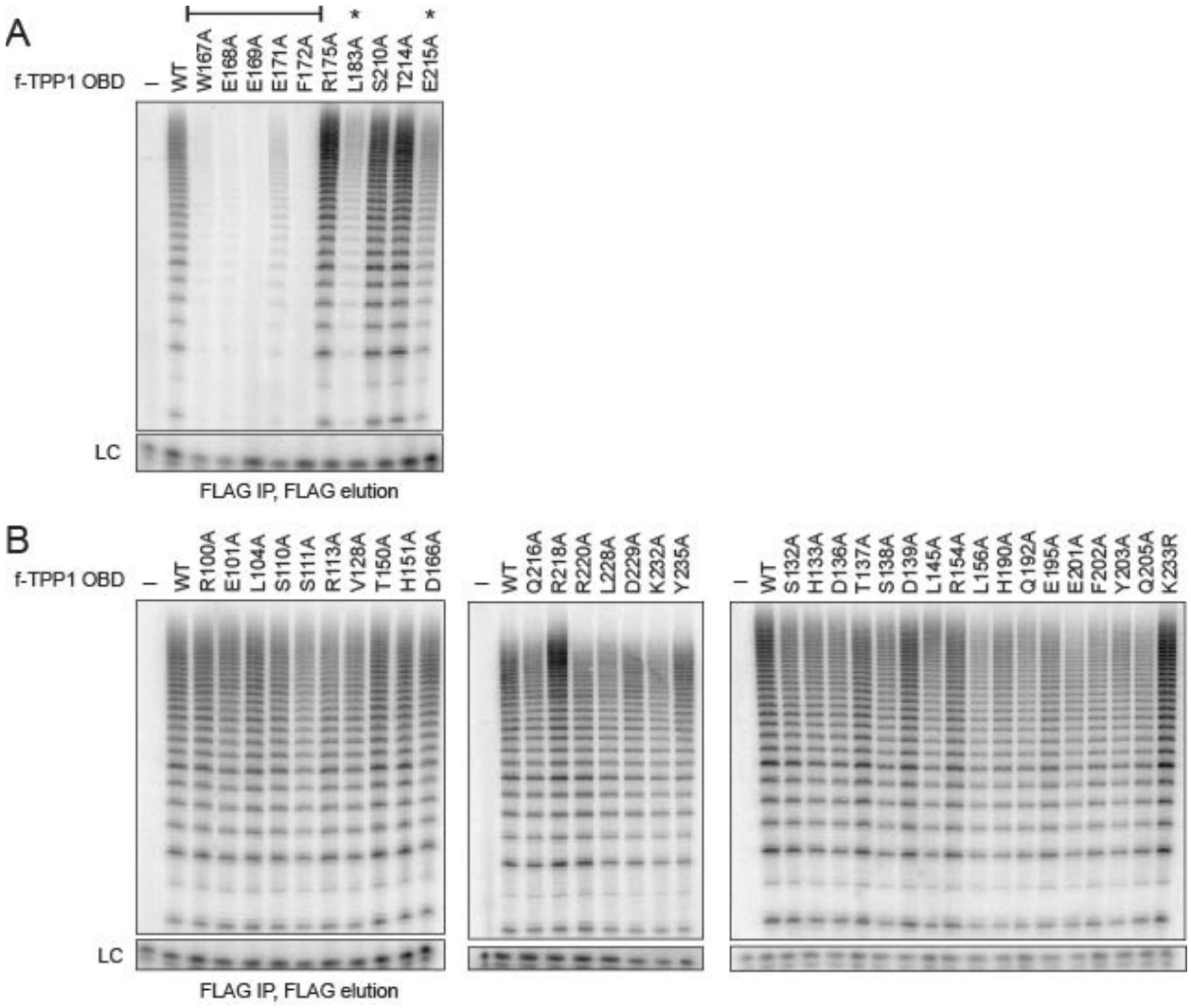

Figure 5: Sequence dependence of TPP1 OBD association with telomerase holoenzyme co-expressed in human cells. *A* and *B*, Telomerase holoenzyme activity co-IP with an f-tagged TPP1 OBD co-expressed with zz-TERT and hTR in human cells. Each panel of activity assays begins with a negative control that monitors holoenzyme activity binding in the absence of an f-tagged TPP1 OBD. The bracket indicates TPP1 OBD variants with reproducibly and severely reduced co-IP of holoenzyme activity; the two additional TPP1 OBD variants indicated with an asterisk reproducibly but less severely compromise holoenzyme co-IP. Equal input and bound amounts of each TPP1 OBD were verified (data not shown).

Figure 6

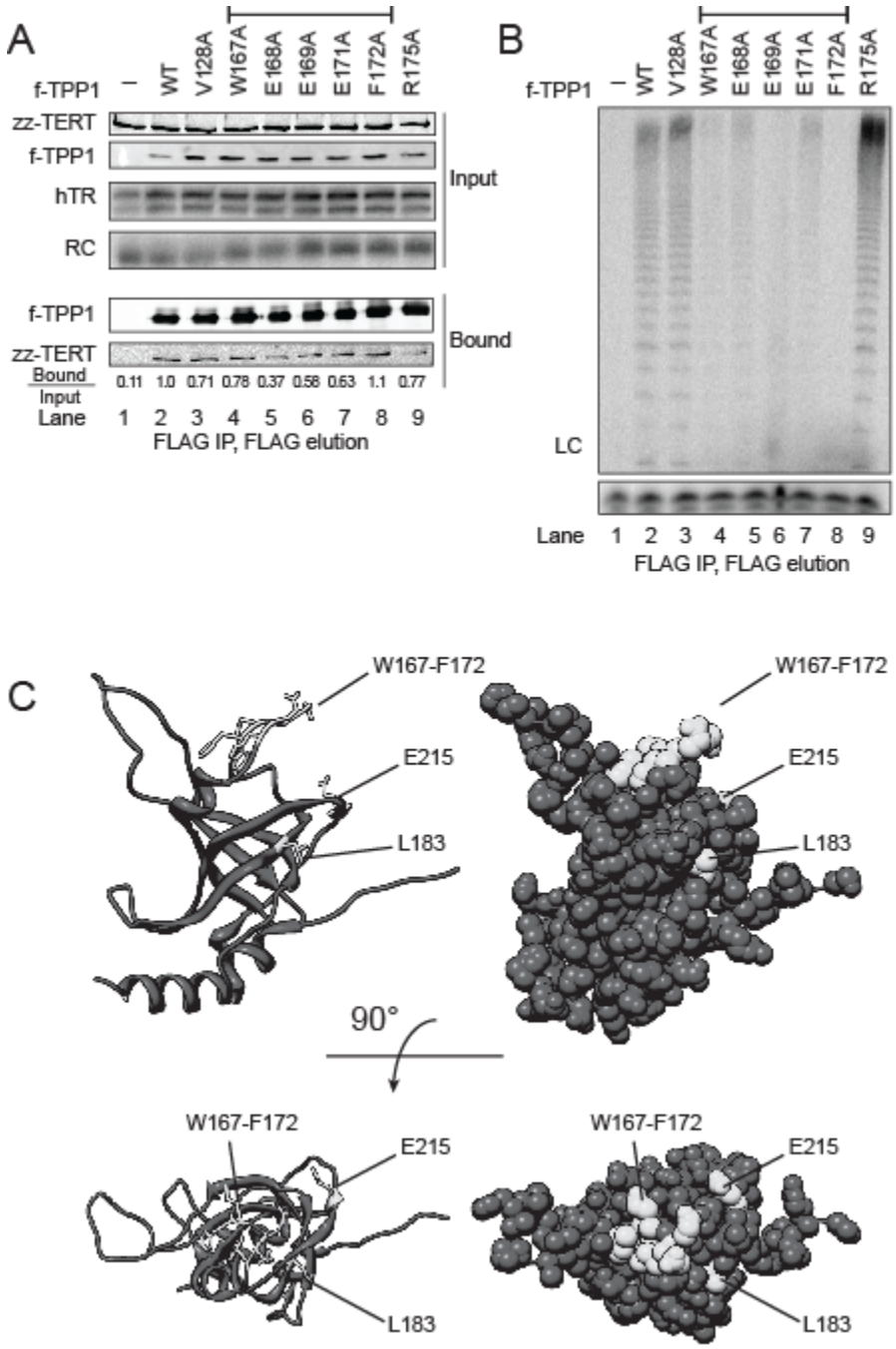

Figure 6: Sequence dependence of full-length TPP1 association with telomerase holoenzyme co-expressed in human cells. *A*, Telomerase zz-TERT and hTR association with f-tagged full-length TPP1 harboring the indicated single amino acid substitution in the OBD, following co-expression in human cells. A negative control monitors holoenzyme subunit binding to resin from cell extract lacking f-tagged TPP1 (lane 1). The bracket indicates the sequence variants with reproducibly and severely reduced co-IP of hTR as quantified by

Bound/Input hTR ratio. *B*, Telomerase holoenzyme activity co-IP by co-expressed f-tagged full-length TPP1 harboring the indicated single amino acid substitution in the OBD. The bracket indicates the sequence variants with reproducibly and severely reduced co-IP of holoenzyme activity. *C*, Ribbon and space-fill representations of human TPP1 OBD structure {}. The amino acids with side-chains shown here to be important for holoenyzme binding are indicated in lighter shading against the rest of the protein and labeled.

CHAPTER FOUR

Genetic dissection of multiple roles for human TPP1 in stem cell telomere length homeostasis

Abstract

Telomere homeostasis is essential for the long-term survival of both stem cells and cancer cells. To maintain telomeres, telomerase is recruited to chromosome ends by the shelterin protein complex. An understanding of the requirements for telomerase recruitment, its regulation, and the consecutive steps of telomerase action at telomeres is elusive. The shelterin protein TPP1 can facilitate telomerase recruitment through a region termed the TEL patch. Using genome editing in human stem cells we demonstrate that TEL patch deficient cells phenocopy telomerase-deficient cells and thereby establish TPP1's essential role in telomerase-mediated telomere maintenance. Intragenic complementation of TEL patch-deficient cells revealed that TPP1 also functions in telomerase activation following recruitment and that a distinct surface of TPP1 determines responsiveness of telomerase to telomere length, which controls telomere length homeostasis. This genetic dissection of separable TPP1 functions uncovers new steps of telomerase action in stem cells and new avenues for selective telomerase inhibition.

Introduction

The balance of human development and tumor suppression requires that telomeres of embryonic stem cells have appropriate length. While the human embryo must have telomeres long enough to support the proliferative demand of a developing organism, they also should be short enough so that telomere attrition can serve as a barrier to tumorigenesis(Gilson and Ségal-Bendirdjian, 2010). Therefore, elucidating the regulatory mechanisms controlling human telomere homeostasis is fundamental for understanding normal stem cell renewal and its deregulation in cancer. In addition, long-term stem cell function critically depends on genome integrity, which requires the protective function of telomeres provided by the shelterin protein complex(Palm and de Lange, 2008).While shelterin proteins protect ends to give telomere stability, shelterin subunits can also inhibit, activate, and modulate the processivity of new telomeric repeat synthesis by telomerase(Nandakumar and Cech, 2013; Palm and de Lange, 2008). To understand this complexity, an experimental system is needed that can dissect function of telomerase without impacting end-protection. Studies using genetically engineered mice are complicated by the atypically long telomeric repeat tracts observed in standard mouse strains(Kipling and Cooke, 1990). Studies using RNA interference to deplete shelterin proteins in tumor cells lines such as HeLa cells are limited by residual wild-type protein and by tumor-selected changes in telomere number and telomerase regulation(Bryan et al., 1998; Kim et al., 1994; Nakashima et al., 2013). Here, we introduce a genetically defined system that overcomes these limitations, allowing us to uncover the mechanisms by which shelterin regulates telomerase function in human stem cells.

Studies in tumor cells have shown that human telomere integrity requires shelterin protein complexes comprising POT1 bound to single-stranded telomeric repeats, TRF1 and TRF2 bound to double-stranded telomeric repeats, and TIN2 and TPP1 bridging the direct DNA binding proteins(Cesare and Karlseder, 2012; Nandakumar and Cech, 2013; Palm and de Lange, 2008). The interdependence of TPP1, POT1, and other shelterin components makes it challenging to dissect their individual contributions to telomere length homeostasis. While depletion and overexpression data established TPP1 and POT1 as negative regulators of telomere length(Baumann and Price, 2010; Churikov and Price, 2008; Hockemeyer et al., 2007; Houghtaling et al., 2004b; Liu et al., 2004; Loayza and De Lange, 2003a; Ye et al., 2004), both proteins can also facilitate telomerase action. The TPP1 OB-fold (OB) and specifically a patch containing acidic residues, termed the TEL patch, is involved in TPP1 association with telomerase(Abreu et al., 2010; Nandakumar et al., 2012; Sexton et al., 2012; Tejera et al., 2010; Wang et al., 2007; Zhong et al., 2012). TPP1 that either lacks the OB (ΔOB) or is mutated in the TEL patch fails to interact with telomerase or to sustain telomere length but maintains shelterin integrity. Furthermore, the TPP1 OB alone is sufficient to localize telomerase to an ectopic site(Zhong et al., 2012). However, it is currently unknown whether this mode of recruitment is either essential and/or exclusive in human cells.

Adjacent to the TPP1 OB is the POT1 binding domain (PBD), which mediates the TPP1-POT1 interaction that brings POT1 to telomeres in vivo and increases POT1 DNA binding affinity in vitro(Abreu et al., 2010; Wang et al., 2007). Purified recombinant TPP1-POT1 stimulates the repeat addition processivity (RAP) of human telomerase ~3-fold, and TPP1 alone stimulates activity up to 1.5-fold, dependent on specific residues in the TERT N-terminal (TEN) domain(Wang et al., 2007; Zaug et al., 2010). TEL patch mutations reduce TPP1-POT1 stimulation of RAP, telomerase recruitment to telomeres, telomere length, and ectopic recruitment of telomerase to tethered TPP1 OB(Nandakumar et al., 2012; Sexton et al., 2012; Zhong et al., 2012). Conversely, mutations in the TERT TEN domain can also abrogate RAP stimulation in vitro (G100V) or telomerase recruitment to telomeres in vivo (R132D)(Sexton et al., 2012; Stern et al., 2012; Zaug et al., 2010). A current challenge in the field involves relating in vitro biochemical observations to in vivo telomere length regulation. Studies in budding and fission yeast have shown that telomerase physical recruitment to telomeres is a step distinguishable from telomerase activation and that both steps are required for telomere elongation(Chan et al., 2008; Evans and Lundblad, 1999; Jun et al., 2013). However, analogous in vivo steps of telomerase activation in mammalian cells remain undefined.

Here we describe the genetic analysis of requirements for human telomerase action at telomeres using human embryonic stem cells (hESCs), primary human cells with physiological telomere length homeostasis(Marión and Blasco, 2010; Thomson, 1998). By targeted gene replacement, we show that the TEL patch of TPP1 is essential for telomere maintenance, with telomere shortening upon TEL patch deletion that is indistinguishable from shortening following genetic disruption of TERT. Fusion of TERT to TPP1 or increased telomerase access to single-stranded chromosome 3' ends does not bypass the requirement for TEL patch function, demonstrating that the TEL patch has a function beyond telomerase recruitment. Moreover, TPP1 OB function does not require a contiguous POT1-TPP1-telomerase ternary complex or TPP1 phosphorylation sites. A distinctive phenotype was observed with mutation of the TPP1 residue L104, which altered the stable set-point of telomere length. These separation of function phenotypes genetically define an unexpected multiplicity of roles for human TPP1 in stem cell telomere length homeostasis and provide further insight into potential mechanisms for blocking telomerase action as cancer therapies.

Materials and Methods

hESC culture

Cell culture was carried out as described previously(Soldner et al., 2009). All hESC lines were maintained on a layer inactivated mouse embryonic fibroblasts (MEFs) in hESC medium (DMEM/F12 [Invitrogen] supplemented with 15% fetal bovine serum [Hyclone], 5% KnockOutTM Serum Replacement [Invitrogen], 1 mM glutamine [Invitrogen], 1% nonessential amino acids [Invitrogen], 0.1 mM β-mercaptoethanol [Sigma], penicillin/streptomycin [Gibco], and 4 ng/ml FGF2 [R&D systems]). Cultures were passaged every 5-7 days either manually or enzymatically with collagenase typeIV (Invitrogen; 1.5 mg/ml) and gravitational sedimentation by washing 3x in wash media (DMEM/F12 [Invitrogen] supplemented with 5% fetal bovine serum [Hyclone], and pennecillin/streptomycin [Gibco]).

ZFN-mediated genome editing

Gene targeting with zinc finger nucleases was performed as previously described(Hockemeyer et al., 2009, 2011). TPP1 targeted to the AAVS1 locus was removed with co-transfection of Cre recombinase mRNA and NLS-GFP mRNA (Stemgent) using previously described transfection protocols(Hockemeyer et al., 2009), followed by sorting of GFP expressing cells and culture of clonally derived ES colonies with verification of LoxP site recombination of ES lines by PCR. Targeting of the last exon of the TPP1 genomic locus was excluded due to the presence of the overlapping immediate neighboring gene RLTPR, transcribed in the opposite sense as TPP1.

IF and scoring for nuclear blebbing and TIFs

For analysis by IF cells were washed with PBS, incubated with PBS + 0.1 % Triton X-100 and washed 1x with PBS where indicated (pre-permeablization), fixed with 3.7% formaldehyde in PBS, permeabilized with PBS + 0.5% Triton X-100, and blocked with PBS + 0.1% Triton X-100 with 3% horse serum. Fixed cells were incubated with antibodies against OCT4 (Abnova), FLAG (M2 Sigma), TRF2 (Imgenex), γ-H2AX (Millipore) TRF1 (gift of Titia de Lange), and GFP (Abnova) in blocking solution, followed by secondary antibodies. Cells were imaged on a Zeiss Observer.Z1 and images were processed using Axiovision rel. 4.7.

Scoring of blebbed nuclei was performed single blind. Box plots show scoring of 8 individual colonies per cell line at a time point approximately 2 weeks before death of the homozygous TPP1 ΔL-GFP line. P values are derived from a Tukey HSD test performed after significance was determined with an initial ANOVA. Scoring of TIFs was performed single blind. Bar graph shows scoring of indicated lines with p value determined by Fisher's exact test.

ChIP, Detection of RNA, Southern blotting, and telomerase catalytic activity

Chromatin immunoprecipitation was performed as previously described(Loayza and De Lange, 2003b). Protein G conjugated Dyna beads (Invitrogen) were used to IP antibodies. RNA

was detected by blot hybridization as previously described(Sexton et al., 2012). Southern blots for detection of genomic insertions were performed as previously described(Hockemeyer et al., 2011). TRAP assay was performed as previously described using TSNT (AATCCGTCGAGCAGAGTTAAAAGGCCGAGAAGCGAT) as an internal control (Kim et al., 1994). Direct primer extension assay for telomerase activity was performed as previously described(Sexton et al., 2012).

Detection of telomere length

For preparation of genomic DNA, hESC lines were washed with PBS, then removed using 1.5 mg/ml collagenase type IV from a plate containing a MEF feeder layer and washed 3x in wash media by gravitational sedimentation to minimize contaminating MEF cells. Genomic DNA was then prepared as in Southern blot protocol. Resuspended genomic DNA was digested with MboI and AluI overnight at 37°C. The resulting DNA was normalized and run on 0.75% agarose (Seakem ME Agarose, Lonza), dried under vacuum for 2 hrs at 50°C, denatured in 0.5 M NaOH, 1.5 M NaCl for 30 mins, shaking at 25°C, neutralized with 1 M Tris pH 6.0, 2.5 M NaCl shaking at 25°C, 2x for 15 mins each. Then the gel was pre-hybridized in Church's buffer (1% BSA, 1mM EDTA, 0.5M $NaP0_4$ pH7.2, 7% SDS) for 1 hr at 50°C before adding telomeric probe (PNK γ-32P ATP end-labeled [T2AG3]3). Gel was washed 3x 30 min in 4x SSC and 1x 30 min in 4x SSC + 0.1% SDS before exposing on a phosphorimager screen.

While this method removes the vast majority of mouse feeder cells, the signal from mouse telomeres is disproportionate to human telomeres due to amplified relative length and concentration into a smaller area(Kipling and Cooke, 1990). Because MEF telomeres are size-resolved from human telomeres they do not interfere with analysis of hESC telomere length.

Results

To conduct a genetic analysis of human TPP1 requirements for telomerase action, we edited the TPP1 locus of WIBR#3 hESCs to express a TPP1 variant in which the acidic loop of the TEL patch (amino acids 166-172) was replaced with a GSSG linker (TPP1 ΔL) (Fig. 1a). This allele, as predicted by previous studies in tumor cells(Nandakumar et al., 2012; Sexton et al., 2012; Zhong et al., 2012), entirely eliminates the ability of TPP1 to co-purify active telomerase when over-expressed in HEK293T cells (Extended data fig. 1). In addition to mutating the TEL patch, our editing strategy introduced a GFP-tag at the C-terminus of the endogenous locus TPP1 ΔL variant. The resulting TPP1 ΔL-GFP protein localized to the telomere as determined by immunofluorescence (IF) and ChIP analysis, corroborating previous HeLa cell over expression studies concluding that the TEL patch is dispensable for its telomere localization (Fig. 1b,c)(Abreu et al., 2010). We analyzed telomere length dynamics in heterozygous (ΔL/+) and homozygous (ΔL/ΔL) targeted hESCs. Telomere length remained stable in heterozygous ΔL/+ cells (n=2) but progressively decreased in homozygous ΔL/ΔL cells (n=4) (Fig. 1d,e). Initially, TPP1 ΔL/ΔL cells proliferated at a wild-type rate, with doubling times indistinguishable from heterozygous ΔL/+ and parental hESCs. However, an abrupt decrease in proliferation was observed over approximately two weeks when telomeres reached 2.5 to 3 kb in average length, and all cells died ~90 days after targeting. Interestingly, even at very late time points about 80 days after targeting, ΔL/ΔL hESC cultures still contained mostly pluripotent cells monitored at the single-cell level for OCT4 expression by IF (Fig. 1f). However, these OCT4-positive cells at late time points had an evident change in nuclear morphology, with lobulated, blebbed nuclei indicative of cells undergoing apoptosis (Fig. 1f,g). Control experiments conducted in parallel established that this telomere shorting phenotype is specific to the ΔL Tel-patch mutations and that telomeres are maintained in cells that express wild-type TPP1-GFP from the endogenous locus. These experiments also confirm independently that loss of the TPP1 OB fold leads to telomere shortening and cell death in a telomere length-dependent manner (Extended data fig. 2). We conclude that telomerase action on telomeres through TPP1 TEL patch function provides an essential step of telomere maintenance in hESCs.

In order to determine whether telomere shortening imposed by absence of the TEL patch is a complete or only partial inhibition of telomerase action, we generated TERT-deficient (TERT-/-) WIBR#3 hESCs by integrating a STOP cassette into the first exon of the TERT locus (Fig. 2a). We compared phenotypes between TERT-/- (n=3) and TPP1 ΔL/ΔL cells. While telomerase activity was readily detectable in cell extracts of the parental hESCs, comparable to that of immortalized human cell lines (Extended data fig. 3), it was eliminated by homozygous TERT disruption (Fig. 2b). Homozygous loss of TERT resulted in no detectable change of initial proliferation rates compared to TERT+/- hESCs (n=2) or the parental line. As expected, TERT-/- cells exhibited progressive telomere shortening, while TERT+/- cells exhibited detectable but modest shortening suggestive of TERT haploinsufficiency (Fig. 2c,d). The rate of telomere shortening and the post-targeting days of continuous passage prior to cell death were

indistinguishable from TPP1 ΔL lines. TERT-/- cells exhibited reduced proliferation starting about 75 days after the loss of telomerase function and presented the same nuclear blebbing and cell sloughing observed for TPP1 ΔL/ΔL cells (Fig. 2e,f). Around 90 days after telomerase loss, corresponding with telomere lengths of approximately 2.5 to 3 kb, proliferating cells were no longer detectable in the TERT-/- hESCs, phenocopying the proliferative limit as well as telomere shortening phenotype of TPP1 ΔL/ΔL cells. Additionally, double-targeted TERT-/- and TPP1 ΔL/ΔL clones die with kinetics indistinguishable from singly targeted lines (Extended data fig. 4). We conclude that loss of the TPP1 TEL patch imposes a complete loss of telomerase-mediated telomere elongation.

Many factors contribute directly or indirectly to telomerase action at telomeres, including telomere length, shelterin component abundance and telomerase levels (Extended data fig. 5)(Nandakumar and Cech, 2013; Palm and de Lange, 2008; Stern et al., 2012; Stewart et al., 2012b; Zhao et al., 2011). To investigate whether telomere maintenance in TPP1 ΔL/ΔL hESCs can be rescued by increased expression level of TERT or TPP1 ΔL, we used safe harbor transgenesis to overexpress FLAG-tagged TPP1 (TPP1-F), TPP1 ΔL (TPP1 ΔL-F), or TERT (F-TERT) in TPP1 ΔL/ΔL cells (Fig. 3a and Extended data fig. 6). IF confirmed that both TPP1-F and TPP1 ΔL-F localized to telomeres (Fig. 3b), and immunoblot analysis confirmed over expression of F-TERT from the AAVS1 locus (Extended data fig. 6d), which in hESCs was accompanied by modest increase of telomerase activity in cell extracts (Extended data fig. 3). Independent of whether individual clonal cell lines or pooled cell populations derived from targeting were analyzed (Fig. 3c,d), only TPP1-F but not TPP1 ΔL-F or TERT overexpression rescued telomere shortening and deferred nuclear blebbing and cell death in TPP1 ΔL cells. This resulted in telomere elongation and maintenance at lengths comparable to control cells (Fig. 3c-e, n=5).

Defects in the physical recruitment of telomerase to telomeres can be suppressed by direct fusion of TERT to a telomeric DNA binding domain or protein(Armbruster et al., 2004; Evans and Lundblad, 1999). To test whether the failure of TPP1 ΔL cells to maintain telomeres can be rescued by fusion to TERT, we targeted the AAVS1 locus for integration of a transgene expressing an F-tagged TERT fusion with TPP1 ΔL (Fig. 4a). For comparison, in parallel we targeted AAVS1 to express F-TERT, the F-TERT R132D variant that retains wild-type telomerase activity but prevents association with TPP1 and telomeres(Stern et al., 2012), TPP1-F-TERT, TPP1 ΔL-F-TERT R132D, TPP1-F, or TPP1 N with an N-terminal extension derived from the endogenous locus (Fig. 4a and Extended data fig. 7)(Cristofari et al., 2007b). All of these polypeptides localized to telomeres (Fig. 4b). We compared this set of proteins for their ability to confer telomere length maintenance to both a homozygous TERT null cell line and homozygous TPP1 ΔL cell line. In the TERT-/- cells, only constructs containing wild-type TERT were able to rescue telomere length maintenance (Fig. 5c, n=3). In TERT-/- cells expressing TPP1 ΔL-F-TERT R132D, telomeres shortened at a rate indistinguishable from the untargeted parental cells (Fig. 4c). In TPP1 ΔL/ΔL cells, telomere length maintenance was rescued only by TPP1-F or TPP1-N but not with TPP1 ΔL-F-TERT or TPP1 ΔL-F-TERT R132D fusion proteins

(Fig. 4c). Taken together, these findings indicate that the TPP1-F-TERT fusion protein provides TPP1 and TERT function but does not suppress the TPP1 ΔL or TERT R132D defect in telomerase action at telomeres.

To test whether the TEL patch remains essential for telomerase action on a more accessible chromosome end, we made use of a previously described POT1 variant lacking its N-terminal DNA binding OB fold, shown to strongly induce telomere elongation and Telomere-Dysfunction-Induced Foci (TIF) (Loayza and De Lange, 2003a; Takai et al., 2003; Xin et al., 2007). We targeted the AAVS1 locus of the homozygous TPP1 ΔL cell line to express F-POT1 ΔOB, which localized to telomeres (Fig. 4b) but did not rescue telomere shortening (Fig. d) or change the continuous passage interval to cell death relative to untargeted parental cells. As a control, we confirmed that expression of POT1 ΔOB induced telomere elongation in the heterozygous TPP1 ΔL/+ cells (Extended data fig. 8).

When added to in vitro telomerase activity assays, the TPP1-POT1 heterodimer increases telomerase enzyme processivity(Wang et al., 2007). To investigate whether a contiguous ternary complex of POT1, TPP1 and telomerase is required for telomerase activity on telomeres in vivo, we targeted the AAVS1 locus to express TPP1 ΔPBD, a TPP1 variant that lacks the interaction domain with POT1(Baumann and Price, 2010). The combination of TPP1-telomerase interaction mediated by TPP1 ΔPBD and TPP1-POT1 interaction mediated by TPP1 ΔL rescued viability of TPP1 ΔL/ΔL cells and allowed moderate telomere elongation (Fig. 4d)(Liu et al., 2004; Xin et al., 2007), despite the absence of a contiguous ternary POT1-TPP1-telomerase complex. In agreement with previously studies, we verified that TPP1 lacking the PBD has no defect in associating with active telomerase when overexpressed from HEK293T cells (data not shown). TPP1 ΔPBD-F caused an increase in TIF formation as compared to both parental and TPP1-F rescued lines, indicating some deprotection of telomere ends (Extended data fig. 8). Moreover, despite the fact that TPP1 OB expression alone in human cells was sufficient to direct telomerase relocalization(Zhong et al., 2012), neither an OB-F or OB ΔL-F construct targeted to the AAVS1 locus could maintain telomeres or cell viability (Fig. 4d and Extended data fig. 9).

The assays above use a genetic complementation approach to resolve how different TPP1 domains function in shelterin interactions and telomerase elongation of telomeres. To investigate whether TPP1 OB has additional roles in telomere elongation other than telomerase recruitment, we targeted the AAVS1 locus to express TPP1-F variants containing single amino acid substitutions on different surfaces of the OB fold (Fig 5a). We made mutations within the TEL patch but beyond the acidic residues of the loop that were not covered by the ΔL construct (L212, L183, E215). We also substituted amino acid L104 situated on the opposite side of the OB from the TEL patch. The L104A substitution did not notably reduce OB association with telomerase (Nandakumar et al., 2012; Sexton et al., 2012). However, L104A abrogated POT1-dependent RAP stimulation(Nandakumar et al., 2012). Near L104, we mutated S111 to S111A or S111R because phosphorylation of this site is thought to allow S-phase-specific TPP1-telomerase interaction(Zhang et al., 2013). We also mutated the only consensus Akt phosphorylation site in TPP1 at S498 to generate S498A and S498E, because Akt

phosphorylation of TPP1 is thought to modulate telomerase-TPP1 interaction by affecting putative TPP1 homodimerization(Han et al., 2013). These TPP1 substitution variants variably reduced association with telomerase assayed by over expression in HEK293Ts (Fig. 5b).

The ability of each mutant to rescue telomere maintenance was compared to rescue with TPP1-F or TPP1 N, targeted and passaged in parallel. As expected, all of these TPP1 proteins colocalized with telomeres by IF (Extended data fig. 9). TPP1-F and TPP1 N elongated telomeres and conferred extended proliferation, as did all of the phosphorylation-site mutants. Disruption of E215 or L183 resulted in partial telomere elongation (Fig. 5c). Cells expressing TPP1 L212A displayed a hypomorphic phenotype, delaying but not averting cell death. Surprisingly, each L104 substitution rescued cell viability but did not increase telomere length, instead allowing maintenance of very short telomeres similar to those of untargeted parental cells near the time of their death. This failure of telomere elongation following substitution of L104 occurs despite its ability to associate with similar levels of activity as E215, which readily elongated telomeres (Fig. 5b,c). A similar phenotype became apparent when analyzing telomere length over time in TPP1 ΔPBD-F cells. Although TPP1 ΔPBD-F restored long-term viability telomeres remained equally short as in TPP1 L104A (Fig. 5d,e). These results suggest that TPP1 ΔPBD, L104A, L104E, and L104R do not compromise recruitment of telomerase but rather change the telomere length set-point at which telomerase maintains telomeres (Fig. 5d,e). We conclude that L104, and perhaps the TPP1-POT1 heterodimer, participate in a step of telomerase action at telomeres that is responsive to absolute telomere length, distinct from what we demonstrate is a genetically essential TPP1 TEL patch function in telomerase recruitment at any telomere length (Fig. 5d,e).

Discussion

In this study we used state-of-the-art genome editing technology in hESCs to make specific genetic substitutions of TPP1 as the strategy for establishing TPP1 requirements for telomerase action, while preserving its essential role in maintaining telomere integrity as a part of shelterin. Our data demonstrate that the TEL patch provides essential means by which telomerase maintains the telomere (Fig. 5f i-iii). We show that deletion of the TEL patch phenocopies telomerase deletion, supporting that TERT and the TEL patch lie in the same pathway of telomere maintenance. The TEL patch remained essential even when liberating the chromosome 3' terminus by expressing a POT1 without DNA binding activity(Loayza and De Lange, 2003b). Conversely, TPP1 missing the PDB could complement TPP1 ΔL (Fig. 5f iv), indicating that direct association with a TPP1-POT1 heterodimer is not necessary for telomerase action at telomeres. However, telomeres regained only intermediate length, suggesting that POT1 in a ternary POT1-TPP1-telomerase complex may stimulate telomerase action, perhaps by enhancing association with single-stranded DNA(Baumann and Price, 2010). We note that testing the regulatory potential of higher-order cellular assemblies of shelterin proteins remains in important topic for future studies.

Genetic screens in yeast and expression knockdown and overexpression data in human tumor cells have explored the pathways that participate in telomere length maintenance. Here, we show that TPP1 variants can modulate the responsiveness of telomerase action to telomere length in non-transformed human primary stem cells. While mutagenesis of TPP1 phosphorylation sites did not have any apparent functional impact, substitutions of L104, L183, L212, and E215 did affect telomere maintenance. The observation that TPP1 L104 substitutions and TPP1 ΔPBD rescue TPP1 ΔL cell viability while maintaining very short but stable telomeres separates a particular telomere length homeostasis set-point from telomere maintenance and the long-term renewal of hESCs. Detectable recruitment of telomerase to the telomererequires the TEL patch, while an L104-dependent second step regulates telomerase action, possibly in concert with or requiring contact by POT1 (Fig. 5f iv-v). The capacity of a cell to return telomeres to a genetically controlled length is particularly relevant because tumor cell lines often fail to elongate telomeres despite having comparable levels of telomerase. This data provides insights into the mechanisms by which stem cells determine an appropriate telomere length set point, which ultimately determines the replicative capacity of differentiated cell types in the human soma.

Mechanisms that could mediate this telomerase activation and/or relief of repression are not understood at biochemical level in any organism, but at a genetic level our findings have parallels with results in yeast. The budding yeast TPP1-like protein Est3p is required for telomere elongation even if TERT is bound to a telomere(Evans and Lundblad, 1999; Lue et al., 2013; Tuzon et al., 2011), and the fission yeast Tpz1-interacting Ccq1 protein promotes telomere elongation independent of its role in telomerase recruitment to telomeres or opening of telomeric chromatin(Jun et al., 2013). We propose that TPP1, in the physiological context of human stem

cells, has a double-function of recruiting telomerase as well as initiating a subsequent step that facilitates chromosome 3' end extension by new repeat synthesis. Disruption of the genetically essential TPP1 TEL patch or the TPP1 surface perturbed by L104 substitution each limited telomere elongation in hESCs without compromising shelterin integrity. Through several independent genetic experiments we provide in vivo evidence that telomerase action at telomeres is also regulated by shelterin after recruitment. These findings are highly relevant as they reveal novel targets for cancer therapeutics that could selectively inhibit telomerase action and demonstrate for the first time the power of genome editing in hPSCs for structure-function and epistasis analyses.

Figure 1

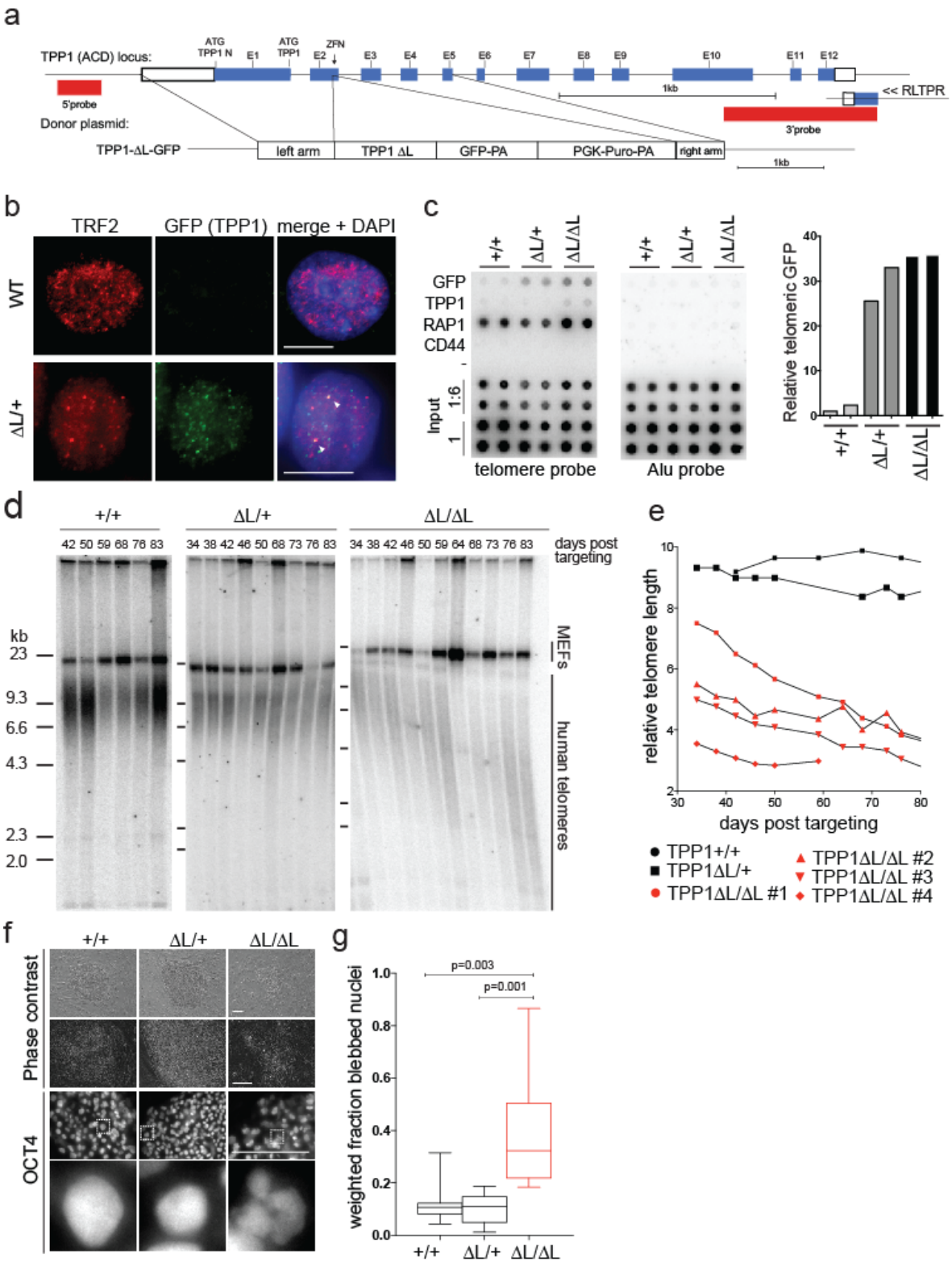
a
TPP1 (ACD) locus:
ATG TPP1 N
E1
ATG TPP1
E2
ZFN
E3
E4
E5
E6
E7
E8
E9
E10
E11
E12
1kb
<< RLTPR
5'probe
3'probe
Donor plasmid:
TPP1-ΔL-GFP
left arm
TPP1 ΔL
GFP-PA
PGK-Puro-PA
right arm
1kb
b
TRF2
GFP (TPP1)
merge + DAPI
WT
ΔL/+
c
+/+
ΔL/+
ΔL/ΔL
GFP
TPP1
RAP1
CD44
Input
1:6
1
telomere probe
Alu probe
Relative telomeric GFP
d
+/+
ΔL/+
ΔL/ΔL
42 50 59 68 76 83
34 38 42 46 50 68 73 76 83
34 38 42 46 50 59 64 68 73 76 83
days post targeting
kb
23
9.3
6.6
4.3
2.3
2.0
MEFs
human telomeres
e
relative telomere length
days post targeting
TPP1+/+
TPP1ΔL/+
TPP1ΔL/ΔL #1
TPP1ΔL/ΔL #2
TPP1ΔL/ΔL #3
TPP1ΔL/ΔL #4
f
+/+
ΔL/+
ΔL/ΔL
Phase contrast
OCT4
g
p=0.003
p=0.001
weighted fraction blebbed nuclei
+/+
ΔL/+
ΔL/ΔL

Figure 1: The TPP1 TEL patch is essential for telomere maintenance in hESCs. a, Targeting schematic for ZFN-mediated cutting and homology-mediated introduction of C-terminally GFP-tagged TPP1 ΔL. **b,** IF of WT or heterozygous TPP1 ΔL-GFP cells stained against GFP (TPP1) and TRF2. White arrowheads indicate robust protein signal colocalization. Scale bar is 5 μm. **c,** ChIP of WT or heterozygous or homozygous TPP1 ΔL-GFP cell extracts assayed in duplicate. Quantification of relative levels of telomeric repeat association with GFP normalized to input telomere signal is at right. **d,** Telomere restriction fragment length assay showing telomere length time course of WT or heterozygous or homozygous TPP1 ΔL-GFP lines. **e,** Quantification of telomeric repeat hybridization signal lengths in homozygous TPP1 ΔL-GFP cell lines as compared with WT and heterozygous TPP1 ΔL-GFP lines. **f,** Phase contrast images of late time point colony morphology, top. Bottom, IF of late time point hESC colonies stained against OCT4 with magnification of representative nuclei below. Scale bar is 200 μm. **g,** Box plot of quantification of nuclear blebbing.

Figure 2

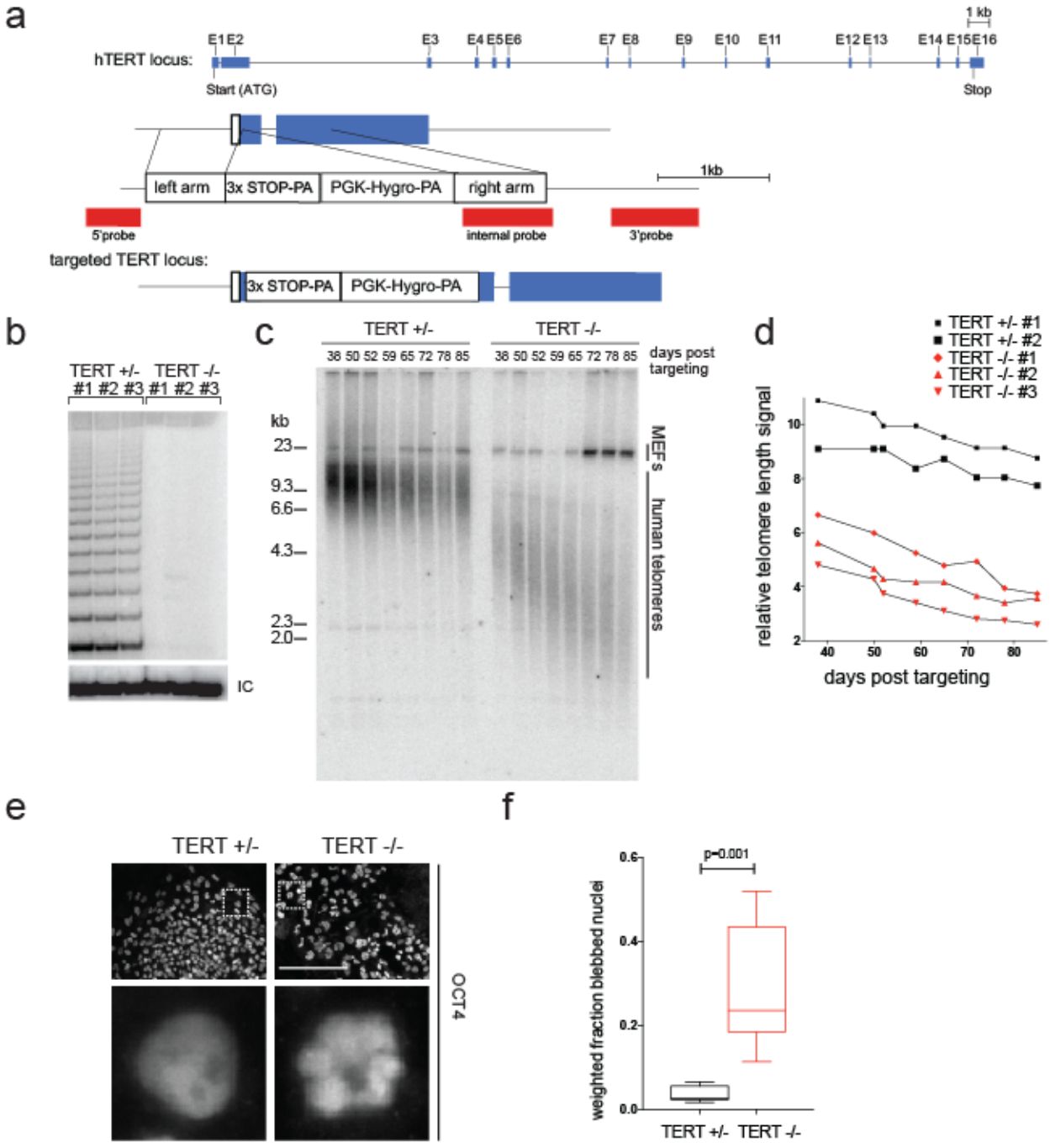

Figure 2: TERT knockout phenocopies the TPP1 ΔL time course of failures in telomere maintenance and cellular renewal. a, Targeting schematic for ZFN-mediated cutting and homology-mediated introduction of a stop cassette into the endogenous TERT locus. **b,** TRAP assay of whole cell extracts from the indicated cell lines using 333 ng total protein and subsequent 1:4 dilutions. IC, internal control. **c,** Telomere restriction fragment length assay of

TERT +/- and -/- hESC cell lines. **d,** Quantification of telomeric repeat hybridization signal lengths in TERT +/- and TERT -/- lines. **e,** IF of late time point TERT +/- and -/- cell lines stained against OCT4. Scale bar is 200 µm. **f,** Box plot quantification of nuclear blebbing.

Figure 3

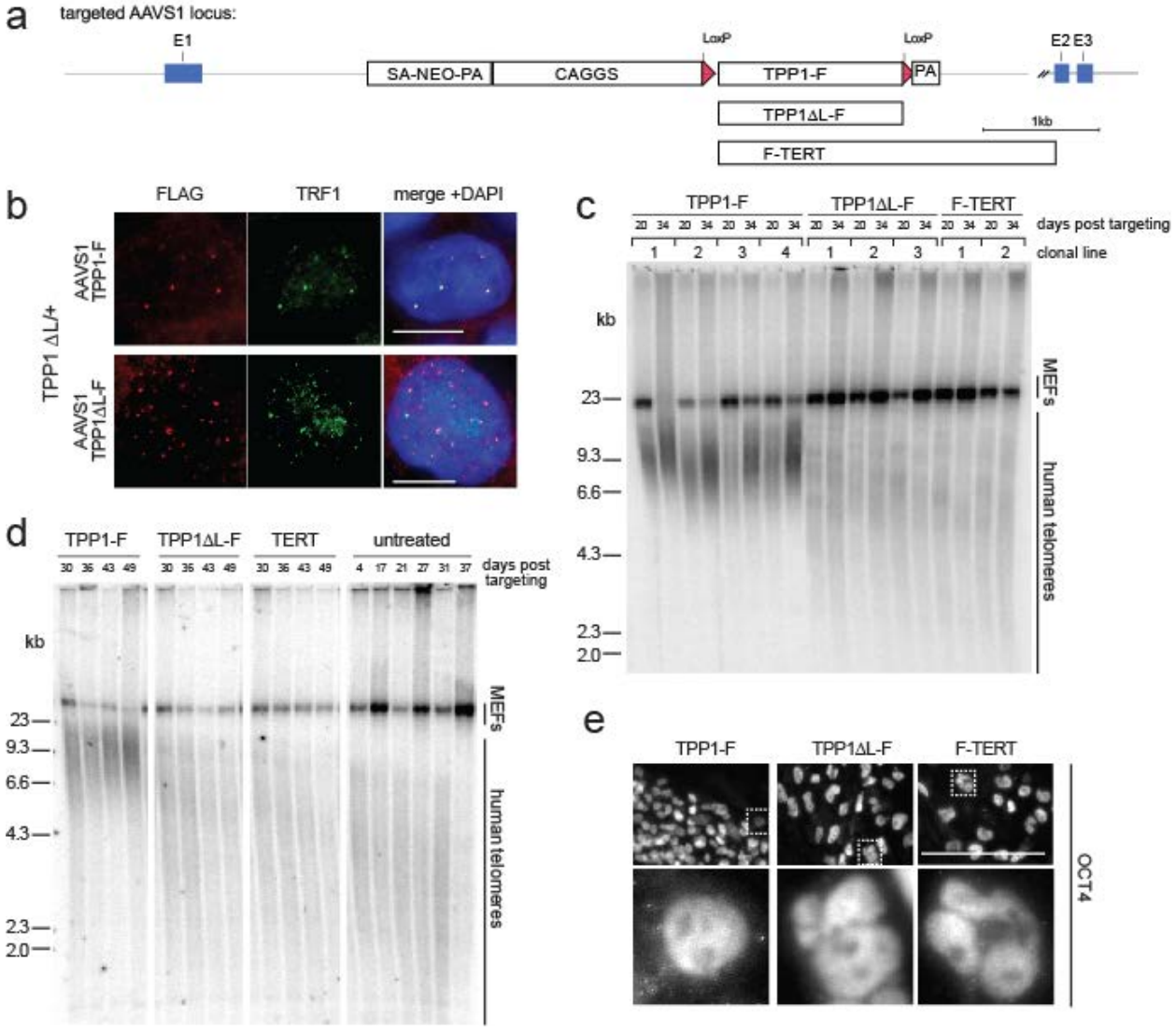

Figure 3: The TPP1 TEL-patch functional requirement is not bypassed by over-expression of telomere or telomerase proteins. a, Targeting schematic of variants introduced at AAVS1 locus. **b,** IF of TPP1-F and TPP1 ΔL-F in a heterozygous TPP1 ΔL-GFP background stained against FLAG and TRF1. **c,** Telomere restriction fragment length assay of a TPP1 ΔL-GFP homozygous line with overexpressed TERT, TPP1-F, or TPP1 ΔL-F. Individual cell clones are indicated by brackets, each with two time points. **d,** Telomere restriction fragment length assay of cell populations from a TPP1 ΔL-GFP cell line with over-expressed F-TERT, TPP1-F, or TPP1 ΔL-F compared to the parental homozygous TPP1 ΔL-GFP. **e,** IF of late time-point hESC colonies stained against OCT4. Scale bar is 200 μm.

Figure 4

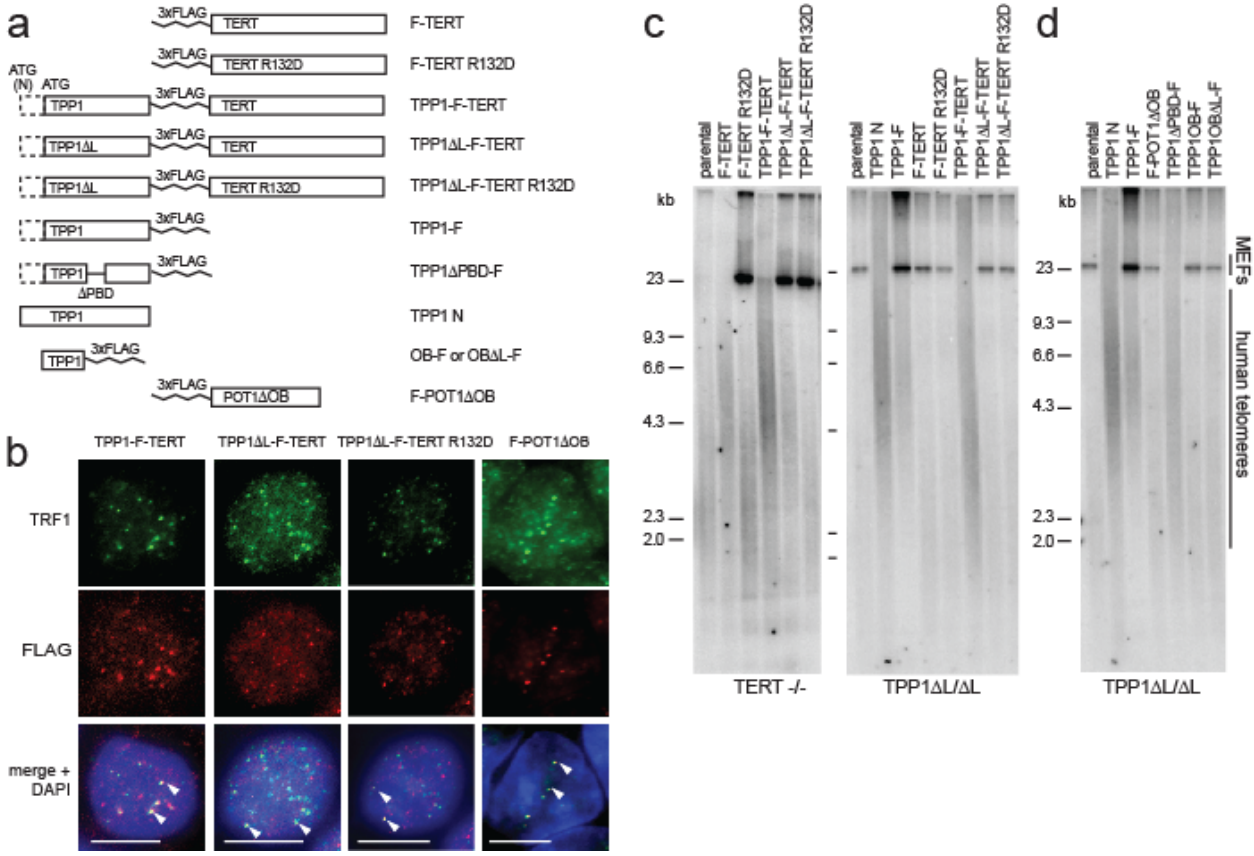

Figure 4: Telomere-localized TERT and release of the DNA 3' end are not sufficient to rescue TEL patch deficient cells. a, Schematic of variants used to complement ΔL/ΔL lines. **b,** IF of TPP1-F-TERT fusions and F-POT1ΔOB. White arrowheads indicate robust protein signal colocalization. Scale bar is 5 μm. **c,d** Telomere lengths of TERT -/- and TPP1 ΔL/ΔL expressing rescue-assay variants.

Figure 5

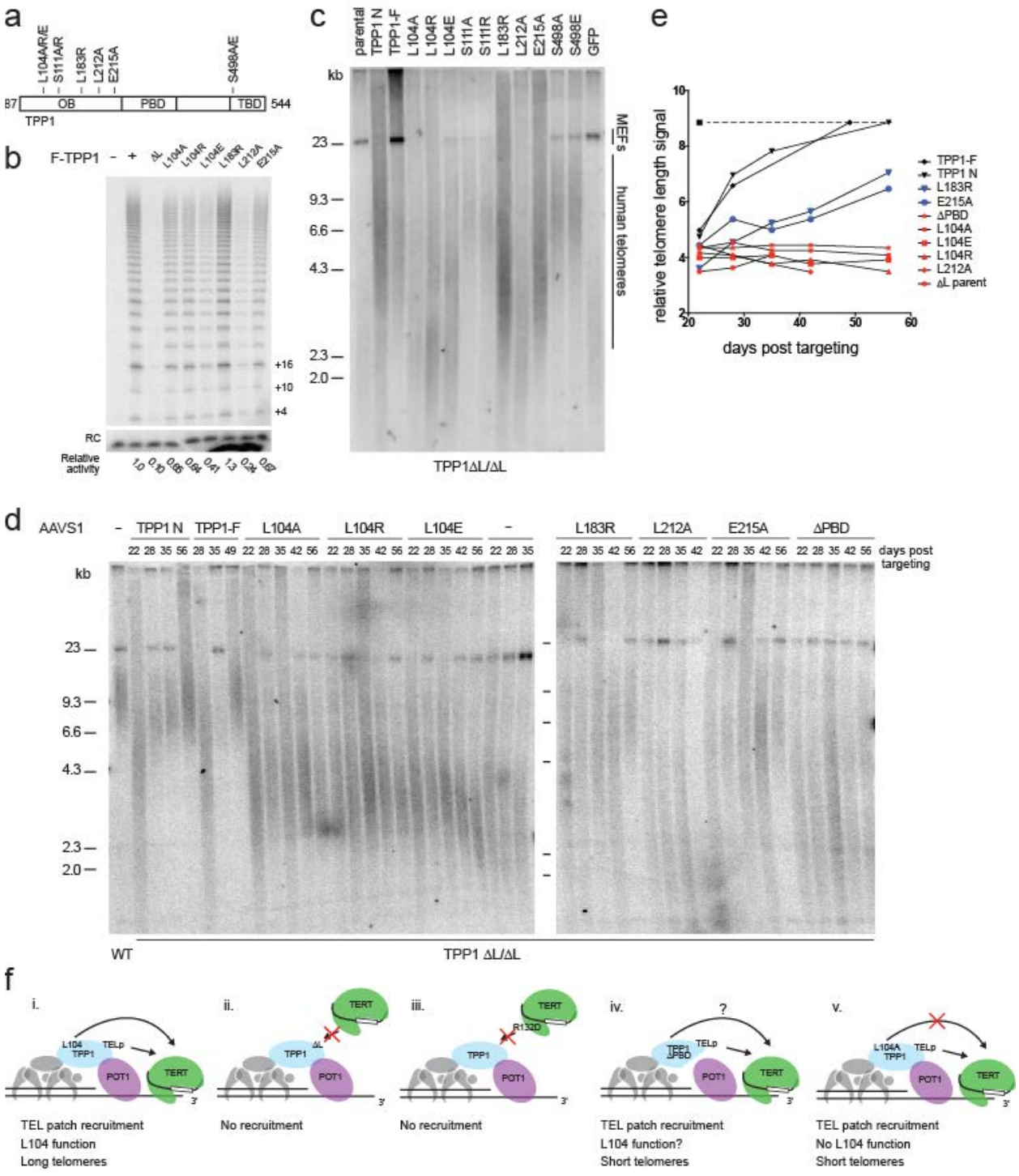

Figure 5: The L104 residue confers sensitivity of telomerase action to telomere length. a, Schematic of TPP1 variants used for overexpression at the AAVS1 locus. **b,** Primer extension of F-TPP1 variants from HEK293T cells. **c,** Telomere length of TPP1 ΔL/ΔL lines

rescued with TPP1 variants. **d**,Time course of telomere lengths from selected TPP1 variant rescue lines. **e,** Time course of telomere lengths for cell lines from **d**. Dotted line indicates WT hESC telomere length. **f,** Schematic of TPP1 functions at telomeres.

Extended data figure 1

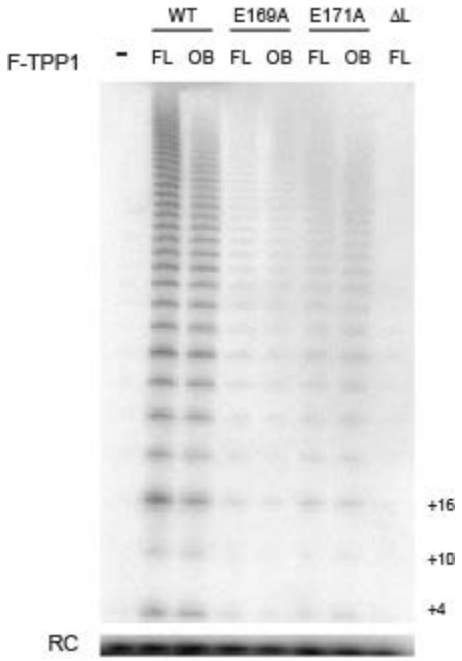

Extended data fig. 1. The TEL patch loop deletion (ΔL) eliminates association with functional telomerase. a, Telomerase catalytic activity from HEK293T overexpression and FLAG IP of F-TPP1, zz-TERT and hTR in primer extension assay. RC, recovery control.

Extended data figure 2

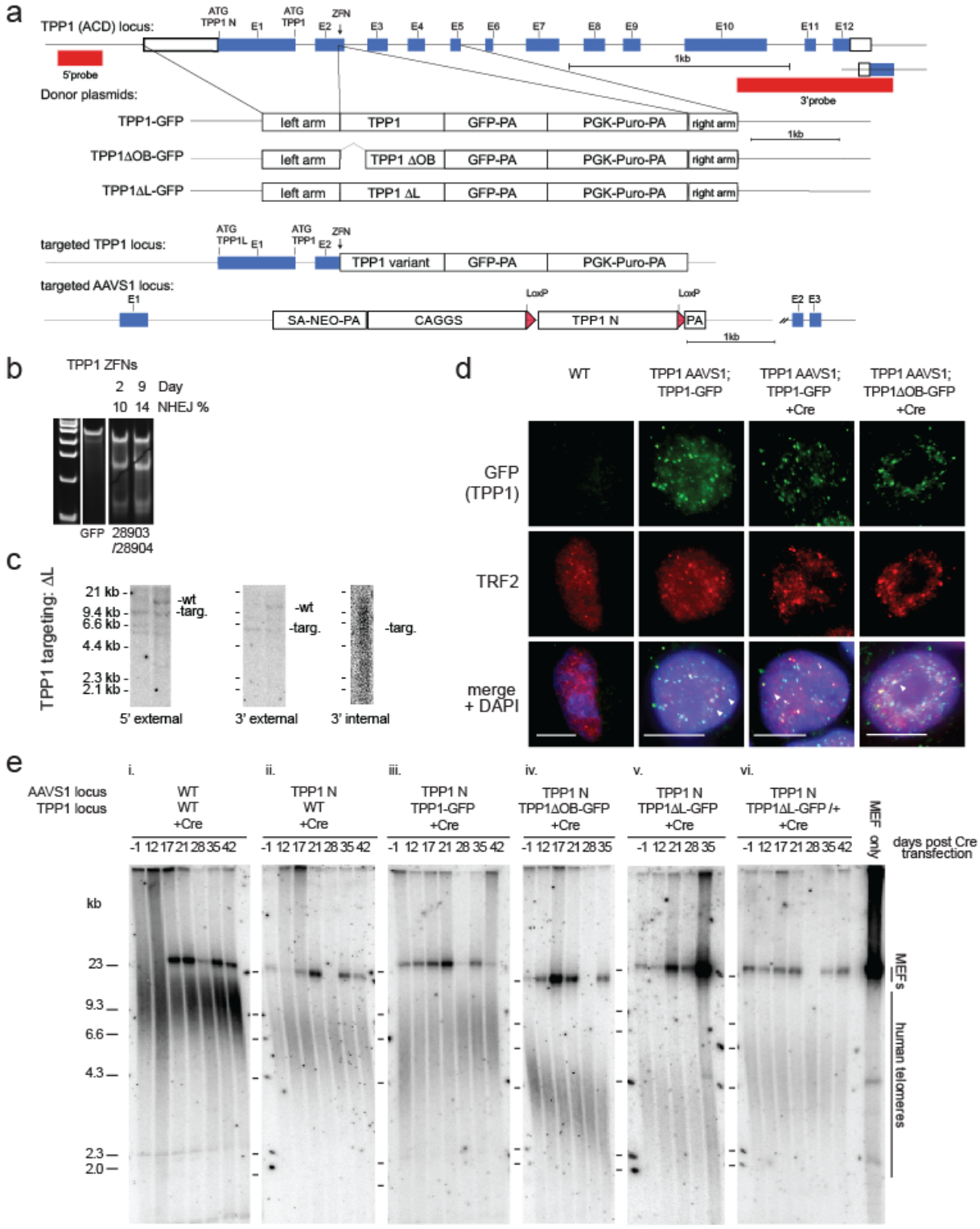

Extended data fig. 2.The TPP1 TEL patch is genetically essential for telomere maintenance in hESCs. a, Targeting schematic for ZFN-mediated cutting and homology-

mediated introduction of C-terminally GFP-tagged TPP1 variants into the TPP1 (ACD) locus and AAVS1 locus. TPP1 N represents TPP1 cDNA derived from translation initiation at an ATG which includes 86 amino acids N-terminal of a second ATG, which begins the region of TPP1 homolog conservation[20,32]. **b,** Efficiency of cutting by transfected ZFNs of PCR-amplified genomic locus of target genes by Cel-1 assay[42]. **c,** Southern of HindIII-digested genomic DNA from TPP1-targeted lines. **d,** IF of TPP1 Cre-conditional cell lines stained against GFP (TPP1) and endogenous TRF2. White arrowheads indicate robust protein signal colocalization. Scale bar is 5 μm. **e,** Telomere restriction fragment length assay showing telomere length time course of variant lines and a single sample of mouse embryonic fibroblast feeder layer genomic DNA.

Extended data figure 3

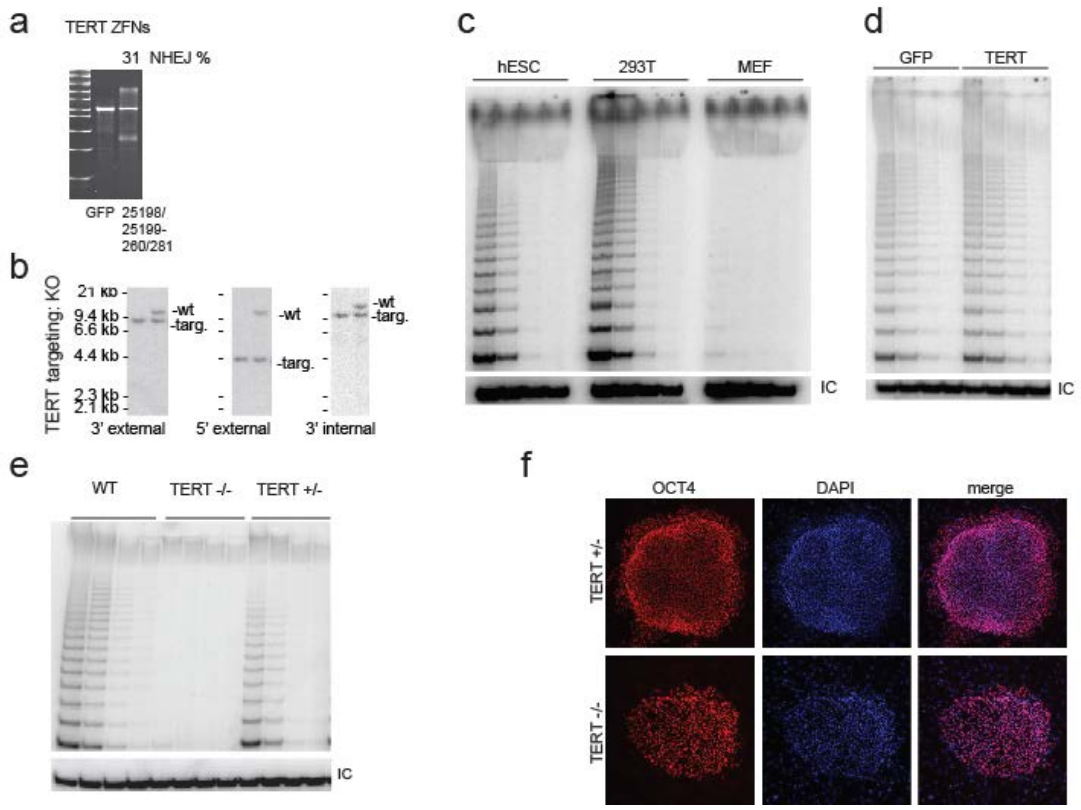

Extended data fig. 3. Telomerase activity levels and pluripotency in hESCs and targeted lines. a, Efficiency of cutting by transfected ZFNs of PCR-amplified genomic locus of target genes by Cel-1 assay. **b,** Southern blot of HindIII-digested genomic DNA from TERT-targeted lines indicating size of DNA fragments for correctly targeted lines. **c,** TRAP assay of whole cell extract from HEK293T cells, WT hESCs, and MEFs alone using 333 ng total protein and subsequent 1:4 dilutions. IC, internal control. **d,** TRAP assay showing telomerase activity from hESCs transiently transfected to express TERT or GFP with protein concentration as in ***a***. **d,** TRAP assay of WT, TERT -/-, or TERT +/- lines with protein concentration as in **a.** Note that WT here is the same set shown in Extended data fig. 4, cropped from the same gel. **e,** IF of TERT -/- and TERT +/- lines approximately 1 week before TERT -/- cells died, stained against OCT4 and counter-stained with DAPI.

Extended data figure 4

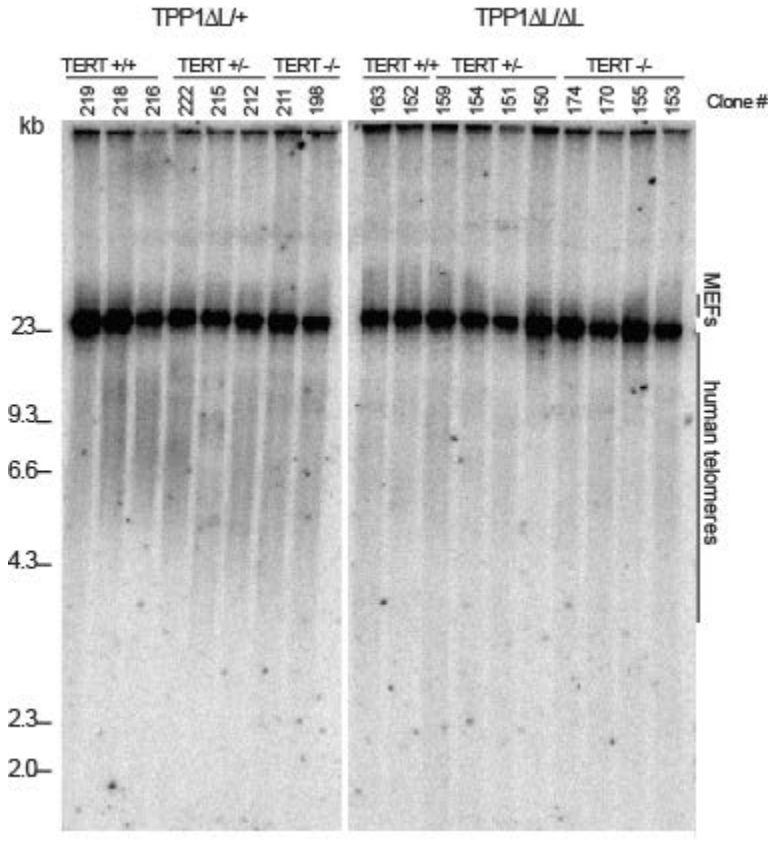

Extended data fig. 4. Double knockout epistasis test for TPP1 and TERT. Telomere lengths from clonal lines from targeting TERT for knockout in either a TPP1 ΔL/ΔL or TPP1 ΔL/+ background. Homozygous, heterozygous, and undisrupted locus clones for TERT KO are shown. All cell lines showed telomere shortening and died with indistinguishable kinetics.

Extended data figure 5

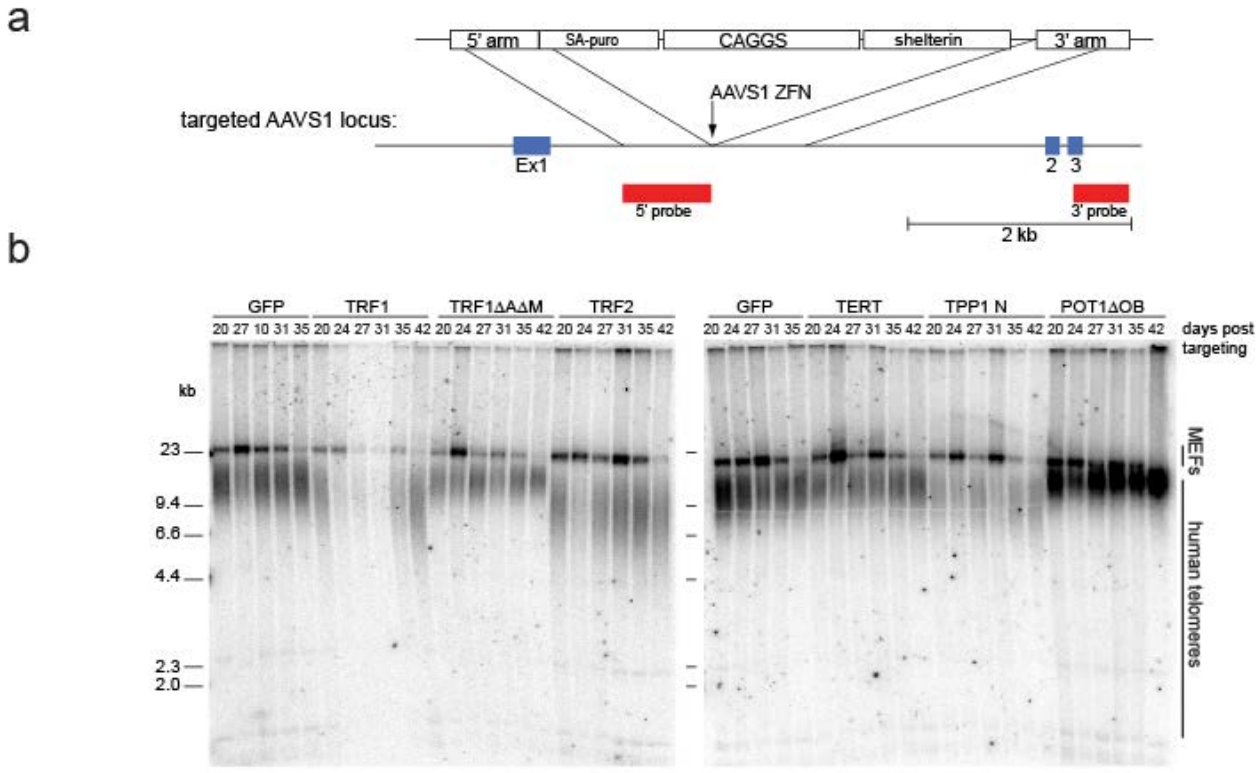

Extended data fig. 5. Overexpression of shelterin components affects telomere length homeostasis. a, Targeting schematic for introduction of shelterin components and TERT at the AAVS1 locus. **b,** Telomere length of cells containing constructs indicated over time, TRF1ΔAΔM is deleted for the myb and acidic domains.

Extended data figure 6

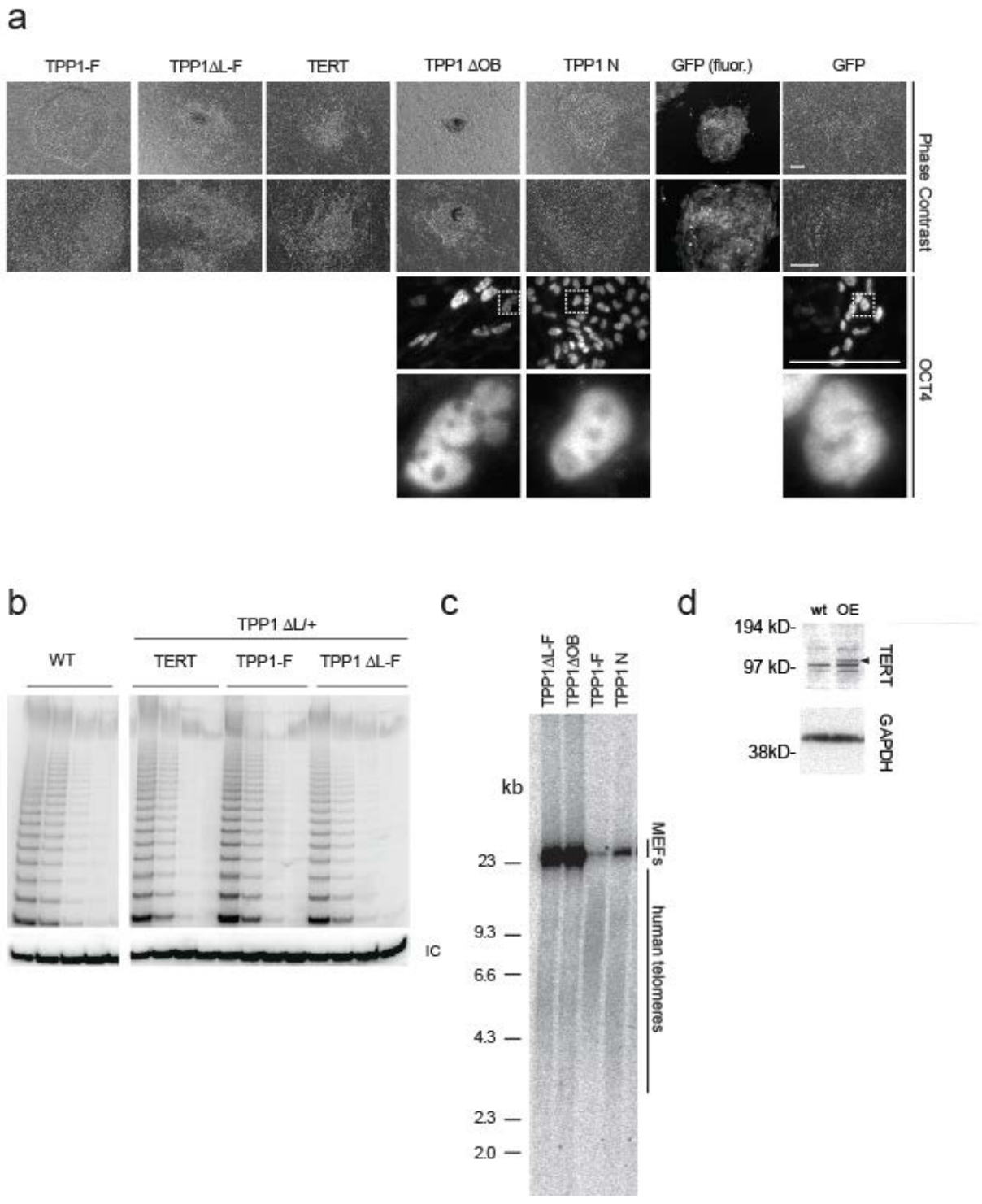

Extended data fig. 6. TPP1 ΔL/ΔL lines require TEL patch for rescue. a, Phase contrast and IF stained against OCT4 in TPP1 ΔL/ΔL lines rescued with indicated constructs. Note that lines missing OCT4 images are shown in the main figures. Scale bar is 200 μm. **b,**

TRAP assay of WT hESCs (same as the set shown in Extended data fig. 3, cropped from the same gel) TPP1 ΔL/ΔL lines rescued with indicated constructs using 333 ng total protein and subsequent 1:4 dilutions. IC, internal control. **c,** Telomere length assay of TPP1 ΔL/ΔL lines rescued with indicated constructs at late time point, approximately 2 weeks before death of TPP1 ΔL/ΔL parent cells. **d,** Immunoblot of overexpression of TERT from the AAVS1 locus.

Extended data figure 7

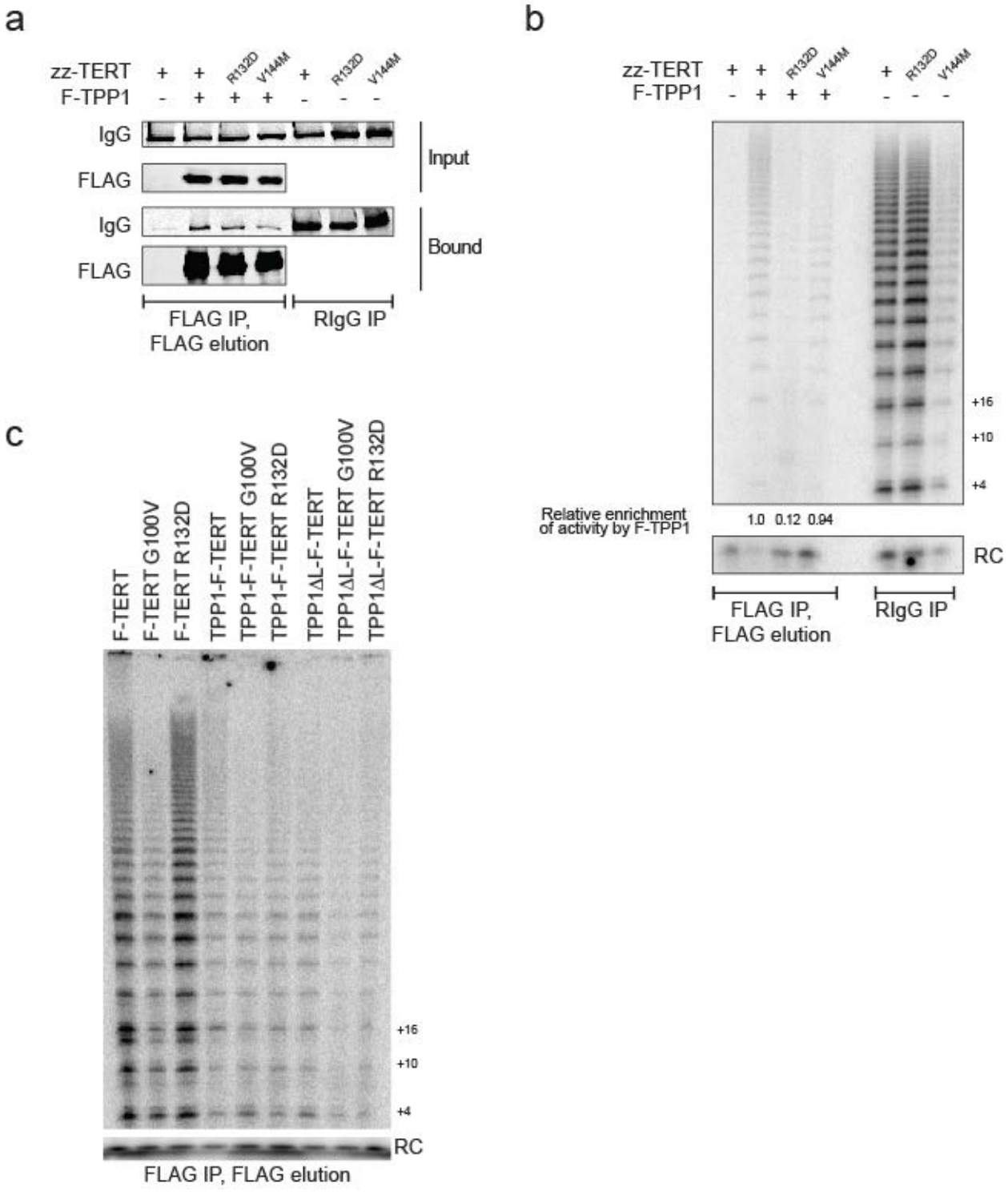

Extended data fig. 7. TPP1 does not functionally associate with TERT R132D. a, Immunoblot of F-TPP1 or zz-TERT overexpressed in HEK293T cells and purified as indicated.

RIgG, rabbit immunoglobulin G. **b,** Direct telomerase catalytic activity assay of purifications from ***a***. Relative enrichment was FLAG IP normalized to RIgG. RC, recovery control. **c,** Direct telomerase catalytic activity assay of TPP1-F-TERT fusion proteins and controls as indicated.

Extended data figure 8

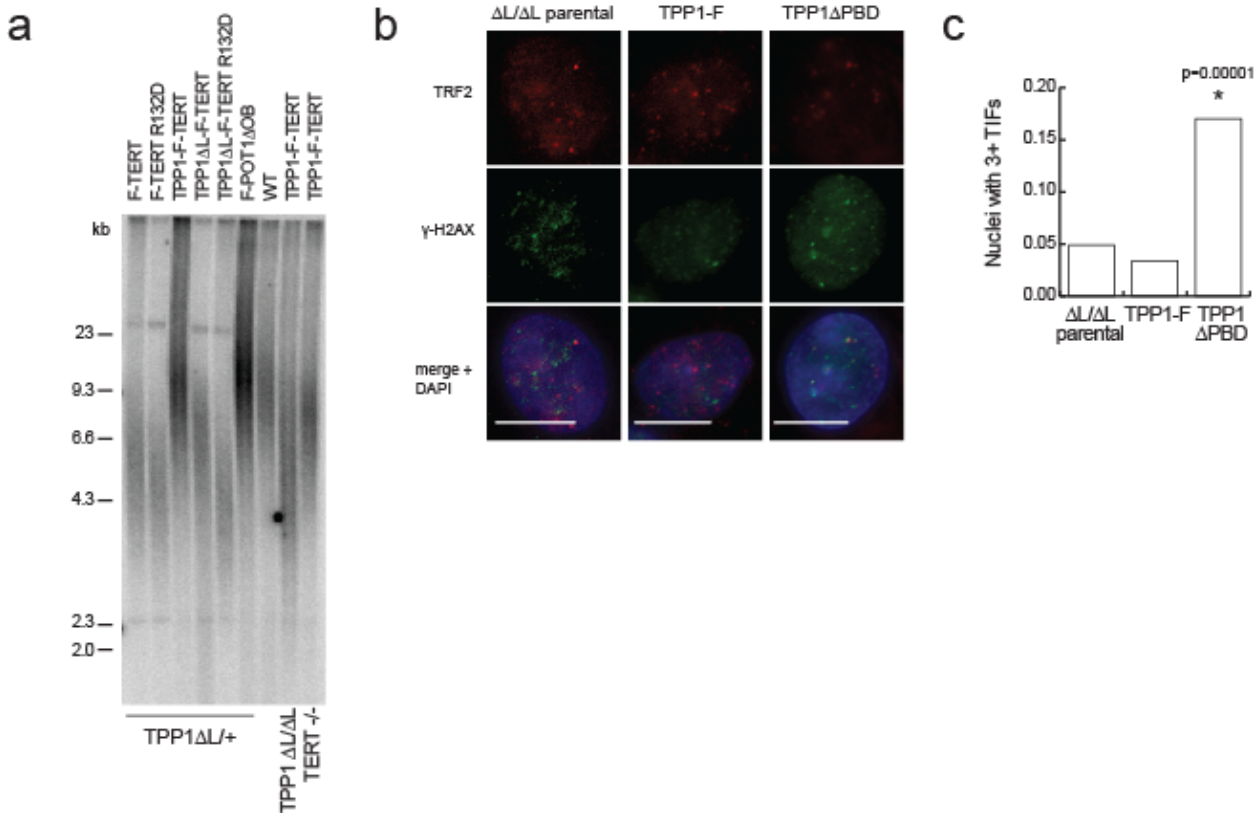

Extended data fig. 8. Tethered TERT maintains telomeres in the presence of WT TPP1. a, Telomere lengths of cell lines with AAVS1-targeted fusion constructs and F-POT1 ΔOB in TPP1 ΔL/+ cell background at approximately 75 days after targeting. Also shown are telomere lengths of TPP1 ΔL/ΔL or TERT -/- lines maintained for approximately 90 days after targeting to express TPP1-F-TERT. **b,** IF of TIFs in TPP1 ΔL/ΔL parental line, or rescue with TPP1 ΔPBD-F and TPP1-F stained against the DNA damage indicator γH2AX and TRF2, counterstained with DAPI. **c,** Quantification of TIFs from ***b***, p value determined by fisher's exact test.

Extended data figure 9

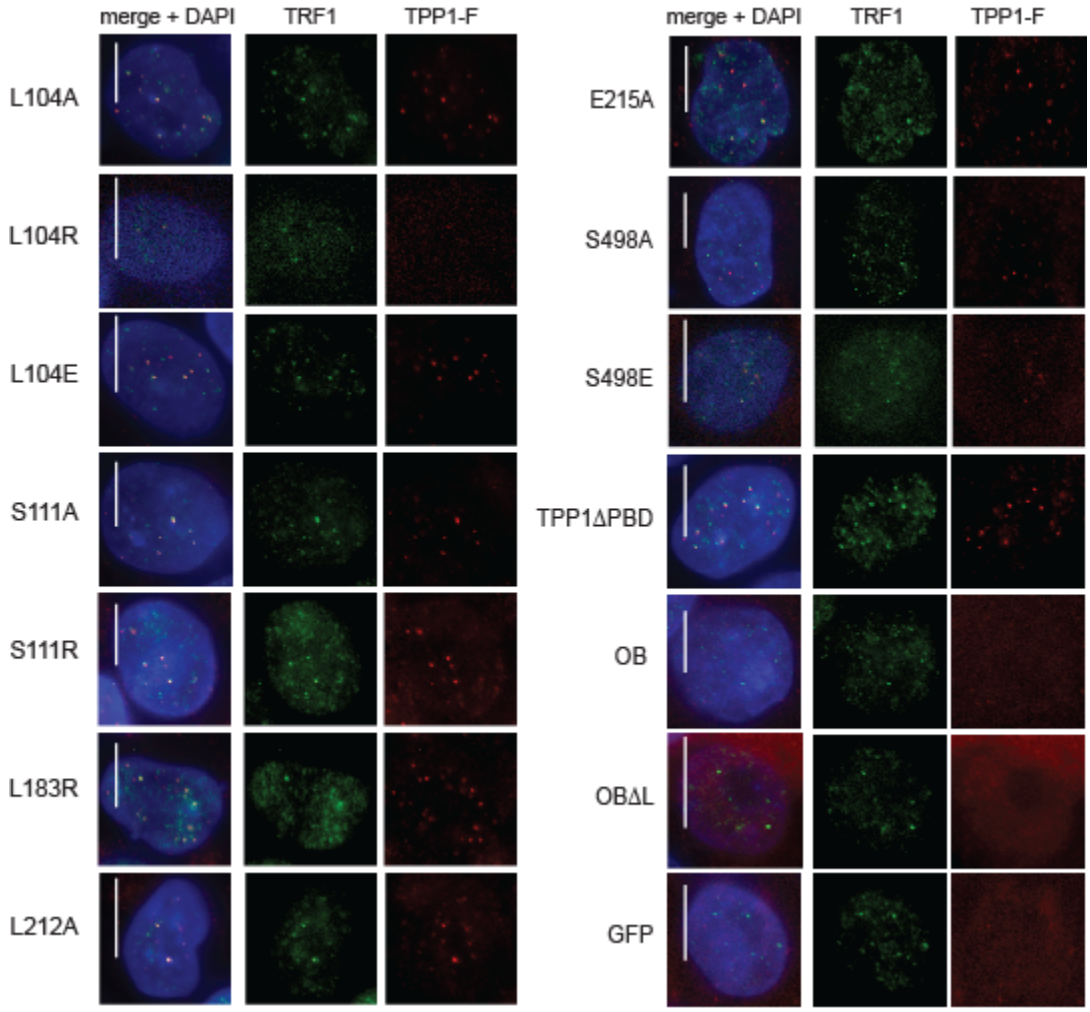

Extended data fig. 9. TPP1 variants localize to the telomere. IF of TPP1-F variants, costained against FLAG and TRF1, counterstained with DAPI. Note that upon fixation and permeablization, GFP fluorescence normally visible in live cells is lost allowing for staining against TRF2 and GFP.

Extended data table 1

Strain	Genotype (all in WIBR#3, NIH line # 78)	Clonal at AAVS1 (Y/N)?	Figure introduced
UCBDH1	*AAVS1::TPP1-N-NEO/AAVS1*	Y	Ext. 2
UCBDH2	*AAVS1::TPP1-N-NEO/AAVS1, TPP1::TPP1-GFP-PURO/TPP1::TPP1-GFP-PURO*	Y	Ext. 2
UCBDH3	*AAVS1::TPP1-N-NEO/AAVS1, TPP1::TPP1ΔL-GFP-PURO/TPP1::TPP1ΔL-GFP-PURO*	Y	Ext. 2
UCBDH4	*AAVS1::TPP1-N-NEO/AAVS1, TPP1::TPP1ΔL-GFP-PURO/TPP1*	Y	Ext. 2
UCBDH5	*AAVS1::TPP1-N-NEO/AAVS1, TPP1::TPP1ΔOB-GFP-PURO/TPP1::TPP1ΔOB-GFP-PURO*	Y	Ext. 2
UCBDH6	*TPP1::TPP1ΔL-GFP/TPP1::TPP1ΔL-GFP*	Y	Fig. 1
UCBDH7	*TPP1::TPP1ΔL-GFP/TPP1*	Y	Fig. 1
UCBDH8	*TERT::3xS-HYGRO/TERT::3xS-HYGRO*	Y	Fig. 2
UCBDH9	*TERT::3xS-HYGRO/TERT*	Y	Fig. 2
UCBDH10	*AAVS1::TPP1-F-NEO/AAVS1,TPP1::TPP1-GFP-PURO/TPP1::TPP1-GFP-PURO*	Y	Fig. 3
UCBDH11	*AAVS1::TPP1ΔL-F-NEO/AAVS1, TPP1::TPP1-GFP-PURO/TPP1::TPP1-GFP-PURO*	Y	Fig. 3
UCBDH12	*AAVS1::TPP1-N-NEO/AAVS1, TPP1::TPP1-GFP-PURO/TPP1::TPP1-GFP-PURO*	N	Ext. 6
UCBDH13	*AAVS1::TPP1-F-NEO/AAVS1,TPP1::TPP1-GFP-PURO/TPP1*	N	Fig. 3
UCBDH14	*AAVS1::TPP1ΔL-F-NEO/AAVS1, TPP1::TPP1-GFP-PURO/TPP1*	N	Fig. 3
UCBDH15	*AAVS1::TERT-NEO/AAVS1, TPP1::TPP1-GFP-PURO/TPP1*	N	Fig. 3
UCBDH16	*AAVS1::GFP-NEO/AAVS1, TPP1::TPP1-GFP-PURO/TPP1::TPP1-GFP-PURO*	N	Ext. 6
UCBDH17	*AAVS1::TPP1ΔOB-F-NEO/AAVS1, TPP1::TPP1-GFP-PURO/TPP1::TPP1-GFP-PURO*	Y	Ext. 6
UCBDH18	*AAVS1::TERT-NEO/AAVS1, TPP1::TPP1-GFP-PURO/TPP1::TPP1-GFP-PURO*	Y	Fig. 3
UCBDH19	*TERT::3xS-HYGRO/TERT::3xS-HYGRO, TPP1::TPP1ΔL-GFP/TPP1::TPP1ΔL-GFP*	Y	Ext. 4
UCBDH20	*TERT::3xS-HYGRO/TERT, TPP1::TPP1ΔL-GFP/TPP1::TPP1ΔL-GFP*	Y	Ext. 4
UCBDH21	*TERT::3xS-HYGRO/TERT, TPP1::TPP1ΔL-GFP/TPP1::TPP1ΔL-GFP*	N	Fig. 3
UCBDH22	*AAVS1::F-TERT-NEO/AAVS1, TPP1::TPP1-GFP-PURO/TPP1::TPP1-GFP-PURO*	N	Fig. 4
UCBDH23	*AAVS1::F-TERTR132D-NEO/AAVS1, TPP1::TPP1-GFP-PURO/TPP1::TPP1-GFP-PURO*	N	Fig. 4
UCBDH24	*AAVS1::TPP1-F-TERT-NEO/AAVS1, TPP1::TPP1-GFP-PURO/TPP1::TPP1-GFP-PURO*	N	Fig. 4
UCBDH25	*AAVS1::TPP1ΔL-F-TERT-NEO/AAVS1, TPP1::TPP1-GFP-PURO/TPP1::TPP1-GFP-PURO*	N	Fig. 4
UCBDH26	*AAVS1::TPP1ΔL-F-TERTR132D-NEO/AAVS1, TPP1::TPP1-GFP-PURO/TPP1::TPP1-GFP-PURO*	N	Fig. 4
UCBDH27	*AAVS1::F-POT1ΔOB-NEO/AAVS1, TPP1::TPP1-GFP-PURO/TPP1::TPP1-GFP-PURO*	N	Fig. 4
UCBDH28	*AAVS1::F-TERT-NEO/AAVS1, TERT::3xS-HYGRO/TERT::3xS-HYGRO*	N	Fig. 4
UCBDH29	*AAVS1::F-TERTR132D-NEO/AAVS1, TERT::3xS-HYGRO/TERT::3xS-HYGRO*	N	Fig. 4
UCBDH30	*AAVS1::TPP1-F-TERT-NEO/AAVS1, TERT::3xS-HYGRO/TERT::3xS-HYGRO*	N	Fig. 4
UCBDH31	*AAVS1::TPP1ΔL-F-TERT-NEO/AAVS1, TERT::3xS-HYGRO/TERT::3xS-HYGRO*	N	Fig. 4
UCBDH32	*AAVS1::TPP1ΔL-F-TERTR132D-NEO/AAVS1, TERT::3xS-HYGRO/TERT::3xS-HYGRO*	N	Fig. 4
UCBDH33	*AAVS1::F-TERT-NEO/AAVS1, TPP1::TPP1ΔL-GFP/TPP1*	N	Ext. 8
UCBDH34	*AAVS1::F-TERTR132D-NEO/AAVS1, TPP1::TPP1ΔL-GFP/TPP1*	N	Ext. 8
UCBDH35	*AAVS1::TPP1-F-TERT-NEO/AAVS1, TPP1::TPP1ΔL-GFP/TPP1*	N	Ext. 8
UCBDH36	*AAVS1::TPP1ΔL-F-TERT-NEO/AAVS1, TPP1::TPP1ΔL-GFP/TPP1*	N	Ext. 8
UCBDH37	*AAVS1::TPP1ΔL-F-TERTR132D-NEO/AAVS1, TPP1::TPP1ΔL-GFP/TPP1*	N	Ext. 8
UCBDH38	*AAVS1::F-POT1ΔOB-NEO/AAVS1, TPP1::TPP1ΔL-GFP/TPP1*	N	Ext. 8

UCBDH39	*AAVS1::TPP1L104A-F-NEO/AAVS1, TPP1::TPP1-GFP-PURO/TPP1::TPP1-GFP-PURO*	N	Fig. 5
UCBDH40	*AAVS1::TPP1L104R-F-NEO/AAVS1, TPP1::TPP1-GFP-PURO/TPP1::TPP1-GFP-PURO*	N	Fig. 5
UCBDH41	*AAVS1::TPP1L104E-F-NEO/AAVS1, TPP1::TPP1-GFP-PURO/TPP1::TPP1-GFP-PURO*	N	Fig. 5
UCBDH42	*AAVS1::TPP1S111A-F-NEO/AAVS1, TPP1::TPP1-GFP-PURO/TPP1::TPP1-GFP-PURO*	N	Fig. 5
UCBDH43	*AAVS1::TPP1S111R-F-NEO/AAVS1, TPP1::TPP1-GFP-PURO/TPP1::TPP1-GFP-PURO*	N	Fig. 5
UCBDH44	*AAVS1::TPP1L183R-F-NEO/AAVS1, TPP1::TPP1-GFP-PURO/TPP1::TPP1-GFP-PURO*	N	Fig. 5
UCBDH45	*AAVS1::TPP1L212A-F-NEO/AAVS1, TPP1::TPP1-GFP-PURO/TPP1::TPP1-GFP-PURO*	N	Fig. 5
UCBDH46	*AAVS1::TPP1E215A-F-NEO/AAVS1, TPP1::TPP1-GFP-PURO/TPP1::TPP1-GFP-PURO*	N	Fig. 5
UCBDH47	*AAVS1::TPP1S498A-F-NEO/AAVS1, TPP1::TPP1-GFP-PURO/TPP1::TPP1-GFP-PURO*	N	Fig. 5
UCBDH48	*AAVS1::TPP1S498E-F-NEO/AAVS1, TPP1::TPP1-GFP-PURO/TPP1::TPP1-GFP-PURO*	N	Fig. 5
UCBDH49	*AAVS1::TPP1OB-F-NEO/AAVS1, TPP1::TPP1-GFP-PURO/TPP1::TPP1-GFP-PURO*	N	Fig. 4
UCBDH50	*AAVS1::TPP1OBΔL-F-NEO/AAVS1, TPP1::TPP1-GFP-PURO/TPP1::TPP1-GFP-PURO*	N	Fig. 4
UCBDH51	*AAVS1::TPP1ΔPBD-F-NEO/AAVS1, TPP1::TPP1-GFP-PURO/TPP1::TPP1-GFP-PURO*	N	Fig. 4
UCBDH52	*AAVS1::GFP-NEO/AAVS1, TPP1::TPP1-GFP-PURO/TPP1::TPP1-GFP-PURO*	N	Fig. 4
UCBDH53	*AAVS1::F-POT1ΔOB-N-PURO/AAVS1*	N	Ext. 5
UCBDH54	*AAVS1::TRF1ΔΔM-PURO/AAVS1*	N	Ext. 5
UCBDH55	*AAVS1::TERT-PURO/AAVS1*	N	Ext. 5
UCBDH56	*AAVS1::GFP-PURO/AAVS1*	N	Ext. 5
UCBDH57	*AAVS1::TRF2-PURO/AAVS1*	N	Ext. 5

Extended data table 1: List of cell lines modified for these studies. All lines were clonally selected for TPP1 and TERT targeting. Clonal selection for AAVS1 targeting is indicated. Where AAVS1-targeted lines were not clonally selected, the efficiency of targeting predicts heterozygocity at the AAVS1 locus in the population.

REFERENCES

Abreu, E., Aritonovska, E., Reichenbach, P., Cristofari, G., Culp, B., Terns, R.M., Lingner, J., and Terns, M.P. (2010). TIN2-tethered TPP1 recruits human telomerase to telomeres in vivo. Mol. Cell. Biol. *30*, 2971–2982.

Antal, M., Boros, E., Solymosy, F., and Kiss, T. (2002). Analysis of the structure of human telomerase RNA in vivo. Nucleic Acids Res. *30*, 912–920.

Armbruster, B.N., Banik, S.S.R., Guo, C., Smith, A.C., and Counter, C.M. (2001). N-Terminal Domains of the Human Telomerase Catalytic Subunit Required for Enzyme Activity in vivo . Mol. Cell. Biol. *21* , 7775–7786.

Armbruster, B.N., Etheridge, K.T., Broccoli, D., and Counter, C.M. (2003). Putative Telomere-Recruiting Domain in the Catalytic Subunit of Human Telomerase . Mol. Cell. Biol. *23* , 3237–3246.

Armbruster, B.N., Linardic, C.M., Veldman, T., Bansal, N.P., Downie, D.L., and Counter, C.M. (2004). Rescue of an hTERT Mutant Defective in Telomere Elongation by Fusion with hPot1 . Mol. Cell. Biol. *24* , 3552–3561.

Artandi, S.E., and Attardi, L.D. (2005). Pathways connecting telomeres and p53 in senescence, apoptosis, and cancer. Biochem. Biophys. Res. Commun. *331*, 881–890.

Avilion, A.A., Piatyszek, M.A., Gupta, J., Shay, J.W., Bacchetti, S., and Greider, C.W. (1996). Human Telomerase RNA and Telomerase Activity in Immortal Cell Lines and Tumor Tissues . Cancer Res. *56* , 645–650.

Batista, L.F.Z., Pech, M.F., Zhong, F.L., Nguyen, H.N., Xie, K.T., Zaug, A.J., Crary, S.M., Choi, J., Sebastiano, V., Cherry, A., et al. (2011). Telomere shortening and loss of self-renewal in dyskeratosis congenita induced pluripotent stem cells. Nature *474*, 399–402.

Baumann, P., and Price, C. (2010). Pot1 and telomere maintenance. FEBS Lett. *584*, 3779–3784.

Bianchi, A., and Shore, D. (2008). How telomerase reaches its end: mechanism of telomerase regulation by the telomeric complex. Mol. Cell *31*, 153–165.

Blackburn, E.H., and Collins, K. (2011). Telomerase: An RNP Enzyme Synthesizes DNA . Cold Spring Harb. Perspect. Biol. *3* .

Blackburn, E.H., Greider, C.W., and Szostak, J.W. (2006). Telomeres and telomerase: the path from maize, Tetrahymena and yeast to human cancer and aging. Nat. Med. *12*, 1133–1138.

Bryan, T.M., and Baumann, P. (2010). G-quadruplexes: from guanine gels to chemotherapeutics. Methods Mol. Biol. *608*, 1–16.

Bryan, T.M., Englezou, A., Dunham, M.A., and Reddel, R.R. (1998). Telomere length dynamics in telomerase-positive immortal human cell populations. Exp. Cell Res. *239*, 370–378.

Cairney, C.J., and Keith, W.N. (2008). Telomerase redefined: Integrated regulation of hTR and hTERT for telomere maintenance and telomerase activity. Biochimie *90*, 13–23.

Cesare, A.J., and Karlseder, J. (2012). A three-state model of telomere control over human proliferative boundaries. Curr. Opin. Cell Biol. *24*, 731–738.

Chan, A., Boulé, J.-B., and Zakian, V.A. (2008). Two pathways recruit telomerase to Saccharomyces cerevisiae telomeres. PLoS Genet. *4*, e1000236.

Chen, J.-L., and Greider, C.W. (2003). Template boundary definition in mammalian telomerase. Genes Dev. *17*, 2747–2752.

Chen, J.-L., and Greider, C.W. (2005). Functional analysis of the pseudoknot structure in human telomerase RNA. Proc. Natl. Acad. Sci. U. S. A. *102*, 8080–5; discussion 8077–9.

Chen, J.L., Blasco, M.A., and Greider, C.W. (2000). Secondary structure of vertebrate telomerase RNA. Cell *100*, 503–514.

Chen, L.-Y., Redon, S., and Lingner, J. (2012). The human CST complex is a terminator of telomerase activity. Nature *488*, 540–544.

Churikov, D., and Price, C.M. (2008). Pot1 and cell cycle progression cooperate in telomere length regulation. Nat. Struct. Mol. Biol. *15*, 79–84.

Cifuentes-Rojas, C., and Shippen, D.E. (2012). Telomerase regulation. Mutat. Res. Mol. Mech. Mutagen. *730*, 20–27.

Cohen, S.B., Graham, M.E., Lovrecz, G.O., Bache, N., Robinson, P.J., and Reddel, R.R. (2007). Protein Composition of Catalytically Active Human Telomerase from Immortal Cells . Sci. *315* , 1850–1853.

Collie, G.W., Haider, S.M., Neidle, S., and Parkinson, G.N. (2010). A crystallographic and modelling study of a human telomeric RNA (TERRA) quadruplex. Nucleic Acids Res. *38*, 5569–5580.

Collins, K. (2006). The biogenesis and regulation of telomerase holoenzymes. Nat. Rev. Mol. Cell Biol. *7*, 484–494.

Collins, K. (2008). Physiological assembly and activity of human telomerase complexes. Mech. Ageing Dev. *129*, 91–98.

Collins, K. (2011). Single-stranded DNA repeat synthesis by telomerase. Curr. Opin. Chem. Biol. *15*, 643–648.

Counter, C.M., Hahn, W.C., Wei, W., Caddle, S.D., Beijersbergen, R.L., Lansdorp, P.M., Sedivy, J.M., and Weinberg, R.A. (1998). Dissociation among in vitro telomerase activity, telomere maintenance, and cellular immortalization . Proc. Natl. Acad. Sci. *95* , 14723–14728.

Creacy, S.D., Routh, E.D., Iwamoto, F., Nagamine, Y., Akman, S.A., and Vaughn, J.P. (2008). G4 resolvase 1 binds both DNA and RNA tetramolecular quadruplex with high affinity and is the major source of tetramolecular quadruplex G4-DNA and G4-RNA resolving activity in HeLa cell lysates. J. Biol. Chem. *283*, 34626–34634.

Cristofari, G., Adolf, E., Reichenbach, P., Sikora, K., Terns, R.M., Terns, M.P., and Lingner, J. (2007a). Human Telomerase RNA Accumulation in Cajal Bodies Facilitates Telomerase Recruitment to Telomeres and Telomere Elongation. Mol. Cell *27*, 882–889.

Cristofari, G., Sikora, K., and Lingner, J. (2007b). Telomerase unplugged. ACS Chem. Biol. *2*, 155–158.

Daniel, M., Peek, G.W., and Tollefsbol, T.O. (2012). Regulation of the human catalytic subunit of telomerase (hTERT). Gene *498*, 135–146.

Deng, Z., Norseen, J., Wiedmer, A., Riethman, H., and Lieberman, P.M. (2009). TERRA RNA Binding to TRF2 Facilitates Heterochromatin Formation and ORC Recruitment at Telomeres. Mol. Cell *35*, 403–413.

Egan, E.D., and Collins, K. (2010). Specificity and Stoichiometry of Subunit Interactions in the Human Telomerase Holoenzyme Assembled In vivo. Mol. Cell. Biol. *30*, 2775–2786.

Egan, E.D., and Collins, K. (2012). Biogenesis of telomerase ribonucleoproteins . RNA *18* , 1747–1759.

Errington, T.M., Fu, D., Wong, J.M.Y., and Collins, K. (2008). Disease-associated human telomerase RNA variants show loss of function for telomere synthesis without dominant-negative interference. Mol. Cell. Biol. *28*, 6510–6520.

Evans, S.K., and Lundblad, V. (1999). Est1 and Cdc13 as comediators of telomerase access. Science *286*, 117–120.

Feuerhahn, S., Iglesias, N., Panza, A., Porro, A., and Lingner, J. (2010). TERRA biogenesis, turnover and implications for function. FEBS Lett. *584*, 3812–3818.

Fu, D., and Collins, K. (2003). Distinct biogenesis pathways for human telomerase RNA and H/ACA small nucleolar RNAs. Mol. Cell *11*, 1361–1372.

Fu, D., and Collins, K. (2006). Human telomerase and Cajal body ribonucleoproteins share a unique specificity of Sm protein association. Genes Dev. *20*, 531–536.

Fu, D., and Collins, K. (2007). Purification of human telomerase complexes identifies factors involved in telomerase biogenesis and telomere length regulation. Mol. Cell *28*, 773–785.

Gilson, E., and Ségal-Bendirdjian, E. (2010). The telomere story or the triumph of an open-minded research. Biochimie *92*, 321–326.

Gros, J., Guédin, A., Mergny, J.-L., and Lacroix, L. (2008). G-Quadruplex formation interferes with P1 helix formation in the RNA component of telomerase hTERC. Chembiochem *9*, 2075–2079.

Gu, P., Min, J.-N., Wang, Y., Huang, C., Peng, T., Chai, W., and Chang, S. (2012). CTC1 deletion results in defective telomere replication, leading to catastrophic telomere loss and stem cell exhaustion. EMBO J *31*, 2309–2321.

Han, X., Liu, D., Zhang, Y., Li, Y., Lu, W., Chen, J., and Songyang, Z. (2013). Akt regulates TPP1 homodimerization and telomere protection. Aging Cell *12*, 1091–1099.

Harley, C.B. (2008). Telomerase and cancer therapeutics. Nat. Rev. Cancer *8*, 167–179.

Hockemeyer, D., Palm, W., Else, T., Daniels, J.-P., Takai, K.K., Ye, J.Z.-S., Keegan, C.E., de Lange, T., and Hammer, G.D. (2007). Telomere protection by mammalian Pot1 requires interaction with Tpp1. Nat. Struct. Mol. Biol. *14*, 754–761.

Hockemeyer, D., Soldner, F., Beard, C., Gao, Q., Mitalipova, M., DeKelver, R.C., Katibah, G.E., Amora, R., Boydston, E.A., Zeitler, B., et al. (2009). Efficient targeting of expressed and silent genes in human ESCs and iPSCs using zinc-finger nucleases. Nat. Biotechnol. *27*, 851–857.

Hockemeyer, D., Wang, H., Kiani, S., Lai, C.S., Gao, Q., Cassady, J.P., Cost, G.J., Zhang, L., Santiago, Y., Miller, J.C., et al. (2011). Genetic engineering of human pluripotent cells using TALE nucleases. Nat. Biotechnol. *29*, 731–734.

Houghtaling, B.R., Cuttonaro, L., Chang, W., and Smith, S. (2004a). A dynamic molecular link between the telomere length regulator TRF1 and the chromosome end protector TRF2. Curr. Biol. *14*, 1621–1631.

Houghtaling, B.R., Cuttonaro, L., Chang, W., and Smith, S. (2004b). A dynamic molecular link between the telomere length regulator TRF1 and the chromosome end protector TRF2. Curr. Biol. *14*, 1621–1631.

Huen, J., Kakihara, Y., Ugwu, F., Cheung, K.L.Y., Ortega, J., and Houry, W.A. (2010). Rvb1-Rvb2: essential ATP-dependent helicases for critical complexes. Biochem. Cell Biol. *88*, 29–40.

Hug, N., and Lingner, J. (2006). Telomere length homeostasis. Chromosoma *115*, 413–425.

Iwamoto, F., Stadler, M., Chalupníková, K., Oakeley, E., and Nagamine, Y. (2008). Transcription-dependent nucleolar cap localization and possible nuclear function of DExH RNA helicase RHAU. Exp. Cell Res. *314*, 1378–1391.

Jády, B.E., Richard, P., Bertrand, E., and Kiss, T. (2006). Cell cycle-dependent recruitment of telomerase RNA and Cajal bodies to human telomeres. Mol. Biol. Cell *17*, 944–954.

Jankowsky, E., and Fairman, M.E. (2007). RNA helicases--one fold for many functions. Curr. Opin. Struct. Biol. *17*, 316–324.

Jun, H.-I., Liu, J., Jeong, H., Kim, J.-K., and Qiao, F. (2013). Tpz1 controls a telomerase-nonextendible telomeric state and coordinates switching to an extendible state via Ccq1. Genes Dev. *27*, 1917–1931.

Kim, N.W., Piatyszek, M.A., Prowse, K.R., Harley, C.B., West, M.D., Ho, P.L.C., Coviello, G.M., Wright, W.E., Weinrich, S.L., and Shay, J.W. (1994). Specific Association of Human Telomerase Activity with Immortal Cells and Cancer. Science (80-.). *266*, 2011–2015.

Kipling, D., and Cooke, H.J. (1990). Hypervariable ultra-long telomeres in mice. Nature *347*, 400–402.

Lansdorp, P.M. (2005). Role of Telomerase in Hematopoietic Stem Cells. Ann. N. Y. Acad. Sci. *1044*, 220–227.

Latrick, C.M., and Cech, T.R. (2010). POT1-TPP1 enhances telomerase processivity by slowing primer dissociation and aiding translocation. EMBO J. *29*, 924–933.

Lattmann, S., Giri, B., Vaughn, J.P., Akman, S.A., and Nagamine, Y. (2010). Role of the amino terminal RHAU-specific motif in the recognition and resolution of guanine quadruplex-RNA by the DEAH-box RNA helicase RHAU. Nucleic Acids Res. *38*, 6219–6233.

Lee, J., Mandell, E.K., Tucey, T.M., Morris, D.K., and Lundblad, V. (2008). The Est3 protein associates with yeast telomerase through an OB-fold domain. Nat. Struct. Mol. Biol. *15*, 990–997.

Lee, J., Mandell, E.K., Rao, T., Wuttke, D.S., and Lundblad, V. (2010). Investigating the role of the Est3 protein in yeast telomere replication. Nucleic Acids Res. *38*, 2279–2290.

Lee, S.R., Wong, J.M.Y., and Collins, K. (2003). Human telomerase reverse transcriptase motifs required for elongation of a telomeric substrate. J. Biol. Chem. *278*, 52531–52536.

Li, S., Makovets, S., Matsuguchi, T., Blethrow, J.D., Shokat, K.M., and Blackburn, E.H. (2009). Cdk1-dependent phosphorylation of Cdc13 coordinates telomere elongation during cell-cycle progression. Cell *136*, 50–61.

Li, X., Nishizuka, H., Tsutsumi, K., Imai, Y., Kurihara, Y., and Uesugi, S. (2007). Structure, interactions and effects on activity of the 5'-terminal region of human telomerase RNA. J. Biochem. *141*, 755–765.

Liu, D., Safari, A., O'Connor, M.S., Chan, D.W., Laegeler, A., Qin, J., and Songyang, Z. (2004). PTOP interacts with POT1 and regulates its localization to telomeres. Nat. Cell Biol. *6*, 673–680.

Loayza, D., and De Lange, T. (2003a). POT1 as a terminal transducer of TRF1 telomere length control. Nature *423*, 1013–1018.

Loayza, D., and De Lange, T. (2003b). POT1 as a terminal transducer of TRF1 telomere length control. Nature *424*, 1013–1018.

Lue, N.F., Yu, E.Y., and Lei, M. (2013). A popular engagement at the ends. Nat. Struct. Mol. Biol. *20*, 10–12.

Marión, R.M., and Blasco, M.A. (2010). Telomeres and telomerase in adult stem cells and pluripotent embryonic stem cells. Adv. Exp. Med. Biol. *695*, 118–131.

Mattern, K.A., Swiggers, S.J.J., Nigg, A.L., Löwenberg, B., Houtsmuller, A.B., and Zijlmans, J.M.J.M. (2004). Dynamics of protein binding to telomeres in living cells: implications for telomere structure and function. Mol. Cell. Biol. *24*, 5587–5594.

McKerlie, M., and Zhu, X.-D. (2011). Cyclin B-dependent kinase 1 regulates human TRF1 to modulate the resolution of sister telomeres. Nat Commun *2*, 371.

Meyerson, M., Counter, C.M., Eaton, E.N., Ellisen, L.W., Steiner, P., Caddle, S.D., Ziaugra, L., Beijersbergen, R.L., Davidoff, M.J., Liu, Q., et al. (1997). hEST2, the Putative Human Telomerase Catalytic Subunit Gene, Is Up-Regulated in Tumor Cells and during Immortalization. Cell *90*, 785–795.

Min, B., and Collins, K. (2009). An RPA-Related Sequence-Specific DNA-Binding Subunit of Telomerase Holoenzyme Is Required for Elongation Processivity and Telomere Maintenance. Mol. Cell *36*, 609–619.

Mitchell, J.R., and Collins, K. (2000). Human telomerase activation requires two independent interactions between telomerase RNA and telomerase reverse transcriptase. Mol. Cell *6*, 361–371.

Mitchell, J.R., Wood, E., and Collins, K. (1999). A telomerase component is defective in the human disease dyskeratosis congenita. Nature *402*, 551–555.

Miyake, Y., Nakamura, M., Nabetani, A., Shimamura, S., Tamura, M., Yonehara, S., Saito, M., and Ishikawa, F. (2009). RPA-like Mammalian Ctc1-Stn1-Ten1 Complex Binds to Single-Stranded DNA and Protects Telomeres Independently of the Pot1 Pathway. Mol. Cell *36*, 193–206.

Nakashima, M., Nandakumar, J., Sullivan, K.D., Espinosa, J.M., and Cech, T.R. (2013). Inhibition of telomerase recruitment and cancer cell death. J. Biol. Chem. *288*, 33171–33180.

Nandakumar, J., and Cech, T.R. (2013). Finding the end: recruitment of telomerase to telomeres. Nat. Rev. Mol. Cell Biol. *14*, 69–82.

Nandakumar, J., Bell, C.F., Weidenfeld, I., Zaug, A.J., Leinwand, L.A., and Cech, T.R. (2012). The TEL patch of telomere protein TPP1 mediates telomerase recruitment and processivity. Nature *492*, 285–289.

O'Sullivan, R.J., and Karlseder, J. (2010). Telomeres: protecting chromosomes against genome instability. Nat. Rev. Mol. Cell Biol. *11*, 171–181.

Palm, W., and de Lange, T. (2008). How shelterin protects mammalian telomeres. Annu Rev Genet *42*, 301–334.

Price, C., Boltz, K.A., Chaiken, M.F., Stewart, J.A., Beilstein, M.A., and Shippen, D.E. (2010). Evolution of CST function in telomere maintenance. Cc *9*, 3157–3165.

Rai, R., Li, J.-M., Zheng, H., Lok, G.T.-M., Deng, Y., Huen, M.S.-Y., Chen, J., Jin, J., and Chang, S. (2011). The E3 ubiquitin ligase Rnf8 stabilizes Tpp1 to promote telomere end protection. Nat. Struct. Mol. Biol. *18*, 1400–1407.

Randall, A., and Griffith, J.D. (2009). Structure of long telomeric RNA transcripts: the G-rich RNA forms a compact repeating structure containing G-quartets. J. Biol. Chem. *284*, 13980–13986.

Robart, A.R., and Collins, K. (2010). Investigation of human telomerase holoenzyme assembly, activity, and processivity using disease-linked subunit variants. J. Biol. Chem. *285*, 4375–4386.

Robart, A.R., and Collins, K. (2011). Human Telomerase Domain Interactions Capture DNA for TEN Domain-Dependent Processive Elongation. Mol. Cell *42*, 308–318.

Savage, S.A., and Alter, B.P. (2009). Dyskeratosis congenita. Hematol. Oncol. Clin. North Am. *23*, 215–231.

Sexton, A.N., and Collins, K. (2011). The 5′ Guanosine Tracts of Human Telomerase RNA Are Recognized by the G-Quadruplex Binding Domain of the RNA Helicase DHX36 and Function To Increase RNA Accumulation. Mol. Cell. Biol. *31*, 736–743.

Sexton, A.N., Youmans, D.T., and Collins, K. (2012). Specificity requirements for human telomere protein interaction with telomerase holoenzyme. J. Biol. Chem. *287*, 34455–34464.

Shay, J.W., and Keith, W.N. (2008). Targeting telomerase for cancer therapeutics. Br. J. Cancer *98*, 677–683.

Soldner, F., Hockemeyer, D., Beard, C., Gao, Q., Bell, G.W., Cook, E.G., Hargus, G., Blak, A., Cooper, O., Mitalipova, M., et al. (2009). Parkinson's disease patient-derived induced pluripotent stem cells free of viral reprogramming factors. Cell *136*, 964–977.

Stern, J.L., and Bryan, T.M. (2008). Telomerase recruitment to telomeres. Cytogenet. Genome Res. *122*, 243–254.

Stern, J.L., Zyner, K.G., Pickett, H.A., Cohen, S.B., and Bryan, T.M. (2012). Telomerase Recruitment Requires both TCAB1 and Cajal Bodies Independently . Mol. Cell. Biol. *32* , 2384–2395.

Stewart, J.A., Wang, F., Chaiken, M.F., Kasbek, C., Chastain, P.D., Wright, W.E., and Price, C.M. (2012a). Human CST promotes telomere duplex replication and general replication restart after fork stalling. EMBO J *31*, 3537–3549.

Stewart, J.A., Chaiken, M.F., Wang, F., and Price, C.M. (2012b). Maintaining the end: roles of telomere proteins in end-protection, telomere replication and length regulation. Mutat. Res. *730*, 12–19.

Takai, H., Smogorzewska, A., and de Lange, T. (2003). DNA damage foci at dysfunctional telomeres. Curr. Biol. *13*, 1549–1556.

Takai, K.K., Hooper, S.M., Blackwood, S.L., Gandhi, R., and de Lange, T. (2010). In vivo stoichiometry of shelterin components. J Biol Chem.

Talley, J.M., DeZwaan, D.C., Maness, L.D., Freeman, B.C., and Friedman, K.L. (2011). Stimulation of yeast telomerase activity by the ever shorter telomere 3 (Est3) subunit is dependent on direct interaction with the catalytic protein Est2. J. Biol. Chem. *286*, 26431–26439.

Tejera, A.M., Stagno d'Alcontres, M., Thanasoula, M., Marion, R.M., Martinez, P., Liao, C., Flores, J.M., Tarsounas, M., and Blasco, M.A. (2010). TPP1 is required for TERT recruitment, telomere elongation during nuclear reprogramming, and normal skin development in mice. Dev. Cell *18*, 775–789.

Thomson, J.A. (1998). Embryonic Stem Cell Lines Derived from Human Blastocysts. Science (80-.). *282*, 1145–1147.

Tomlinson, R.L., Ziegler, T.D., Supakorndej, T., Terns, R.M., and Terns, M.P. (2006). Cell Cycle-regulated Trafficking of Human Telomerase to Telomeres . Mol. Biol. Cell *17* , 955–965.

Tomlinson, R.L., Abreu, E.B., Ziegler, T., Ly, H., Counter, C.M., Terns, R.M., and Terns, M.P. (2008). Telomerase Reverse Transcriptase Is Required for the Localization of Telomerase RNA to Cajal Bodies and Telomeres in Human Cancer Cells . Mol. Biol. Cell *19* , 3793–3800.

Tran, H., Schilling, M., Wirbelauer, C., Hess, D., and Nagamine, Y. (2004). Facilitation of mRNA Deadenylation and Decay by the Exosome-Bound, DExH Protein RHAU. Mol. Cell *13*, 101–111.

Tuzon, C.T., Wu, Y., Chan, A., and Zakian, V.A. (2011). The Saccharomyces cerevisiae telomerase subunit Est3 binds telomeres in a cell cycle- and Est1-dependent manner and interacts directly with Est1 in vitro. PLoS Genet. *7*, e1002060.

Tycowski, K.T., Shu, M.D., Kukoyi, A., and Steitz, J.A. (2009). A Conserved WD40 Protein Binds the Cajal Body Localization Signal of scaRNP Particles. Mol. Cell *34*, 47–57.

Vaughn, J.P., Creacy, S.D., Routh, E.D., Joyner-Butt, C., Jenkins, G.S., Pauli, S., Nagamine, Y., and Akman, S.A. (2005). The DEXH protein product of the DHX36 gene is the major source of tetramolecular quadruplex G4-DNA resolving activity in HeLa cell lysates. J. Biol. Chem. *280*, 38117–38120.

Venteicher, A.S., Abreu, E.B., Meng, Z., McCann, K.E., Terns, R.M., Veenstra, T.D., Terns, M.P., and Artandi, S.E. (2009). A Human Telomerase Holoenzyme Protein Required for Cajal Body Localization and Telomere Synthesis . Sci. *323* , 644–648.

Walne, A.J., and Dokal, I. (2009). Advances in the understanding of dyskeratosis congenita. Br. J. Haematol. *145*, 164–172.

Wan, M., Qin, J., Songyang, Z., and Liu, D. (2009). OB Fold-containing Protein 1 (OBFC1), a Human Homolog of Yeast Stn1, Associates with TPP1 and Is Implicated in Telomere Length Regulation . J. Biol. Chem. *284* , 26725–26731.

Wang, F., Podell, E.R., Zaug, A.J., Yang, Y., Baciu, P., Cech, T.R., and Lei, M. (2007). The POT1-TPP1 telomere complex is a telomerase processivity factor. Nature *445*, 506–510.

Wong., J.M.Y., and Collins, K. (2006). Telomerase RNA level limits telomere maintenance in X-linked dyskeratosis congenita. Genes Dev. *20*, 2848–2858.

Xin, H., Liu, D., Wan, M., Safari, A., Kim, H., Sun, W., O/'Connor, M.S., and Songyang, Z. (2007). TPP1 is a homologue of ciliate TEBP-[bgr] and interacts with POT1 to recruit telomerase. Nature *445*, 559–562.

Xu, Y., Ishizuka, T., Kimura, T., and Komiyama, M. (2010). A U-tetrad stabilizes human telomeric RNA G-quadruplex structure. J. Am. Chem. Soc. *132*, 7231–7233.

Yang, D., He, Q., Kim, H., Ma, W., and Songyang, Z. (2011). TIN2 Protein Dyskeratosis Congenita Missense Mutants Are Defective in Association with Telomerase . J. Biol. Chem. *286* , 23022–23030.

Ye, J.Z.-S., Hockemeyer, D., Krutchinsky, A.N., Loayza, D., Hooper, S.M., Chait, B.T., and de Lange, T. (2004). POT1-interacting protein PIP1: a telomere length regulator that recruits POT1 to the TIN2/TRF1 complex. Genes Dev. *18*, 1649–1654.

Yen, W.-F., Chico, L., Lei, M., and Lue, N.F. (2011). Telomerase regulatory subunit Est3 in two Candida species physically interacts with the TEN domain of TERT and telomeric DNA. Proc. Natl. Acad. Sci. U. S. A. *108*, 20370–20375.

Yu, E.Y., Wang, F., Lei, M., and Lue, N.F. (2008). A proposed OB-fold with a protein-interaction surface in Candida albicans telomerase protein Est3. Nat. Struct. Mol. Biol. *15*, 985–989.

Zaug, A.J., Podell, E.R., Nandakumar, J., and Cech, T.R. (2010). Functional interaction between telomere protein TPP1 and telomerase. Genes Dev. *24*, 613–622.

Zhang, Y., Chen, L.-Y., Han, X., Xie, W., Kim, H., Yang, D., Liu, D., and Songyang, Z. (2013). Phosphorylation of TPP1 regulates cell cycle-dependent telomerase recruitment. Proc. Natl. Acad. Sci. U. S. A. *110*, 5457–5462.

Zhao, Y., Sfeir, A.J., Zou, Y., Buseman, C.M., Chow, T.T., Shay, J.W., and Wright, W.E. (2009). Telomere extension occurs at most chromosome ends and is uncoupled from fill-in in human cancer cells. Cell *138*, 463–475.

Zhao, Y., Abreu, E., Kim, J., Stadler, G., Eskiocak, U., Terns, M.P., Terns, R.M., Shay, J.W., and Wright, W.E. (2011). Processive and Distributive Extension of Human Telomeres by Telomerase under Homeostatic and Nonequilibrium Conditions. Mol. Cell *42*, 297–307.

Zhong, F.L., Batista, L.F.Z., Freund, A., Pech, M.F., Venteicher, A.S., and Artandi, S.E. (2012). TPP1 OB-fold domain controls telomere maintenance by recruiting telomerase to chromosome ends. Cell *150*, 481–494.